Draft for open comment

Tropospheric Ozone Assessment Report: Critical review of changes in the tropospheric ozone burden and budget from 1960-2100

Author Team: A.T. Archibald, J. L. Neu, Y. Elshorbany, O. R. Cooper, P.J. Young, H. Akiyoshi, R.A. Cox, M. Coyle, R. Derwent, M. Deushi, A. Finco, G.J. Frost, I. E. Galbally, G. Gerosa, C. Granier, P.T. Griffiths, R. Hossaini, L. Hu, P.Jöckel, B. Josse, M. Y. Lin, M. Mertens, O. Morgenstern, M. Naja, V. Naik, S. Oltmans, D.A. Plumer, L.E. Revell, A. Saiz-Lopez, P. Saxena, Y.M. Shin, I. Shahid, D. Shallcross, S. Tilmes, T. Trickl, T. J. Wallington, T. Wang, H. M. Worden, G. Zeng

The Tropospheric Ozone Assessment Report (TOAR) is a current IGAC activity (http://www.igacproject.org/activities/TOAR) with a mission to provide the research community with an up-to-date scientific assessment of tropospheric ozone's global distribution and trends from the surface to the tropopause.

Guided by this mission, TOAR has two goals:

1) Produce the first tropospheric ozone assessment report based on the peer-reviewed literature and new analyses.

2) Generate easily accessible, documented data on ozone exposure and dose metrics at hundreds of measurement sites around the world (urban and non-urban), freely accessible for research on the global-scale impact of ozone on climate, human health and crop/ecosystem productivity.

The report is being written as a series of eight stand-alone publications to be submitted for peer-review to *Elementa: Science of the Anthropocene*, an open-access, non-profit science journal founded by five US research Universities and published by University of California Press (www.elementascience.org). Prior to submission each paper will be posted to the TOAR webpage (http://www.igacproject.org/activities/TOAR/OpenComments) for a 30-day open comment period. We invite members of the atmospheric and biological sciences communities as well as the general public to read the papers and provide comments if they wish to do so. The open comment period will last for 30 days for each paper, with the draft papers posted to the website as they become available.

To provide comments on this particular paper, please send an e-mail to lead authors Alex Archibald (ata27@cam.ac.uk) and Jessica Neu (Jessica.L.Neu@jpl.nasa.gov).

Title:

Tropospheric Ozone Assessment Report: Critical review of changes in the tropospheric ozone burden and budget from 1960-2100.

Authors:

A.T. Archibald[1,2,*], J. L. Neu[3], Y. Elshorbany[4], O. R. Cooper[5,6], P.J. Young[7,8,9], H. Akiyoshi[10], R.A. Cox[1], M. Coyle[11,12], R. Derwent[13], M. Deushi[14], A. Finco[15], G.J. Frost[6], I. E. Galbally[16], G. Gerosa[15], C. Granier[6], P.T. Griffiths[1,2], R. Hossaini[7], L. Hu[17], P.Jöckel[18], B. Josse[19], M. Y. Lin[20], M. Mertens[18], O. Morgenstern[21], M. Naja[22], V. Naik[20], S. Oltmans[6], D.A. Plumer[23], L.E. Revell[24], A. Saiz-Lopez[25], P. Saxena[26], Y.M. Shin[1], I. Shahid[27], D. Shallcross[28], S. Tilmes[29], T. Trickl[30], T. J. Wallington[31], T. Wang[32], H. M. Worden[29], G. Zeng[21].

Affiliations:

1 Department of Chemistry, University of Cambridge, Lensfield Road, CB2 1EW, UK.

2 National Centre for Atmospheric Science, UK.

3 NASA Jet Propulsion Laboratory, 4800 Oak Grove Drive, Pasadena, CA, USA.

4 College of Arts and Sciences, University of South Florida, St. Petersburg, FL, USA

5 Cooperative Institute for Research in Environmental Sciences, University of Colorado, Boulder, USA

6 NOAA Earth System Research Laboratory, Chemical Sciences Division, Boulder, USA

7 Lancaster Environment Centre, Lancaster University, Lancaster, UK.

8 Centre of Excellence for Environmental Data Science, Lancaster University, Lancaster, LA1 4AP

9 Pentland Centre for Sustainability in Business, Lancaster University, Lancaster, LA1 4YX

10 Climate Modeling and Analysis Section, Center for Global Environmental Research, National Institute for Environmental Studies, 16-2 Onogawa, Tsukuba, Ibaraki 305-8506, Japan.

11 UKCEH Edinburgh, Bush Estate, Penicuik, Midlothian, EH26 0QB UK

12 The James Hutton Institute, Craigiebuckler, Aberdeen, UK, AB15 8QH

13 rdscientific, Newbury, Berkshire RG14 6LH, United Kingdom.

14 Meteorological Research Institute, Japan Meteorological Agency, 1-1 Nagamine, Tsukuba, Ibaraki 305-0052 Japan.

15 Dipartimento di Matematica e Fisica, Università Cattolica del S.C., via musei 41, 25121 Brescia (Italy).

16 Climate Science Centre, CSIRO Aspendale Australia

17 Department of Chemistry and Biochemistry, University of Montana, Missoula, USA

18 Deutsches Zentrum für Luft und Raumfahrt (DLR), Institut für Physik der Atmosphäre, Oberpfaffenhofen, Germany.

19 Centre National de Recherches Météorologiques, Université de Toulouse, Météo-France, CNRS, Toulouse, France

20 Atmospheric & Oceanic Sciences, Princeton University, NOAA Geophysical Fluid Dynamics Laboratory, USA.

21 National Institute of Water & Atmospheric Research Ltd (NIWA), 301 Evans Bay Parade Hataitai Wellington New Zealand.

22 Aryabhatta Research Institute of Observational Sciences, Nainital, Uttarakhand, 263001, India.

23 Environment and Climate Change Canada.

24 School of Physical and Chemical Sciences, University of Canterbury, Private Bag 4800, Christchurch 8140, New Zealand.

25 Department of Atmospheric Chemistry and Climate, Institute of Physical Chemistry Rocasolano, Spanish National Research Council (CSIC), Madrid, Spain.

26 School of Environmental Sciences, Jawaharlal Nehru University, New Delhi, India.

27 Institute of Space Technology, Islamabad, Pakistan.

28 School of Chemistry, Cantock's Close, University of Bristol, BS8 1TS, UK.

29 Atmospheric Chemistry Observations & Modeling Laboratory National Center for Atmospheric Research, Boulder, CO, USA.

30 Karlsruher Institut für Technologie, IMK-IFU, Garmisch-Partenkirchen, Germany.

31 Research & Advanced Engineering, Ford Motor Company, Dearborn, MI 48121-2053, USA.

32 Department of Civil and Environmental Engineering, The Hong Kong Polytechnic University, Hong Kong, China.

Email: ata27@cam.ac.uk

Abstract:

Tropospheric ozone plays an important role within the Earth system. At high concentrations it has negative impacts on air quality, climate, human health and ecosystem productivity. It is also a primary source of the hydroxyl radical (OH) and supports an oxidizing capacity that acts to remove atmospheric pollutants. Complex physical and chemical processes control tropospheric ozone, our understanding of which has changed dramatically over the last 60 years. Models are the key tool used to understand the budget of ozone and they highlight that there are many processes which are known to be important in controlling the budget of tropospheric ozone, and as some processes that remain less certain. In this critical review we assess our evolving understanding of these processes, both physical and chemical. We review simulations from the recent IGAC Chemistry Climate Modelling Initiative (CCMI) to assess the changes in the tropospheric ozone burden and its budget from 1960 to 2010. Analysis of these data indicates that there has been moderate growth in the ozone burden over this time period and that the ensemble of models investigated simulate burdens of ozone well within recent satellite estimates. Analysis of the CCMI model ozone budget indicates that the chemical production of ozone in the troposphere on average has plateaued since the 1990s. However, there have been regional shifts in ozone production in the troposphere, driven by the regional evolution of precursor emissions. An analysis of the evolution of tropospheric ozone through the 21st century, as simulated by CMIP5 models, reveals a large source of uncertainty associated with models themselves in the near term (two to three decades) with emissions scenarios dominating uncertainty in the longer-term evolution of tropospheric ozone. This intrinsic model uncertainty prevents robust predictions of near-term changes in the tropospheric ozone burden, and we review how progress can be made to reduce this limitation.

1 Introduction:

Tropospheric ozone is a greenhouse gas and at elevated levels a pollutant detrimental to human health, and crop and ecosystem productivity (LRTAP Convention, 2011; REVIHAAP, 2013; US EPA, 2013; Monks et al., 2015). Since 1990, a large portion of the anthropogenic emissions of gases that react in the atmosphere to produce ozone have shifted from North America and Europe – due to pollution controls – to Asia, driven by economic growth and more limted pollution controls (Granier et al., 2011; Cooper et al., 2014; Zhang et al., 2016; Hoesly et al., 2018). This rapid shift, coupled with limited ozone monitoring in developing nations, has left scientists unable to answer the most basic questions: Which regions of the world have the greatest human and plant exposure to ozone pollution? Is ozone continuing to decline in nations with strong emission controls? To what extent is ozone increasing in the

developing world? How can we best quantify ozone's impact on climate, human health and crop/ecosystem productivity?

To answer these questions, the International Global Atmospheric Chemistry (IGAC) project developed the Tropospheric Ozone Assessment Report (TOAR): Global metrics for climate change, human health and crop/ecosystem research (www.igacproject.org/activities/TOAR). Initiated in 2014, TOAR's mission is to provide the research community with an up-to-date scientific assessment of tropospheric ozone's global distribution and trends from the surface to the tropopause. TOAR's primary goals are to produce the first tropospheric ozone assessment report underpinned by all available surface, ozonesonde, aircraft and satellite observations, to document an understanding of ozone distributions and trends from the peer-reviewed literature and new analyses, and to generate easily accessible, well-documented ozone exposure metrics relevant to human health and ecosystems at thousands of measurement sites around the world. Through the TOAR Surface Ozone Database (Schultz et al., 2017), these ozone metrics are freely accessible for research on the global-scale impact of ozone on climate, human health and crop/ecosystem productivity. The assessment report is organized as a series of papers in a Special Feature of Elementa: Science of the Anthropocene.

In addition to measurements, numerical modeling plays a critical role in understanding the burden and budget of tropospheric ozone (see *TOAR-Model Performance*, (Young et al., 2018)). Atmospheric chemistry models typically incorporate (1) tropospheric (and stratospheric) photochemical reaction schemes, (2) anthropogenic precursor emission inventories, (3) schemes for natural emissions (4) chemical removal of ozone precursors and ozone-destroying constituents, and for the removal of ozone at physical surfaces, and (5) schemes for representing atmospheric fluid dynamics, thermodynamics and radiation. Alleviating uncertainties in model representation of these processes is necessary for improved understanding of the drivers of past and future changes in tropospheric ozone, and how these changes may affect climate, human health, and ecosystems.

This paper, abbreviated as *TOAR-Ozone Budget*, focuses on the physical and chemical processes that affect the budget of ozone in the troposphere. *TOAR-Ozone Budget* begins with a brief historical overview of the evolution of the scientific understanding of tropospheric ozone and the fundamental processes known to control it (Sections 1-3). The main focus of the paper is a detailed analysis of our current understanding of the sources and sinks of ozone in the troposphere (Section 4), whilst we discuss new insights into the chemical and physical processes that control ozone and challenges associated with the accurate simulation and prediction of ozone abundances (Section 5 and 6). Section 7 provides a summary and future outlook.

1.1 A brief History of Tropospheric Ozone Research

The history of tropospheric ozone research has been reviewed in detail recently (Wallington, et al., 2019; Staehelin et al., 2017), and here we provide a brief overview. The greatest challenges in tropospheric ozone research over the last few decades have been quantifying and understanding 1) the role and interactions of physical processes, including transport of ozone-rich air from the stratosphere to the troposphere and the removal of ozone at plant, soil, water, snow and ice surfaces, and 2) chemical processes including the emission and transformation of ozone precursors and the production and destruction of ozone in the troposphere by gas and aerosol phase chemistry. Recently it has been recognized that the rates and spatial distributions of these different processes have changed over the past decades and will most likely continue to change in the future as the locations of precursor emissions change (Zhang et al., 2016).

1.2 Evolution in Understanding of the Physical and Chemical Processes Controlling the Distribution of Ozone

The starting point of this historical review is the identification of the transport of ozone-rich air from the stratosphere into the troposphere (Regener, 1938). Here, we follow the terminology of Stohl et al. (2003) and use stratosphere to troposphere transport (STT) in reference to air and ozone transport from the stratosphere across the tropopause and into the troposphere, and stratosphere-troposphere exchange (STE) in reference to air and ozone exchange across the tropopause in both directions. The large-scale processes driving transport of stratospheric air to the troposphere were first identified with the discovery of the Brewer-Dobson circulation, in which tropospheric air passes into the stratosphere in the upper arm of the ascending Hadley circulation at low latitudes, and stratospheric air returns to the troposphere in mid-latitudes (Brewer 1949). Further analysis showed that most of the actual transport occurs during tropopause folding in the vicinity of a jet stream (Danielson, 1968; Danielsen and Mohnen, 1977; Shapiro, 1976; 1978; 1980; Keyser and Shapiro, 1986), with other mechanisms of STT being subsidence in cut-off lows (Price and Vaughan, 1993) and gravity-wave breaking (Lamarque et al., 1996). Subsequently there have been attempts to quantify STT and its temporal evolution through observational constraints (Murphy and Fahey 1994; Beekmann et al., 1997; Scheel, 2003; Olsen et al. 2004; Stohl et al., 2003; Trickl et al., 2020).

Ozone destruction on surfaces has been recognized since the earliest laboratory experiments (Schönbein, 1840). Early research showed that ozone is present in much lower concentrations in the lower atmosphere than in the upper atmosphere implying one or more ozone loss mechanisms in the troposphere (Hartley, 1881; Fabry and Bousson, 1913; Colange and Lepape 1929, Chapman, 1932). These ideas on the loss of ozone by destruction at the Earth's surface were first formalized by Auer (1939), with the classical view of tropospheric ozone being regulated by STT of ozone and surface destruction being put forth by Junge (1962) (Figure 1a). Figure 1 shows, schematically, how this understanding has evolved over time. By the 1980s (Figure 1b) there were sufficient measurements of ozone deposition rates at the Earth's surface (e.g. Regener, 1957; Galbally 1971), sufficient observations of ozone in surface air and sufficient understanding of the interaction of meteorology and ozone deposition that a global budget of ozone deposition of 1000 ± 500 Tg (O_3) yr^{-1} was estimated by Galbally and Roy (1980). These early studies have been proven accurate, with estimates of STT and dry deposition remaining within a factor of two over the last thirty-years, each having uncertainties of around ± 30% at present.

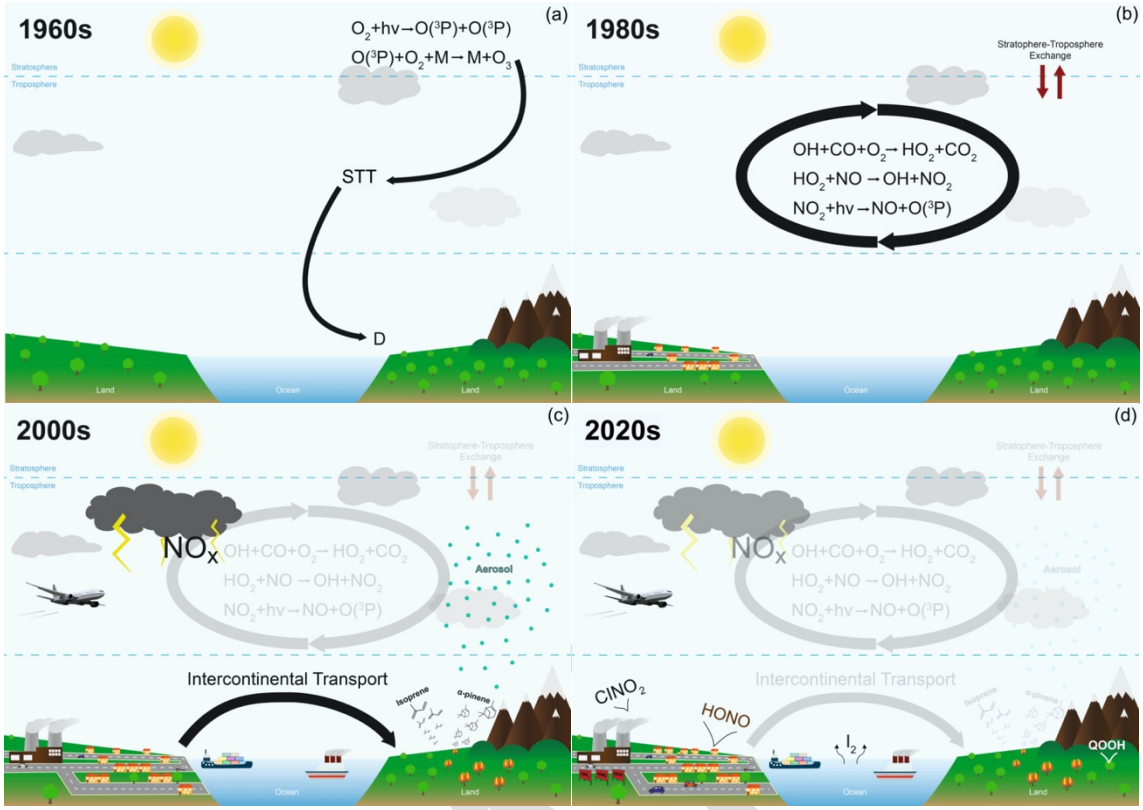

Figure 1: Schematic illustration of how our understanding of the chemical and physical processes controlling tropospheric ozone has evolved. The panels highlight the key processes identified in the different time periods. The labelling of dates in the sub panels (a-d) are indicative.

Up until 1970, there was no knowledge of the kinetic basis of photochemistry of ozone in the lower atmosphere. This changed dramatically when decomposition products of ozone photolysis in the near ultraviolet (UV) were determined, revealing that the long wavelength limit for a significant yield of $O(^1D)$ was 315 nm (Jones and Wayne 1970). Levy (1971) noted that while the majority of $O(^1D)$ atoms are deactivated to ground state $O(^3P)$ atoms through collision with a third molecule (N_2 or O_2), a small fraction react with water vapor to produce hydroxyl radicals (OH). Levy showed that UV radiation in the troposphere and at the Earth's surface was sufficient to initiate the formation of hydroxyl radicals. There was a rapid development of understanding of the photochemistry of the troposphere in the 1970s (Levy 1971, 1972, 1973; Crutzen, 1973; Chameides and Walker, 1973). It was shown that hydroxyl radicals, in the presence of nitrogen oxides and carbon monoxide or volatile organic compounds (VOCs), initiate chemical cycles that, utilizing the oxidation products of carbon monoxide and VOCs, lead to net ozone production (Figure 1b); this chemistry is applicable in both the remote troposphere and the urban atmosphere (Brasseur et al., 1999). The basic mechanism of photochemical production of ozone in the troposphere was confirmed in part by the identification of positive correlations of carbon monoxide and ozone in many regions of the background troposphere (Fishman and Seiler, 1983).

An early combined experimental and modelling study of ozone chemistry in the background troposphere was the Mauna Loa Observatory Photochemistry Experiment in 1988 (MLOPEX), (Ridley et al., 1992, Liu et al., 1992), which was followed by MLOPEX 2 at the same site in 1991 and 1992 (Atlas and Ridley, 1996, Hauglustaine et al., 1996, Brasseur et al., 1996). Since then, it has been shown that net photochemical production of ozone occurs in biomass burning plumes (Jaffe and Wigder, 2012), the polar boundary layer in summer (Oltmans et al., 2008) and in polluted air in snow-covered rural environments in winter (Schnell et al., 2009), as well as in the background troposphere and polluted urban atmosphere. New processes that have been added to the original understanding of tropospheric ozone production and loss processes over the past two decades are discussed in Section 5.

1.3 Regional Differences in Ozone Photochemistry

There are some marked differences in ozone chemistry in remote regions, including the free troposphere, compared to the urban boundary layer (Figure 1c). Methane plays an important role in the free troposphere. The increase in methane over the last decade has been a major driver for increases in background ozone. However, its reactivity makes it a relatively smaller contributor to ozone in the urban atmosphere, where, directly emitted reactive organic compounds dominate ozone production. In remote regions, as well as methane, the VOCs that contribute to ozone chemistry are first- and many-generation oxidation products such as carbon monoxide and a range of oxygenated organic compounds. Another major difference is the availability of NO_x, whose sources are abundant in the urban atmosphere. The primary sources of NO_x in the remote atmosphere are lightning, particularly in the tropical free troposphere (Ridley et al., 1994; Zhang et al., 2003; DeCaria et al., 2005; Schumann and Huntrieser, 2007), and peroxyacetyl nitrate (PAN). In the remote continental boundary layer there are additional sources of soil emission of NOx (Galbally and Roy, 1978; Davidson and Kingerlee 1997) and naturally occurring biomass burning. PAN is a temporary reservoir species for NO_x that is thermally unstable. It is formed primarily in the urban atmosphere from where it can be transported long distances in the free troposphere, facilitating ozone production in the remote atmosphere. In NO_x-poor environments such as the marine boundary layer and much of the free troposphere, ozone is mainly destroyed by photolysis (Ayers et al. 1992). International field experiments (Penkett et al., 1997; Carpenter et al., 1997; Monks et al., 1998) have identified the NO compensation point between ozone production and destruction (Galbally et al., 2000), a key parameter for defining those regions of the troposphere that are net sinks and those that are net sources for tropospheric ozone (Fishman et al., 1979).

A key component of the tropospheric ozone budget is the destruction of ozone at the Earth's surface via deposition, a process absent in the free troposphere. The lack of deposition, coupled with colder temperatures and lower water vapor concentrations, extends the lifetime of ozone in the free troposphere from about a week or so in lower altitudes to a few months in the upper troposphere, based on a globally averaged tropospheric lifetime of 22-23 days (Stevenson et al., 2006). These long atmospheric lifetimes explain the efficiency of the observed transport of ozone from the stratosphere to the middle and lower troposphere and the importance of intercontinental ozone transport in contributing to ozone trends in the background regional atmosphere (Figure 1c). The importance of such long-range transport mechanisms for ozone was recognized in the 1970s (Cox et al., 1975) and formed the corner-stone of the United Nations Economic Commission for Europe (UNECE) Convention on the Long-range Transport of Air Pollution (LRTAP) and continues to be a topic of important research. In the late 1990s, the intercontinental transport of ozone and its precursors from Asia to North America and from North America to Europe was observed, demonstrating the link between the emissions from one continent and the trace gas mixing ratios above a downwind continent (HTAP, 2010).

1.4 Development of Emissions Inventories

On a global scale, the emissions of ozone precursors have increased dramatically over the last 60 years (Hoesly et al., 2018; van Marle et al., 2017; Lamarque et al., 2010). Initially, inventories of ozone precursors were globally integrated estimates (Junge, 1972; Söderlund and Svensson, 1976). Regional emissions inventories were then developed, with the first urban emissions inventory focusing on carbon monoxide, VOCs and NO_x for Los Angeles in the early 1970's to address air quality issues (Roth et al. 1974). A modern approach is the progressive merging of urban, regional and global emission inventories under the IGAC Global Emissions Initiative (GEIA) project (http://www.geiacenter.org/) and the Emissions of atmospheric Compounds and Compilation of Ancillary Data project (ECCAD). The history of these inventories and attempts at their harmonization are discussed by Granier et al. (2011) and references therein. The state of biomass burning and anthropogenic emissions

inventories in 2011 was such that the regional estimates for carbon monoxide and NO_x from different inventories differed by up to a factor of two for the period 1980 to 2005 (Granier et al., 2011). Similar levels of uncertainty may apply to VOC emission estimates too. This highlights the importance for uncertainty estimates associated with emission inventories. While earlier inventories usually completely neglected uncertainty, the latest generation of historic emissions for chemistry-climate model studies are making efforts to move towards enabling quantitative uncertainty estimates (Hoesly et al., 2017).

Another complexity of emission inventories is natural emissions, whose emission rates and their temporal and spatial distribution are dependent on many physical, chemical, and biological processes and states in the environment. Four key processes that contribute to ozone precursor emissions are the production of VOCs from vegetation, NO_x from lightning and soils, and both VOCs and NOx from naturally occurring biomass burning. These processes have been recognized as important contributors to total budgets of NOx and VOCs for many decades, but the problems of quantifying emissions have been formidable. Interactive process-based models now simulate VOC emissions from vegetation, and are embedded within most chemistry climate models, e.g. BEIS (Guenther et al., 1995) and MEGAN (Guenther et al., 2006). However, there is still considerable work to be undertaken in verifying these models (e.g., Marais, et al., 2012; Hu et al., 2015; Emmerson et al., 2016). Similarly, interactive models exist for simulating NO_x emissions from lightning (e.g., those based on Price et al., 1997), but major uncertainties still need to be addressed to refine these models (Schumann and Huntrieser, 2007; Luo et al., 2017; Clark et al., 2017).

2 Physical processes regulating tropospheric ozone

2.1 Loss of ozone to the surface

The ozone deposition process can be described using a resistance analogy, first employed by Galbally and Roy (1980), where the various stages of transfer from the bulk atmosphere to a surface are modelled as serial resistance terms. The destruction at the surface can also be expressed as an equivalent resistance. The advantage of the resistance approach is that the terms are additive, and the reciprocal of the sum of the resistances is the deposition velocity, v_d (Galbally 1974, Galbally and Roy 1980, Wesely 1989), such that

$$v_d = (R_a + R_b + R_c)^{-1} \qquad (2.1)$$

where R_a is the aerodynamic resistance, representing the role of atmospheric turbulence in transporting ozone down from a reference height in the boundary layer (defined by the mixing length); R_b is the resistance arising from molecular diffusion in the sub-laminar boundary layer just above the surface; and R_c is the total surface resistance, arising from when ozone passes through the boundary layer or canopy and makes contact with the surface, where it rapidly reacts and is destroyed. R_c has stomatal and non-stomatal pathways (Figure 2), and is the dominant factor controlling daytime ozone deposition to vegetated surfaces. The rate of this surface destruction is represented by either a combination of cuticular resistance (R_{ct}, which also includes all external plant surfaces) and soil resistance (R_g), or a total surface resistance (R_{st}) for non-vegetated areas, as appropriate.

In the case of plant canopies (which make up a large component of the total ozone deposition flux) there may also be an additional aerodynamic transport term (R_{a_inc}) that represents transport of ozone down to the soil or vegetated understory. It is within the canopy that there may also be gas phase loss of ozone by reaction with NO emitted from the soil and highly reactive VOCs emitted from plants (Kurpius and Goldstein 2003; Fares et al., 2010), and these losses can affect ozone deposition rates over forests and other plant systems with canopies. All these processes and their connections are illustrated in Figure 2.

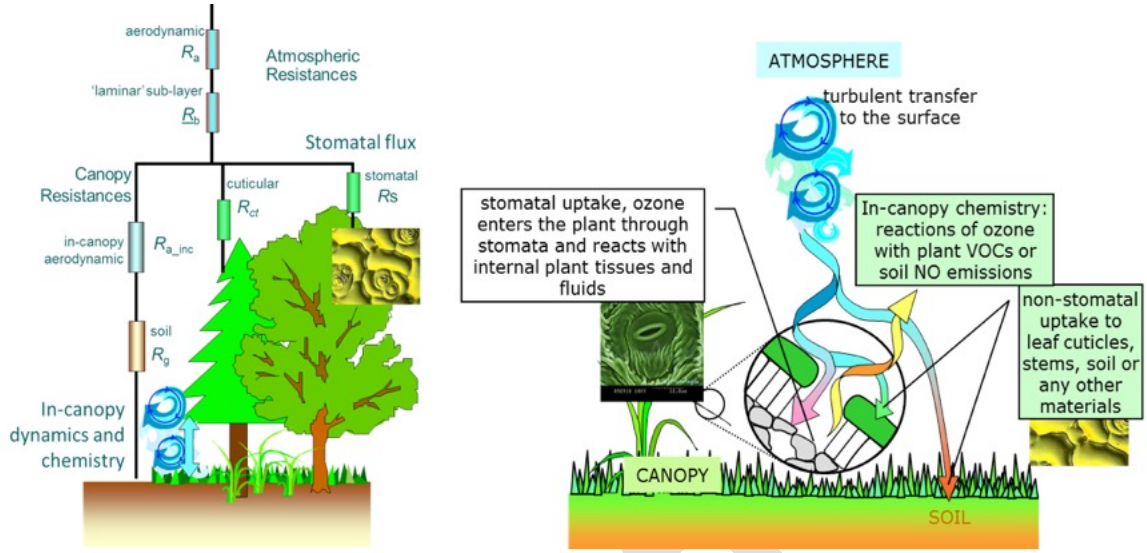

Figure 2: Pathways of ozone deposition on vegetated surfaces (with or without the resistance analogue used to quantify and model the processes).

Over vegetation, ozone can enter the plants' stomata if they are open. The stomatal uptake of ozone is largely regulated by the physiological activity and associated gas exchanges of the vegetation, with light, temperature, and water availability in the plant-soil system as the dominant controlling factors (Gerosa et al., 2009; Fowler et al., 2009; Lin et al., 2019). To estimate the stomatal resistance, it is normally assumed that the concentration of ozone in the intercellular airspace is very small compared to the external concentration, so that it can be neglected. However, studies of plant physiology show that this is not always the case (del a Torre, 2008) and so a modified resistance term may be needed. Furthermore, the widely-used Wesely scheme does not account for the effects of soil moisture or vapor pressure deficits on the stomatal uptake. Recent observational analyses and coupled plant physiology-chemistry-climate models indicate a key role for water availability in modulating ozone deposition rates on seasonal to interannual time scales via changes in stomatal conductance, with the effects on monthly mean daytime v_{d,O_3} variability as large as a factor of two (Lin et al., 2019).

Previously, this stomatal uptake, which can be calculated using plant physiology models, was thought to be the dominant removal process over all vegetated surfaces. The non-stomatal terms were assumed to be constant, only differing depending on whether the surface is dry, wet, or frozen (Wesely, 1989). However, more recent studies have shown that non-stomatal deposition to surfaces can be highly variable and is influenced by temperature, solar radiation, surface moisture and composition, as well as by emissions from the surface. In certain periods and conditions, non-stomatal deposition may dominate surface losses, but there are still large uncertainties in the processes involved (e.g. Clifton et al., 2017; Fowler et al. 2001; Rannik et al. 2012). These concepts are incorporated to some degree in interactive ozone deposition modules within air quality and chemistry climate models (e.g. Tuovinen 2004, Franz 2017; Lin et al., 2019).

A review of ozone deposition estimates from multiple global scale chemistry-climate models was undertaken by Hardacre et al (2015). They looked at 15 models that contributed to the model intercomparison coordinated by the Task Force on Hemispheric Transport of Air Pollution (TF HTAP) (Fiore et al., 2009). Thirteen of these models incorporated a resistance scheme based on the work of Wesely (1989), while the other 2 used prescribed deposition rates (fixed v_d for each land cover class). The calculated annual global deposition fluxes ranged between 818 and 1256 Tg yr^{-1} across the models, with an ensemble mean of 978 ± 127 Tg yr^{-1}, which is similar to predictions from other studies (e.g. Stevenson et al., 2006; Wild, 2007; Young et al., 2013; Young et al., 2018). Comparing the model results with some of the limited measurement data available showed considerable variation in model

performance with season, land cover type and location. The study concluded that uncertainties in deposition to oceans, grasslands and tropical forests were the main cause of differences between the models and that improving them would have the greatest benefit. While the Wesely (1989) scheme has success in some applications (e.g., Silva & Heald, 2018), the lack of sensitivity to soil water availability is problematic, as reviewed by Lin et al. (2019).

Early studies of ozone dry deposition rates and processes for deposition to oceans and snow (Galbally and Roy 1980; Garland et al., 1980) derived deposition rates around an order of magnitude lower than those for soil and plants. More recent studies have established even lower ozone deposition rates over the open ocean (Helmig et al. 2007; Fowler et al. 2009; Ganzeveld et al. 2009; Helmig et al. 2012). These observations can be largely reproduced if the reaction between ozone and iodide ($I^-_{(aq)}$) in the ocean surface layer is included along with turbulent and molecular diffusion processes (Luhar et al., 2017). Incorporating such a deposition scheme into the UKCA chemistry climate model (Luhar et al., 2017) decreases ozone deposition over the ocean by almost half, which corresponds to a 10 % decrease in the model calculated total global ozone deposition. Similar results are obtained in a study of this mechanism with the GEOS-Chem chemical transport model (Pound et al. 2019). An overall downward revision of global ozone deposition rates can be expected as these rates are more widely adopted. The net impact of the ozone-iodide reaction on the ozone budget is not well known, however, given that the ocean surface emits iodine in response to ozone deposition and the released iodine may catalytically destroy ozone in the near surface air, with feedback on other factors such as radiative forcing (Prados-Roman et al., 2015; Sherwen et al 2017). Further model studies are needed to assess the importance of these ozone-iodine feedbacks and reduce the uncertainties in iodine's global impact on ozone.

There are several areas that require further investigation to improve models, allow feedbacks and interactions such as climate change and associated changes in plant activity to be properly assessed, and reduce uncertainty in ozone loss on surfaces. These are: 1) ozone chemistry within plant tissue, on plant and soil surfaces, and within the ocean surface layer; and 2) interactions between ozone deposition and near surface ozone loss via gas phase chemistry, including the coupled ozone deposition and iodine emission cycle at the ocean surface and VOC-ozone reactions in plant canopies; 3) Reduced ozone removal by water-stressed vegetation and associated feedbacks on surface ozone levels during heatwaves and drought. Detailed interactive ozone deposition schemes that include these processes are needed for use in chemistry-climate models to assess how changes in deposition due to changes in land use and climate change affect the global tropospheric ozone budget.

2.2 Transport of ozone from the stratosphere to the troposphere

The stratosphere has long been recognized as an important source of tropospheric ozone. With regard to the impact of stratospheric ozone on the tropospheric ozone budget, the key questions are: 1) what is the net annual flux of ozone from the stratosphere to the troposphere, and what is its interannual variability?; 2) what are the relative contributions of the various STT transport mechanisms (see below) to the annual STT ozone flux?; 3) how well do global atmospheric chemistry models simulate STT transport mechanisms and their contributions to the tropospheric ozone burden?; and 4) how will this source of tropospheric ozone change under climate change, in particular under a geoengineered climate (Xia et al., 2017).

The dynamical processes that transport ozone from the lowermost stratosphere into the troposphere are well understood. These were summarized by Stohl et al. (2003), who reviewed the first 40 years of research on STT, beginning with the pioneering airborne explorations of E. F. Danielsen in 1963 (Danielsen, 1968). At the global scale, STT is driven by the Brewer-Dobson circulation. The 380 K isentropic surface of the extra tropics is a key boundary for quantifying the global annual downward flux of ozone into the troposphere, because any ozone that descends from the stratospheric "overworld" (above 380 K) into the lowermost stratosphere (below 380 K) will eventually enter the troposphere, regardless of the

exact transport mechanism, or the location or timing thereof (Appenzeller et al., 1996; Olsen et al., 2004). Based on MERRA-2 re-analyses, the NH extratropical STT flux has a broad peak from February to May and a minimum in September-October (Jaeglé et al., 2017).

Recent estimates of the flux across the 380 K isentropic surface based on the latest global reanalysis data (with assimilated total column ozone from satellites) are 489 Tg yr^{-1} (NH: 275 Tg yr^{-1}; SH: 214 Tg yr^{-1}) (Olsen et al., 2013), 448 ± 35 Tg yr^{-1} (NH: 256 ± 20; SH: 191 ± 19) (Yang et al., 2016) and 492 Tg yr^{-1} (NH: 281 Tg yr^{-1}; SH: 211 Tg yr^{-1}) (Jaeglé et al., 2017), with the hemispheric disparity arising from the hemispheric asymmetry in the strength of the Brewer-Dobson circulation (stronger in the NH). Estimates of the net stratospheric ozone flux into the troposphere (i.e. the downward flux minus the much smaller flux of tropospheric ozone into the stratosphere) have been inferred from a range of contemporary global atmospheric chemistry models as a residual term of the tropospheric ozone budget, after accounting for the large terms associated with ozone production, loss and surface deposition. TOAR-Model Performance provides a summary of estimates produced from standalone simulations and coordinated activities (ACCENT and ACCMIP; ensembles of opportunity), over the last two decades, which yield a net flux of stratospheric ozone into the troposphere of 520 ± 100 Tg (O_3) yr^{-1} through closure of the ozone budget (Young et al., 2018). Few of the ACCENT and ACCMIP models included full stratospheric chemistry, but following the early work of Jöckel et al. (2006), more and more models are beginning to include this more realistic method of simulating the stratospheric ozone burden. Some of the most recent estimates for the present day from a model with full stratospheric chemistry are 325-360 Tg, at the low end of the ACCENT and ACCMIP ranges (Banerjee et al., 2016; Hu et al., 2017).

The flux estimates above are representative of average conditions, but the values vary interannually due to changes in the stratospheric circulation driven, for example, by El Niño-Southern Oscillation (ENSO) and the stratospheric Quasi-Biennial Oscillation (QBO). Interannual variations in the strength of the stratospheric circulation of around 40% affect the STT flux leading to changes in tropospheric ozone at northern mid-latitudes of around 2%, which is approximately half of the interannual variability (Neu et al., 2014). Olsen et al. (2013) found the extratropical STT ozone flux varied by ± 15% in the NH and ± 6% in the SH from year to year, concluding that $35-39$ years would be required to detect a $2-3\%$ $decade^{-1}$ trend in the STT ozone flux. The STT ozone flux has been affected by the decrease of stratospheric ozone due to ozone depleting substances, but the impact on tropospheric ozone has been relatively small. Hsu and Prather (2009) estimated STT reductions of ~25% in the SH and ~10% in the NH from ozone depletion that occurred from 1979 to 2004, corresponding to a mean decrease in tropospheric ozone of 2.1 nmol/mol and 1 nmol/mol, respectively.

The transport mechanisms by which STT occurs are: 1) intrusions of stratospheric air into the troposphere via the tropopause folds associated with the dry airstream of extratropical cyclones; 2) intrusions of stratospheric air within decaying cut-off lows (a subset of extratropical cyclones); 3) gravity wave breaking; and 4) deep convection penetrating the tropopause (Stohl et al., 2003). A recent analysis of all NH extratropical cyclones for the period 2005–2012 estimates that stratospheric intrusions associated with these cyclones account for 42 ± 20% of the NH extratropical STT ozone flux (Jaeglé et al., 2017). Notable findings regarding the location and seasonality of these intrusions are that shallow intrusions occur most frequently along the subtropical jet stream, a region known for Rossby wave breaking processes conducive to STT, and are particularly prevalent during winter (Scott and Cammas, 2002; Waugh and Funatsu, 2003; Trickl et al., 2011; Homeyer and Bowman, 2013; Nath et al., 2017). Deep intrusions that reach the lower troposphere are frequent at mid-latitudes in winter and spring, with the southwestern USA being a region of high activity, especially in spring. These intrusions also impact the chemistry of the troposphere as they mix with other air masses (Esler et al., 2001); the degree of mixing can be partially gauged via observations of the intrusion's water vapor mixing ratio (Trickl et al., 2016). Intrusions often occur in close proximity to polluted airstreams of extratropical cyclones and over time these air masses can intermingle and eventually mix (Stohl and Trickl, 1999; Parrish et al., 2000; Cooper et al.,

2004; Stohl et al., 2007). Intrusions have also been observed to mix with biomass burning plumes above North America and Europe (Brioude et al., 2007; Trickl et al., 2015).

Although winter and springtime intrusions are cited as most important to the tropospheric burden, summertime stratospheric contributions to tropospheric column ozone amounts (not surface ozone) measured by sondes were estimated at 20-25% over northeastern North America in the 2004 INTEX-A and ICARTT studies (Thompson et al., 2007). The latter budget was based on identification of ozone and potential temperature laminae throughout the soundings. A similar conclusion was reached for the same dataset by Cooper et al. (2006) using the particle-trajectory approach (FLEXPART). A 20-25% contribution for summer STT impacts on tropospheric column ozone was estimated by Collette and Ancellet (2005) using a 30-year European sonde climatology. Furthermore, Stauffer et al., (2018) used a clustering technique and meteorological reanalysis and estimated that, depending on the location, between 25-40% of ozonesonde profiles at midlatitude stations exhibited STT characteristics with anomalously low tropopause heights. The ozonesonde profiles in STT-influenced clusters were not confined to just winter and spring seasons.

Model-based intrusion climatologies and observation-based case studies have demonstrated that high altitude regions such as the western United States (Brioude et al. 2007; Cooper et al., 2004, 2011; Langford et al., 2009, 2015a,b, 2017; Lefohn et al., 2011, 2012, 2014; Lin et al., 2012, 2015; Škerlak et al. 2014, 2019; Dolwick et al. (2015); Lin et al., 2016; Pan et al., 2010; Yates et al., 2013), the Tibetan Plateau (Ding et al., 2006; Cristofanelli, 2010; Chen et al., 2011, 2013; Yin et al., 2017; Škerlak et al. 2019), and the Andes (Anet et al., 2017) are important regions for STT, not only because of frequent deep intrusions but also because their high elevation and very deep daytime boundary layers facilitate the mixing of the diluted intrusions down to the surface. Research aircraft have also documented the occurrence of stratospheric intrusions above Siberia (Berchet et al., 2013), the remote regions of the tropical and mid-latitude South Indian Ocean (Clain et al., 2010; Baray et al., 2012), and at the surface of the high-altitude Antarctic ice sheet (Cristofanelli et al., 2018). The western USA has been intensely studied, with the depth and frequency of the intrusions above the region providing an important test of Eulerian models and global reanalysis data, which have traditionally been limited in their ability to simulate the filamentary features of individual intrusions due to their coarse resolution. However, recent improvements in vertical and horizontal resolution now enable simulation of individual stratospheric intrusions above the western USA and their contribution to surface ozone observations (Lin et al., 2012; Knowland et al., 2017). The interannual variability of intrusions above the region and their impact at the surface have been shown to be strongly influenced by ENSO–driven transport patterns (Lin et al., 2015).

Recent STT research is providing increasing evidence for important interactions between intrusions and deep convection. The potential vorticity anomalies in the mid- and upper troposphere associated with intrusions can trigger deep convection (Waugh and Funatsu, 2003). This can result in mixing between stratospheric and tropospheric air, as observed during a research flight that encountered deep convective clouds penetrating the bottom of an intrusion above Hawaii, with subsequent mixing of tropical tropospheric and mid-latitude stratospheric air masses (Cooper et al. 2005). This phenomenon has also been observed above the western USA during springtime (Homeyer et al., 2011). Deep convective clouds can also entrain ozone-rich lower stratospheric air into the upper troposphere, as observed by three research aircraft on multiple surveys of thunderstorm anvils during the summer 2012 Deep Convective Clouds and Chemistry experiment above the central U.S (Pan et al., 2012, 2014; Schroeder et al., 2014). Tang et al. (2011) used a chemistry-transport model with parameterized deep convection and found that deep convection contributes to half of the STT ozone flux above northern mid-latitudes during June.

3 Chemical processes regulating tropospheric ozone:

Our understanding of the chemical sources and sinks and hence the budget of ozone in the troposphere has increased significantly over the last four decades (Figure 1). Much of the

chemistry is now “textbook”, but the analysis of new laboratory and field observations (enabled by developments in new instruments and improved numerical models) have produced important new discoveries, which we discuss here.

3.1 The photochemical formation mechanism of tropospheric ozone:

It is well established that tropospheric ozone is mainly a secondary photochemical product that results from the photolysis of NO_2.

(R1) $RO_2/HO_2 + NO \rightarrow NO_2 + RO/OH$

(R2) $NO_2 + hv \rightarrow NO + O(^3P)$ ($\lambda \leq 400$ nm)

(R3) $O_2 + O(^3P) + M \rightarrow O_3 + M$

RO_2/HO_2 are organic peroxy radicals (R refer to an alkyl, aryl or alkenyl group) and the hydroperoxy radical respectively. These compounds are key intermediates in the production of ozone in the troposphere (see Section 5.5 for more details) as they convert NO into NO_2 without destroying ozone. They are formed from the oxidation of VOCs and CO with OH. The OH radical is the primary oxidant in the troposphere, for which ozone itself is the primary source via reactions R4 and R5.

(R4) $O_3 + hv \rightarrow O(^1D) + O_2$ ($\lambda \leq 315$ nm)

(R5) $O(^1D) + H_2O \rightarrow 2\ OH$

Several studies have reviewed OH chemical formation in great detail (e.g., Elshorbany et al., 2010b, Stone et al., 2012) and we only briefly mention it here.

Other sources of radicals include alkene ozonolysis (e.g., Paulson and Orlando, 1996; Rickard et al., 1999; Johnson and Marston, 2008), the photolysis of carbonyl compounds, and the photolysis of HONO (Perner and Platt, 1979) (reaction R6).

(R6) $HONO + hv\ (\lambda < 400nm) \rightarrow OH + NO$

This reaction has received attention over the last decade as an important source of OH in the urban atmosphere (Kleffmann et al., 2005, Ren et al., 2006; Dusanter et al, 2009, Elshorbany et al., 2009a, 2012a, 2012b) with associated impacts on the production of ozone (see Section 5.2 for more details).

Recent calculations employing a detailed chemistry scheme (including over 1630 reactions) highlight that secondary production of OH and OH recycling reactions of oxidized VOCs, could outweigh the source of OH in the troposphere from R4 (Lelieveld et al., 2016). But more work is needed to identify the consistency of this result across a range of models.

The ozone forming reactions, R1 to R3, can be considered as a sequence of chain propagating reactions. Under high NO_x conditions, the chain termination is dominated by R7 (where M is a third body), which leads to the formation of nitric acid ($HONO_2$).

(R7) $OH + NO_2 + M \rightarrow HONO_2 + M$

Under low NO_x conditions R10-11 are the more important forms of chain termination.

(R8) $HO_2 + O_3 \rightarrow OH + 2\ O_2$

(R9) $OH + O_3 \rightarrow HO_2 + O_2$

(R10) HO_2 + HO_2 → H_2O_2 + O_2

(R11) HO_2 + RO_2 → ROOH + O_2

In addition to these chemical sinks of ozone, there are a number of physical sinks of ozone – deposition to surfaces (see Section 2.1) and uptake (including of oxidant reservoirs) onto particles (see Section 5.6) – that remove ozone from the troposphere.

Owing to the fast photolysis of NO_2 during the day, reactions that convert NO into NO_2 without the consumption of ozone are considered as ozone producing reactions (i.e. R12a) and reactions which convert NO_2 into other members of the NO_z family (the molecules of oxidized nitrogen (NO_y) excluding NO and NO_2) as ozone destroying (e.g., R7 and R12b). Experimental evidence for a minor, but potentially important, channel of the reaction between HO_2 and NO producing nitric acid ($HONO_2$) (channel 12b) has been reported (Butkovskaya et al., 2005, 2007, 2009). The main sink of $HONO_2$ is surface deposition.

(R12a) HO_2 + NO → HO + NO_2

(R12b) HO_2 + NO + M → $HONO_2$ + M

Several modelling studies (e.g. Søvde et al., 2011; Gottschaldt et al., 2013; Archibald et al., 2019) have investigated the impact of including channel R12b and shown that it could lower tropospheric ozone production rates considerably (20%). Urgent laboratory studies are required to corroborate the $HONO_2$ forming channel R12b.

Traditionally the modeled chemical budget for “ozone” has actually been the budget of odd oxygen (O_x=O_3+$O(^1D)$+$O(^3P)$+NO_2….) to remove the dominance of null-cycles between O_3, and $O(^1D)$ and $O(^3P)$. This diagnosed two terms: the production, predominantly from the conversion of NO to NO_2 via peroxy radicals (R1), and the loss, from the reaction of $O(^1D)$ with H_2O (R5), the direction reaction of HO_x radicals with O_3 (R8 and R9) and other terms. Although this diagnostic framework offered some utility it has not over the years provided significant insight into why the O_3 budgets of different models differed so substantially. Recently, Edwards and Evans (2017), and Bates and Jacob (2019) propose alternative frameworks. Edwards and Evans (2017) showed that tracking the electron spin angular momentum (a spin-budget) within the GEOS-Chem model resulted in a similar results to the traditional model of ozone production in the troposphere described above, but has the advantage of framing the budget in terms of emissions of ozone precursors (VOCs) and specific chemical processes which reduce the efficiency of O_3 production by VOCs. The benefit of this is that more insight can be gained about the role of specific emission changes on the ozone budget (as there is less emphasis on R12a, which ultimately almost every emitted VOC experiences) and specific chemical mechanism details. The spin-budget is similar to the ideas implemented in the Common Representative Intermediates (CRI) mechanism (Jenkin et al., 2008; Jenkin et al., 2019) where individual VOCs are indexed according to their potential to generate RO_2, which propagate NO to NO_2 (F_{NO} in Edwards and Evans (2017)). However, as described, this approach comes at a computational cost as a large amount of output from the model is required. Bates and Jacob (2019) took an alternative approach and extended the idea of chemical families to a wider O_y family (O_y=O_x+O_z). In this framework, O_z represents the ozone forming species such as RO_2 and HO_2 (as well as many other species), without which ozone cannot be produced. Within this “ozone” budget, R1 is an amplifier in the cycling of odd oxygen between O_z and O_x, rather than the main source. These reactions add to the O_y burden,with addition of a primary stratospheric source and photolysis of carbonyl compounds. While the total production and loss of ozone is unchanged by using their budget framework, the lifetime of O_y in the troposphere is dramatically increased (from 24 to 73 days) and the role of the stratosphere is significantly enhanced (acting as a source of 26% of the O_y budget as opposed to 9% of the O_x budget).

These new approaches offer a new capability in our ability to understand the ozone budget within models. However, their relative newness and the need to diagnose a large number of chemical fluxes, has not resulted in these approaches being adopted by the current generation of model inter-comparison exercises. Future efforts may thus allow a better understanding of the model budgets of ozone and why they may disagree with each other.

4 The tropospheric ozone budget

Atmospheric chemistry models are the only tools available to understand the interplay between the complex sources and sinks of tropospheric ozone described above, and hence to understand the response of ozone to changes in these sources and sinks. These models vary greatly in complexity (see Young et al., 2018). Increasingly, models used to study the chemistry of tropospheric ozone include not only the reactions discussed above, but also reactions that are important for stratospheric ozone chemistry (Morgenstern et al., 2017). They can be used to diagnose the spatial and temporal dependence of ozone production in the troposphere, how it has evolved over the past, and, in the case of Chemistry-Climate Models (CCMs), how it will continue to evolve into the future (Young et al., 2018).

Models not only simulate the distribution of ozone; they can also be used to diagnose the ozone budget that controls this distribution. The traditional budget discussed above has four terms: 1) photochemical production (P), whose major terms are described by the constituent reactions of R1 (the number depending on the model's complexity); 2) photochemical loss (L), whose major terms are given by R5, R8 and R9, sometimes including additional minor reactions (e.g. R7, R12 and several others); 3) deposition of ozone to the Earth's surface (D), usually including both dry and wet deposition (which can include loss via clouds); and 4) net transport from the stratosphere (S), which is usually calculated as the residual of the ozone budget, assuming it to be in balance ($S = P - L - D$). S can also be explicitly calculated, but this method is much less frequently used because it is more computationally expensive and traditional definitions of the tropopause surface do not allow for an unambiguous measure of transport in complex dynamical situations (see Prather et al., (2011)).

The first three ozone budget terms (P, L, and D) are usually calculated in each model grid box and can be globally integrated to give the tropospheric ozone budget. The net photochemical tendency (often found in the literature as net chemical production: $d[O_3]/dt|chem = P - L = NCP$) provides a useful measure of regions that are chemical sources and sinks of ozone. An example of the spatial structure in net chemical production is shown in Figure 3 for the UKCA chemistry-climate model under year 2000 conditions (Banerjee et al., 2014).

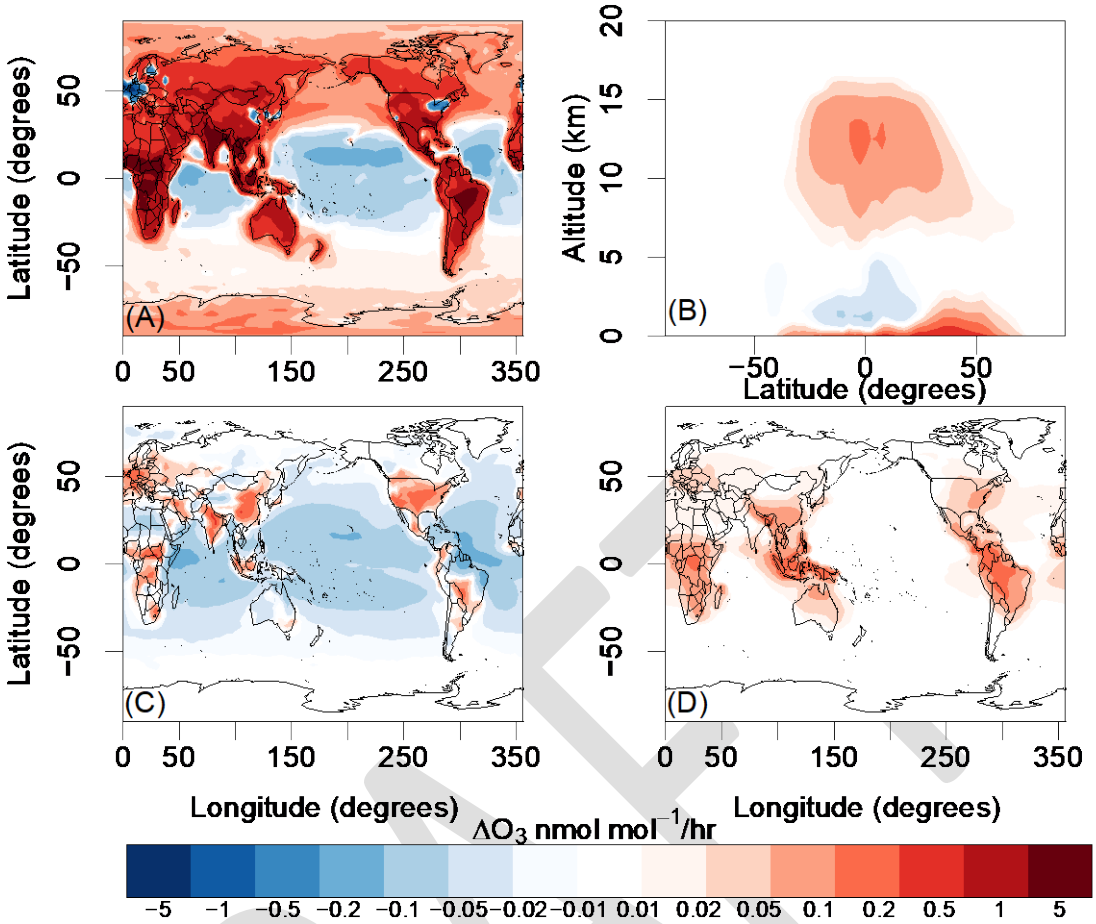

Figure 3: Surface annual mean (panel A) and zonal mean net chemical production (panel B) of ozone from the UKCA model for the year 2000 following the ACCMIP historical scenario (Lamarque et al., 2013). Panels C and D show annual mean net chemical production at 2 km and 8 km respectively.

Figure 3 shows that the most intense net chemical production occurs near the surface over land, with the exception of regions with very high NO_x emissions (e.g. over parts of Western Europe, East Asia and North America). Ozone destruction is widespread over the tropical oceans, especially over the tropical Pacific. Zonally, the net ozone tendency shows a double peak structure in altitude (panel B). Within the boundary layer, ozone production dominates, especially in Northern mid-latitudes. The net ozone tendency decreases with altitude above the boundary layer; in the tropics, photochemical ozone destruction dominates the lower tropospheric signal. The net ozone tendency then has a secondary peak in the tropical upper troposphere, where lightning NO_x emissions have an important role in ozone production (Banerjee et al., 2014). The influence of lightning and deep convection on the net ozone tendency is seen in panel D, where the regions of high annual mean net chemical production at 8 km altitude correlate with regions of high convective activity and outflow.

The majority of the published literature on the tropospheric ozone budget focuses on single model studies. A meta-analysis of the literature is thus problematic because these studies invariably use specific and unique emissions and meteorological conditions, or simulate different periods in time. It is, in principle, considerably easier to quantify and understand the drivers for change in the tropospheric ozone budget from multi-model studies. *TOAR-Model Performance* summarized the present-day ozone budget from a range of different models assessments published between 2005 and 2012 (ACCENT, ACCMIP, and AR5; see Table 8.1 of Young et al. (2018)). These gave an inferred STT (S) of 520 ± 100 Tg (O_3) yr^{-1} and a surface destruction term (D) of 1000 ± 200 Tg (O_3) yr^{-1}. Analysis of multi-model ensembles can prove problematic, however, owing to differences in the level of chemical complexity each

model is capable of representing (especially with respect to non-methane VOCs (NMVOCs); see Young et al. (2013)), as well as other pragmatic decisions made by modelling groups that make different model set ups incongruent (e.g., whether natural emissions evolve with the climate or not). A further specific challenge for the tropospheric ozone budget is in the development of consistent terms of reference for diagnosing the main budget terms, which appears trivial but still to this day causes consternation due largely to disagreements regarding the suite of reactions to be included in the chemical production (P) and loss (L) terms (Young et al., 2013; 2018). For example, there were several models in ACCMIP which incorrectly include terms like R2 in their diagnosed P, rendering a comprehensive assessment of the models impossible (i.e. only 5 out of the 15 models analyzed in Young et al. (2013) had comparable P and L terms).

4.1 How has our understanding of the tropospheric ozone budget changed over time?

As our understanding of the processes that impact tropospheric ozone has changed with time (e.g. Figure 1), so too has the representation of those processes in models. Note that we discuss the change in the ozone budget due to improved knowledge captured through model simulations themselves, not the actual atmospheric trend. Here, we have provided a meta-analysis of the published literature to identify some general features of the changes in model ozone budget terms from the mid-1990s to the present, during which time models have become more sophisticated in their representation of both chemical and physical processes. Hu et al. (2017) recently performed a similar analysis of simulations using the GEOS-Chem chemical transport model (CTM). Here, we examine a range of single model studies and multi model studies. Figure 4 compares calculations from the ACCMIP and ACCENT projects and earlier studies cited by Stevenson et al. (2006) of (a) gross ozone production (P), (b) emissions of NMVOCs and NO_x, (c) STT, and (d) ozone production efficiency (calculated as P/Emissions of NO_x). In all cases, these models analyzed the budget terms for the late 1990s to early 2000s facilitating qualitative comparison.

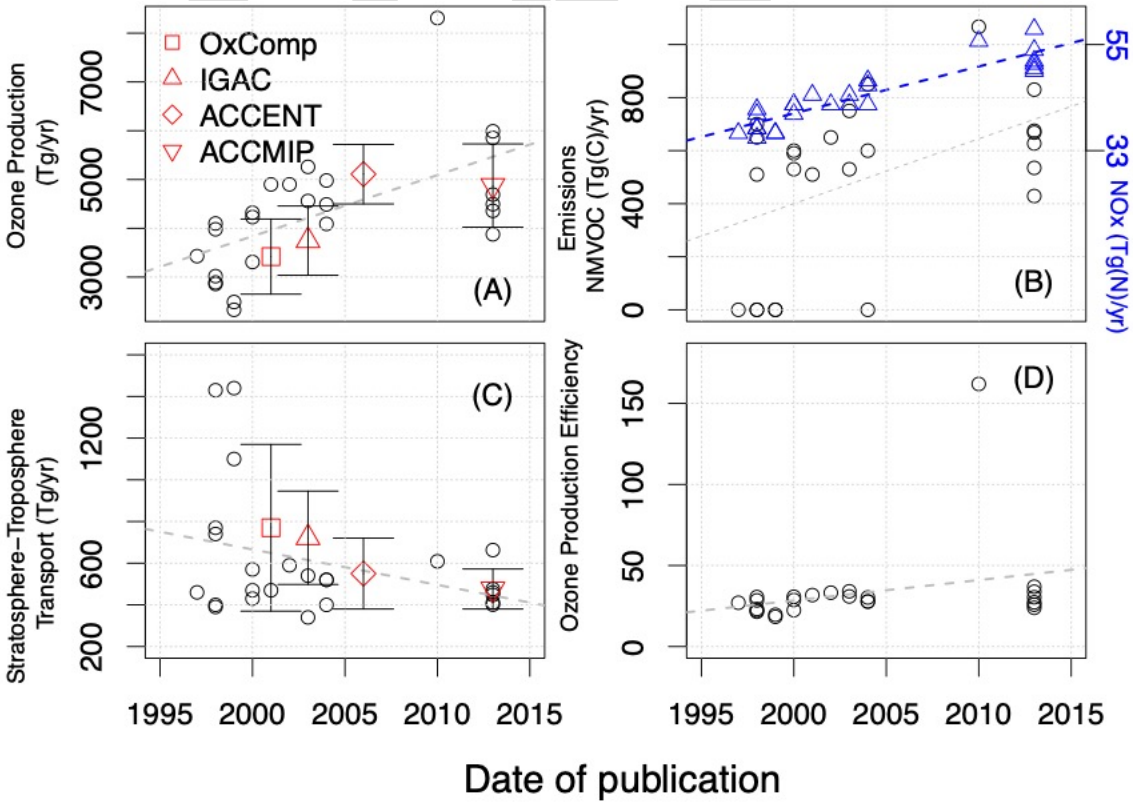

Figure 4: Model simulated (A) production of ozone (B) emissions of NMVOCs and NOx (blue triangles) (C) Stratosphere-Troposphere Transport and (D) Ozone Production Efficiency (Tg ozone produced/Tg NOx emitted), all as a function of publication date. Where data exists, multi model estimates and their uncertainties are indicated. Linear fits through the data are added as dashed lines in each panel, and assessment report means and standard deviations are added to panels a and c.

Several trends are evident from the data in Figure 4. First, there has been an increase in the model-diagnosed photochemical production of ozone as models have evolved over the last two decades (Figure 4a, about 100 Tg per publication year). This in general agrees with the work of Hu et al. (2017) for GEOS-Chem, where the rate of ozone production increased by ~ 80 Tg per publication year. The increase in ozone production (Figure 4a) at first glance coincides with an apparent increase in NMVOC emissions with publication year (Figure 4b), but in reality there are two populations of models: those that include NMVOC emissions (which exhibit a large spread, with average values of 600±200 Tg(C)/yr), and those with zero NMVOC emissions. The models without NMVOC emissions are those focused on stratospheric chemistry, with very simple tropospheric ozone chemistry schemes (i.e. with zero or little NMVOCs). Owing to the high level of scatter it is not possible to confirm if the increase in ozone production is linked to increases in NMVOC in the models. More likely, a major contribution to the increase in P is the increase in NO_x emissions (Figure 4b, blue triangles), which have steadily risen for model studies of the "present day" as emissions inventories have been revised (see Section 6.2 for more on trends and uncertainty in emissions of ozone precursors).

Whilst the ozone production term in models appears to have increased over time, Figure 4c suggests that the STT term has decreased. One explanation for this decrease in modelled STT over the publication period (1998-2013) is the tendency for more recent model studies to include combined stratosphere-troposphere chemistry schemes. These models are more susceptible to errors in large scale transport of ozone from the stratosphere than earlier CTM based studies that applied fixed stratospheric ozone boundary conditions (e.g. OxComp and ACCENT). Hu et al. (2017) hypothesized the change in STT may be related to early model simulations being run at coarse resolution, and a trend for higher resolution model simulations as time has progressed. This resolution change could affect the parameterized vertical transport, in particular deep convection, resulting in lower ozone in the tropical upper troposphere, and hence a lower tropical upwelling flux to compensate for the mid-latitudes downwelling flux. Further targeted studies would be required to clarify the exact mechanisms behind this trend.

Figure 4d shows that the ozone production efficiency (OPE), defined as the ratio of the amount of ozone produced to the NO_x emitted, has increased by 1.2 units per publication year, based on a linear fit to these data. This slight increase in OPE with time could, in principle, account for at least part of the increase in P over this publication record (Figure 4a). One possible cause for the increase in OPE is a redistribution of NO_x emissions; a shift of NO_x emissions to lower latitudes can lead to more efficient ozone production (Zhang et al., 2016). However, it is not possible to definitively identify the cause of the increase in OPE from these multi-model data. The average OPE over the publication period is 27.8 ± 4.85. There is one significant outlier: the CRI-STOCHEM model (Utembe et al., 2010), which has an OPE of 161. This OPE is consistent with the fact that the P term in CRI-STOCHEM is the highest documented in the literature (P = 8310 Tg/yr). CRI-STOCHEM makes use of the CRI mechanism (Jenkin et al. 2008), which is traceable to the Master Chemical Mechanism (Jenkin et al., 1999) and includes a much more complete description of NMVOC than is used in other models. The high P value may reflect greater ozone photochemical production associated with a more complete description of NMVOC chemistry. Interestingly, the ozone burden in CRI-STOCHEM is in broad agreement with other models, as the increased photochemical activity in the model also increases L, which counteracts the effects of such a high P. It is clear that observational constraints on tropospheric OPE rather than just the ozone burden would be very useful for

constraining models. Recent advances in instrumentation may make this possible (Sklaveniti et al., 2018).

Whilst the ACCMIP and ACCENT intercomparisons have generated a large amount of useful data for the community, a lack of consistent model design makes it difficult to understand how model simulations of the ozone budget have evolved over time. For example, the different sets of precursor emissions used in ACCENT and ACCMIP (and the upcoming AerChemMIP) make it difficult to understand what is driving the change in tropospheric ozone from one intercomparison to the next. An outstanding question is how the impacts of changes in chemical mechanisms and rate constants have affected model simulations of the ozone budget. Newsome and Evans, 2018 showed that uncertainty in the inorganic rate constants lead to a notable uncertainty in the calculated composition of the atmosphere. Within the GEOS-Chem model they showed a ~10% uncertainties in the present-day ozone burden and 16% uncertainties in the present day global mean OH due to uncertainties in the inorganic rate constants alone, with even larger changes in tropospheric ozone radiative forcing (16% uncertainties). These uncertainties are comparable to the inter-model variability for these parameters. Hu et al. (2017) have been able to quantify some of this using the GEOS-Chem model and have shown, for example, that changing the representation of isoprene chemistry, in particular a decreased role of isoprene nitrates as sink for NO_x, had a significant effect on tropospheric ozone production rates (increasing P and L by ~ 12%). Moreover, whilst model analysis of the ozone budget provides a means of understanding what drives changes in tropospheric ozone, there are no available observations with which to constrain these model calculations, with the exception of the global ozone burden, and to some extent STT. It is currently impossible to say that a model that simulates a P of 3000 Tg/yr is wrong and one that simulates 7000 Tg/yr is correct. However, with recent aircraft campaigns that are designed to survey the global composition of reactive gases, such as the NASA ATom (Prather et al., 2017) and NERC ACSIS (Sutton et al., 2018) campaigns, there may be additional constraints on the budget in the future.

4.2 Modelled trends in the ozone burden: 1850-2016

The pre-industrial (defined here as the period ca. 1850 CE) burden and distribution of ozone remains highly uncertain despite recent advances in measuring potential ozone proxies in ice cores (Yeung et al., 2019). Ozone concentrations in the 19th century are virtually unknown as reliable rural observations can only be traced back as far as 1896, as assessed by *TOAR-Observations* (Tarasick et al., 2019). At present, model simulations remain our best tools for quantifying changes in the ozone burden since the pre-industrial (Stevenson et al., 2013; Young et al., 2013; Griffiths et al., 2020).

Figure 5 shows the trends in the burden of tropospheric ozone as simulated by a subset of models that took part in the ACCMIP project in support of the Fifth Assessment Report (AR5) of the United Nations Intergovernmental Panel on Climate Change, IPCC (Young et al., 2013), as well as from a subset of models that participated in the Chemistry Climate Model Initiative (CCMI) (Morgenstern et al., 2017). In addition, Figure 5 shows satellite estimates of the tropospheric ozone burden from *TOAR-Climate* (Gaudel et al., 2018). For the models, we define the tropopause using the 125 nmol/mol ozone isopleth determined from monthly mean output; the satellite data are tropospheric columns, with the tropopause levels described by Gaudel et al. (2018). Previous analyses have often used a 150 nmol/mol ozoneapause (Young et al., 2013; Stevenson et al., 2006), however, as discussed in Prather et al. (2011), the global tropospheric ozone burden is sensitive to this definition and we have opted for a lower definition (125 vs 150 nmol/mol) which results in a smaller burden and less stratospheric influence. As the ACCMIP models only provided output as decadal average values, the

annually varying CCMI data have been averaged over each decade. We limit the analysis to the latitude range 60˚S to 60˚N, where the satellite measurements are densest. This geographically limited focus results in a difference between the calculations of the ozone burden presented here from those discussed by Young et al. (2013) for the ACCMIP models, but enables a more robust comparison of the model and satellite data.

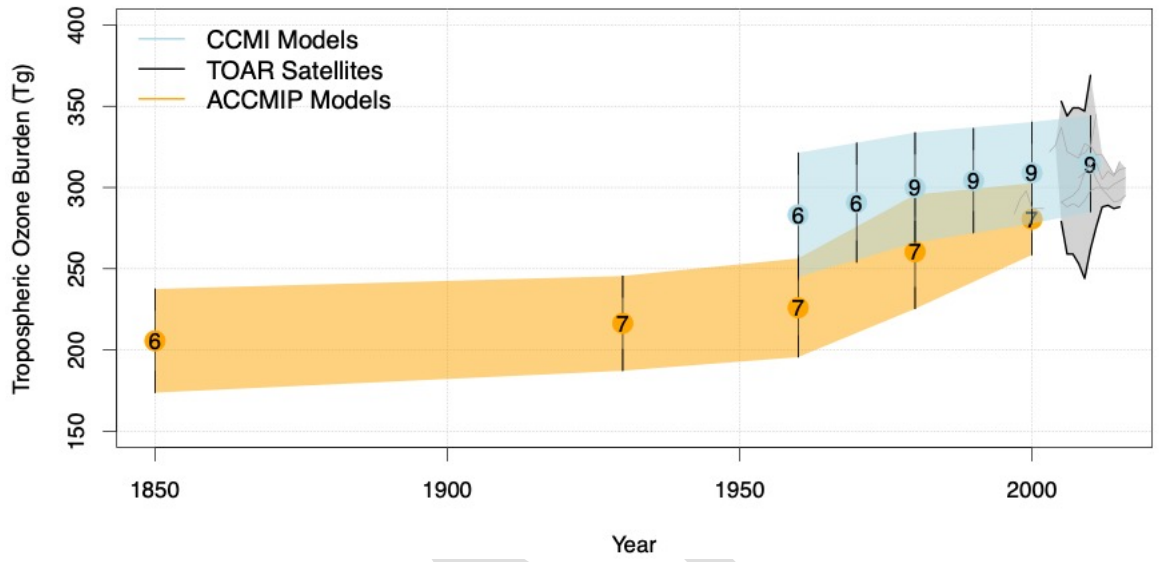

Figure 5: Comparison of modelled (orange and blue envelopes) and satellite-observed (grey envelope) trends in the tropospheric ozone burden between 60˚N and 60˚S. Means of the model data are shown as circles with the vertical lines reflecting ± 1 standard deviation of the mean. The number of models used in calculating the means are displayed in the circles. TOAR Satellites refers to the range of satellite tropospheric ozone burden estimates presented in *TOAR-Climate*.

The model simulations summarized in Figure 5 highlight several key points. Firstly, the tropospheric ozone burden has increased considerably over the historic period. The models indicate that there has been an approximately 30% growth in the burden of ozone over the period 1850-2010, consistent with isotopic constraints using heavy oxygen (^{18}O) from ice cores (Yeung et al., 2019). Simulated increases of the tropospheric ozone burden since the mid-20th century are consistent with that observed at the surface, as assessed by *TOAR-Observations* (Tarasick et al., 2019). Secondly, whilst there is an agreement in the growth of the ozone burden, there is a significant spread in model simulations. However, this spread decreases over the simulation period. For example, the spread in the ACCMIP models, measured as the multi model standard deviation divided by the multi model mean, decreases from 15% in 1850 to 7% in 2000. Similarly, for the CCMI models, the model spread decreases from 13% in 1960 to 9% in 2010. The cause of these features is currently unresolved. Finally, in spite of the large spread in the multi model simulations, both model ensembles lie within the range of satellite estimates of the tropospheric ozone burden, as reviewed by Gaudel et al. (2018).

The overlap between the two model intercomparisons (ACCMIP and CCMI) with each other, and with the TOAR satellite-observations, is promising and highlights a good degree of understanding and capability in simulating the burden of tropospheric ozone. Figure 5 shows that the variability in the CCMI models is larger than the variability in the ACCMIP models. This could be a function of more models being included in the averages (see the numbers in the circles in Figure 5), but importantly the model spread lies within the spread of the satellite-observations, although we note that this is also quite large (21-107 Tg). We can also note that over the period 1960-2000, the ACCMIP models show a stronger increase in the tropospheric ozone burden than the CCMI models (Figure 5).

836 Understanding the causes for the differences in the growth of the ozone burden over this
837 period is an outstanding challenge and would require systematic studies to isolate the key
838 drivers. As Young et al. (2018) highlight, there is need for urgent progress in this area. One
839 consideration, as discussed in general terms in Section 4.1, is the impact of changes in the
840 models themselves; it is possible that models underwent significant process improvements
841 between ACCMIP and CCMI, particularly with respect to the number of models that simulate
842 both stratospheric and tropospheric ozone (Morgenstern et al., 2017). What is certain is that
843 the emissions and boundary conditions used in the ACCMIP and CCMI studies are different
844 (Young et al., 2013; Morgenstern et al., 2017).

845

846

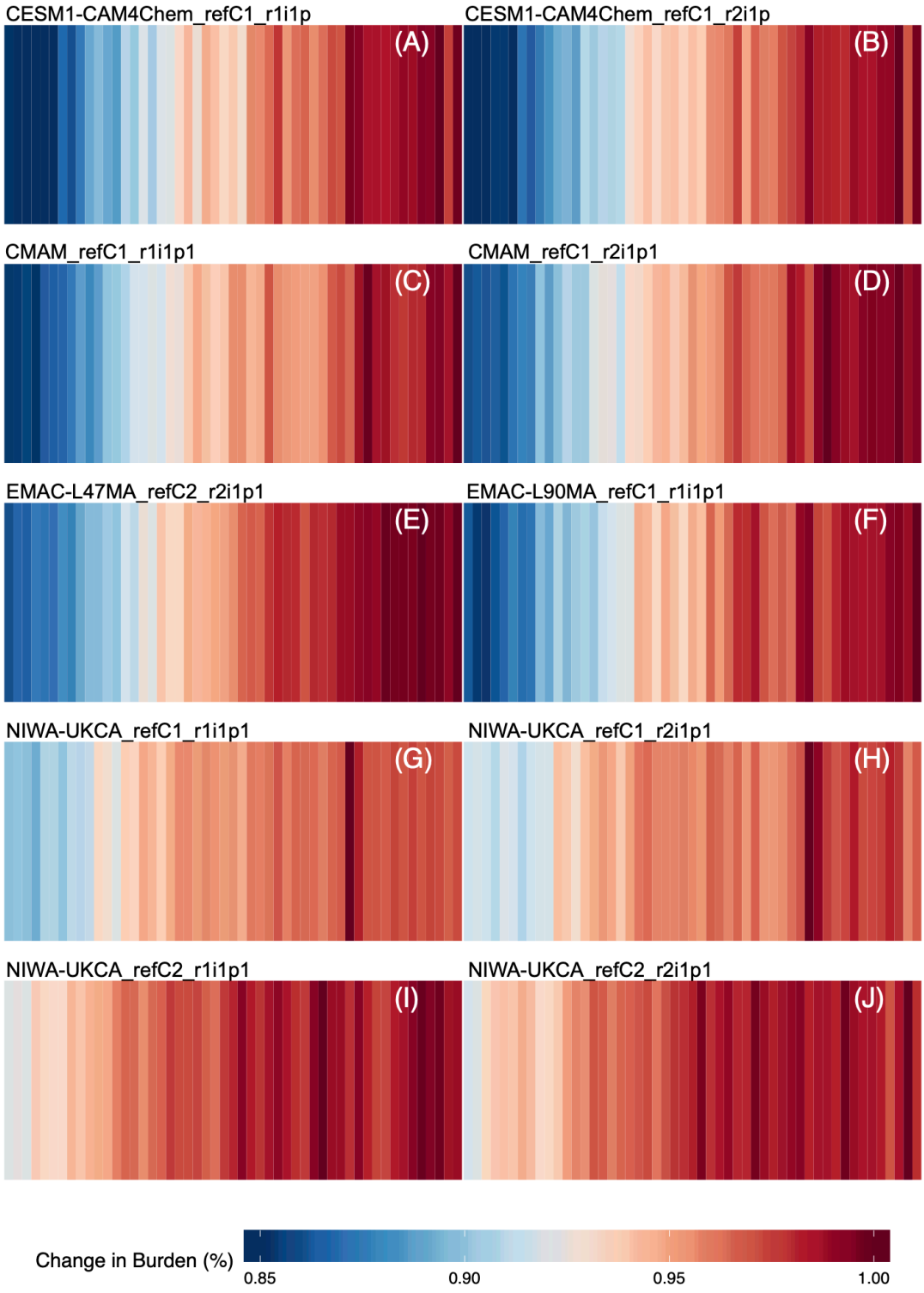

Figure 6: Changes in the tropospheric ozone burden from 1960-2010 relative to the maximum simulated burden over the five decades in a subset of the CCMI models. Each year is plotted as a horizontal coloured bar which represents the fraction of the maximum burden of tropospheric ozone over the time series. Increases in colour from blue to red denote increases in the burden. Individual model simulations are displayed in each panel. Panels (A)-(F) highlight models with significant changes in the burden over the time period of focus. A) CESM1-CAM4Chem_refC1_r1i1p1 B) CESM1-CAM4Chem_refC1_r2i1p1 C) CMAM_refC1_r1i1p1 D) CMAM_refC1_r2i1p1 E) EMAC-L47MA_refC2_r2i1p1 F) EMAC-L90MA_refC1_r1i1p1 G) NIWA-UKCA_refC1_r1i1p1 H) NIWA-UKCA_refC1_r2i1p1 I) NIWA-UKCA_refC2_r1i1p1 J) NIWA-UKCA_refC2_r2i1p1

Young et al. (2018) discuss the history of model intercomparison projects (MIPs) and highlight that CCMI coordinated the largest scale chemistry-climate modelling ozone intercomparison to study the transient evolution of ozone from 1960 through to 2100 (Morgenstern et al., 2017). The CCMI simulations allow us to investigate how well the models agree on the timing of trends in the ozone burden. Figure 6 displays time-series plots of the relative change in the tropospheric ozone burden for a subset of the CCMI models. Each panel in Figure 6 shows an individual simulation with its details (model name, experiment etc.) included in the caption. There were three core types of experiments in the CCMI experimental design: refC1, refC2 and refC1SD. Figure 6 focuses on the refC1 and refC2 simulations, which differ with respect to the time period of the simulations (refC2 runs cover 1960-2100, whereas refC1 covers 1960-2010) and the forcings used (refC1 uses observed historic sea-surface temperature fields, whereas refC2 uses modelled sea-surface fields either in a fully coupled sense or from a separate climate model run). The ozone burdens displayed in Figure 6 have been normalized to the maximum value for each simulation in the time series; this normalization is necessary as there are large absolute differences between models (~ 80 Tg) whereas the trends over the period are much smaller (~ 50 Tg). For the EMAC family of models there are not only differences in the simulations used (refC1 and refC2) but also the model the vertical resolution (47 vs 90 vertical levels) and the fact that EMAC-L47MA_revC2_r2i1p1 was simulated including an interactive deep ocean model. See Jöckel et al. (2016) for more details.

Figure 6 highlights that the CCMI models generally all show increasing burdens of ozone over the period 1960-2010 but that there is a significant amount of spread across the simulations. Broadly speaking, most models tend to agree that the tropospheric ozone burden reached a plateau around 1990-2000, and did not change significantly over the following decade. Figure 6 also highlights that whilst there is spread between simulations from a specific model (i.e. the rows), this is much smaller than the spread between simulations from different models (i.e. the columns) (see Section 4.3 for more on this).

Table 1: Comparison of net chemical production of ozone ($\Delta[O_3]/\Delta t$) computed by a subset of the CCMI models analysed in Figures 5 and 6. The values in the table reflect the decadal averages of the annual mean ozone tendency (Tg/yr). The standard deviation in the decadal mean is presented in parentheses.

Model	**1960**	**1970**	**1980**	**1990**	**2000**	**2010**
CESM1-CAM4Chem	273 (±39)	337 (±44)	405 (±33)	442 (±36)	411 (±32)	396
CMAM	52 (±15)	102 (±28)	142 (±26)	188 (±24)	185 (±15)	174
EMAC-L90MA	495 (±36)	568 (±38)	642 (±25)	683 (±26)	658 (±18)	663 (±18)
GEOSCCM	257 (±24)	309 (±21)	373 (±16)	399 (±23)	370	NA

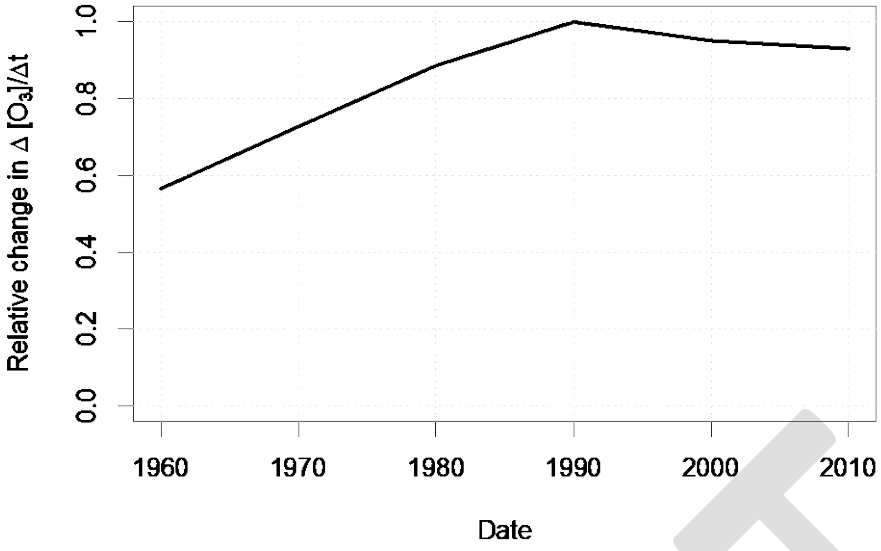

Figure 7**:** Multi model estimates (based on Table 1) of the relative changes (fractional) in the net chemical production of ozone in the troposphere as a function of time. The black solid lines show the multi model mean and the grey envelope the range of the model calculations.

Table 1 shows how the decadal average net chemical tendency (P-L or $d[O_3]/dt_{|chem}$) has changed in a subset of the CCMI models for which these data are available. This quantity diagnoses the net change in the ozone burden as a result of chemical processes only. $d[O_3]/dt_{|chem}$ is analogous to P-L, but differences can arise in the upper troposphere, where traditional diagnosis of P omits the photolysis of O_2 (see Section 3), which can become important in this region (Prather, 2009). As $d[O_3]/dt_{|chem}$ is not tied to accounting for specific reactions, this tends to give a cleaner and "pure" account of the tendency of ozone due to chemical processes. In many respects, the CCMI simulations mirror the results from the ACCMIP models (Young et al., 2013). Firstly, Table 1 in this study and Table 2 of Young et al (2013) both emphasize that, in general, fewer models provide data associated with diagnosing drivers for change in the tropospheric ozone budget than provide data on the ozone burden itself. Table 1 highlights that as with the individual budget terms themselves, there is large spread in the absolute magnitude of the net chemical tendency of tropospheric ozone as simulated in the models. EMAC-L90MA and CMAM have very large and very weak photochemical production of ozone respectively (surprising given the extremely simple tropospheric chemistry in CMAM), while CESM1-CAM4Chem and GEOSCCM fall between the two extremes. However, when comparing the relative trend in the net chemical tendency in tropospheric ozone, it becomes apparent that there is a very high level of agreement between the models. The relative trends in net chemical production over time are plotted for the CCMI models in Table 1 in Figure 7. Figure 7 shows that the relative trend in net chemical production peaked in the 1990s and has levelled off since then i.e. on average the troposphere has provided less of a chemical source of ozone since the 1990s. This result is generally consistent with the trend in the major precursor emissions. Figure 8b shows that emissions of NOx rose only slightly over the period 1990-2010 at the global scale. There is consistency therefore between Figures 5-7, which emphasize that the growth in the burden of ozone in the CCMI models was very small over the period 1960-2010, particularly over the period 1990-2010, where Figure 6 shows that for most models the tropospheric ozone burden has plateaued, and that this muted trend in the ozone burden in a large part may be attributed to a decrease in the rate of net production of ozone in the troposphere (Figure 7).

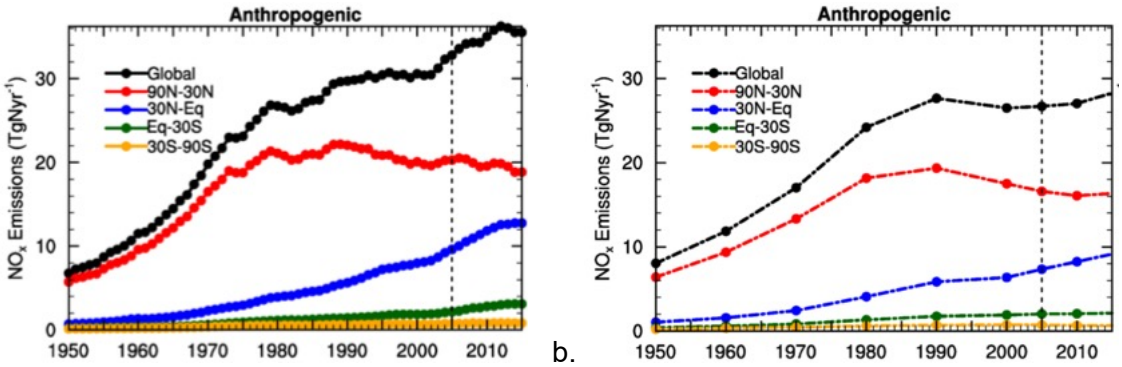

Figure 8: Anthropogenic (land based) NO_x emissions from the a) bottom-up CEDS inventory (Hoesly et al., 2017) for the period 1950-2014 and b) CMIP5 emissions inventory of *Lamarque et al*. (2010) through 2000 and the RCP8.5 scenario thereafter (as used in the CCMI simulations).

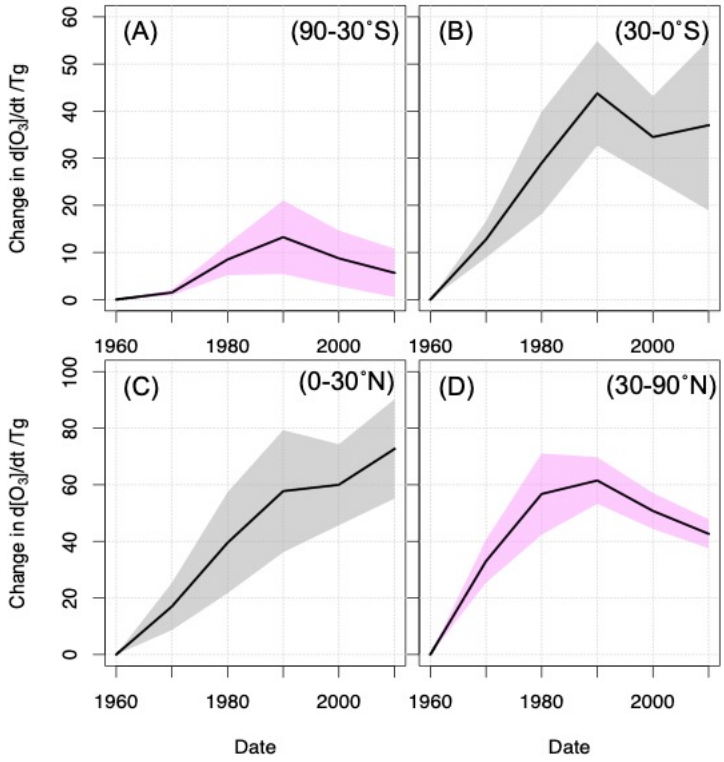

Figure 9: Changes in the decadal average ozone chemical tendency in the troposphere from 1960 to 2010 relative to the 1960 levels, as simulated by a subset of the CCMI models (see Table 1 for details). In all panels the dark line shows the multi model mean change in ozone tendency and the coloured envelope the standard deviation around the multi model mean. Panel (A) shows the relative change in the Southern Hemisphere extratropics (-90˚ to -30˚), panel (B) the Southern Hemisphere tropics (-30˚ to 0˚), panel (C) the Northern Hemisphere tropics (0˚ to 30˚) and panel (D) the Northern Hemisphere extratropics (30˚ to 90˚). Note the NH and SH data are on different y-axis scales.

To further understand the changes in the modeled net chemical production, Figure 9 shows a latitudinal breakdown of the data in Table 1. Figure 9 highlights that the picture at the global scale of a gradual decline in net production of tropospheric ozone since the 1990s (Figure 7) is masked by opposing trends at the hemispheric scale. In fact, there are some complex changes occurring in the tropospheric net chemical production that appear to be associated with the redistribution of global emissions (Figure 8). Normalized to the 1960s, the southern

hemisphere (Figure 9a-b) shows much smaller trends in $d[O_3]/dt_{|chem}$ than the northern hemisphere, where the trends are roughly doubled (note different y-axes for the two hemispheres). The general feature of Figure 9 is that there was global growth in $d[O_3]/dt_{|chem}$ from 1960-1990, but since 1990 two opposing trends are apparent: 1) at high latitudes there has been a decrease in net chemical production of ozone 2) in the tropics there has been a strong increase in net chemical production of ozone, especially in the northern tropics (Figure 9c). However, with such a small number of models, and without good observational constraints on $d[O_3]/dt_{|chem}$, it is hard to be definitive with respect to these trends, but nonetheless these data suggest the need for some further targeted studies to identify and quantify the drivers of these trends and to understand how they will affect the future tropospheric ozone burden. To a first order the main drivers seem partly linked to the variability in emissions of NO_x, as was highlighted in several previous studies (i.e. Parish et al., 2014), but as Figure 8 reflects, there is uncertainty in our understanding of these changes.

4.3 Can we project trends in the tropospheric ozone burden with confidence?

There is robust information suggesting that models have skill in simulating the burden of ozone in the troposphere (Young et al., 2013; 2018) and the results presented above further add to this body of evidence. But do we have confidence in predicting trends in the evolution of tropospheric ozone into the future? While we have the ability to diagnose some of the drivers for changes in tropospheric ozone, particularly the role of chemical production, we cannot presently constrain these drivers. Furthermore, the expected changes in the global tropospheric ozone burden over the next few decades are small and will be difficult to detect given the current observing system (Young et al., 2013; 2018; Griffiths et al., 2020). Even the ACCMIP RCP8.5 scenario, which had the largest projected increases in ozone precursor emissions of any of the representative concentration pathways, led to a predicted increase in global ozone of only 8% from 2000 to 2030 (Young et al., 2013). Given the results from *TOAR-Climate* showing large spatial heterogeneity in measured surface and airborne ozone trends over the past 15 years, the tendency for trends in a given location to be strongly influenced by meteorological variability (e.g. Bloomer et al., 2009; Lin et al., 2014; Strode et al., 2015), and the large differences in satellite measurements of ozone (Gaudel et al., 2018), it is likely that observational records longer than 30 years are required to robustly test modeled ozone trends (e.g., Barnes et al., 2016; Brown-Steiner et al., 2018).

To examine the systematic uncertainties that affect our ability to make confident predictions of the future evolution of tropospheric ozone, we have analysed tropospheric column ozone from a subset of six transient CMIP5 model simulations for three scenarios (RCP2.6, RC4.5 and RCP8.5), relying on the models that included interactive chemistry (the “CHEM” models described by Eyring et al., 2013). Figure 10 shows the future evolution of the tropospheric ozone column (in Dobson Units) (left hand panels) and the fractional variance in the response of the tropospheric column due to internal variability (i.e. short timescale fluctuations driven by natural climatic variability), scenario variability (i.e. driven by the different assumptions about emissions) and intrinsic model differences (right hand panels), following Hawkins and Sutton (2009).

Mirroring the CCMI global burden results (Figure 5), Figure 10a highlights a very modest degree of uncertainty arising from interannual variability at the global scale. A much larger uncertainty comes from the models themselves and, given that there are only three independent models, is likely underestimated compared to using a larger ensemble (e.g., if transient data were available from ACCMIP or ACCENT). This model variability is shown to be the leading source of uncertainty in near term (2000–2030) projections of ozone, but beyond that the largest source of variability comes from which of the three emissions scenarios is followed. Trivially, this term dominates due to the diverging nature of RCP8.5 compared to

the other RCPs. For RCP8.5, the increases in ozone are driven by the projected near doubling of methane concentrations relative to the year 2000, with some contribution from an enhanced net stratospheric source (ref). For the RCP2.6 and RCP4.5, precursor emissions reductions drive the long-term decreases.

With respect to near-term projections, even at the global mean scale, the model diversity alone is high enough to prevent us from distinguishing between ozone concentrations produced under the RCP8.5, RCP 4.5, and RCP2.6 emission scenarios during the period 2000-2015, for which we have a plethora of surface, aircraft, and satellite observations. As shown in Figure 10, ozone predicted by RCP8.5 is not distinct from the other scenarios until after 2020. Based on this limited set of models and three illustrative scenarios, at least another five years of observations are needed before a robust comparison between trends simulated in models and retrieved from observations can be made.

We recognize the shortcomings in this analysis, and a more robust approach will require a larger number of ensemble members from a large number of independent models, spanning a wide range of process complexity to more accurately quantify the role of structural uncertainty in projecting future ozone changes. Furthermore, including additional scenarios that more comprehensively span the range of possible futures, or taking a selective approach to which scenarios are used, would enable a better quantification of the relative role of scenario uncertainty.

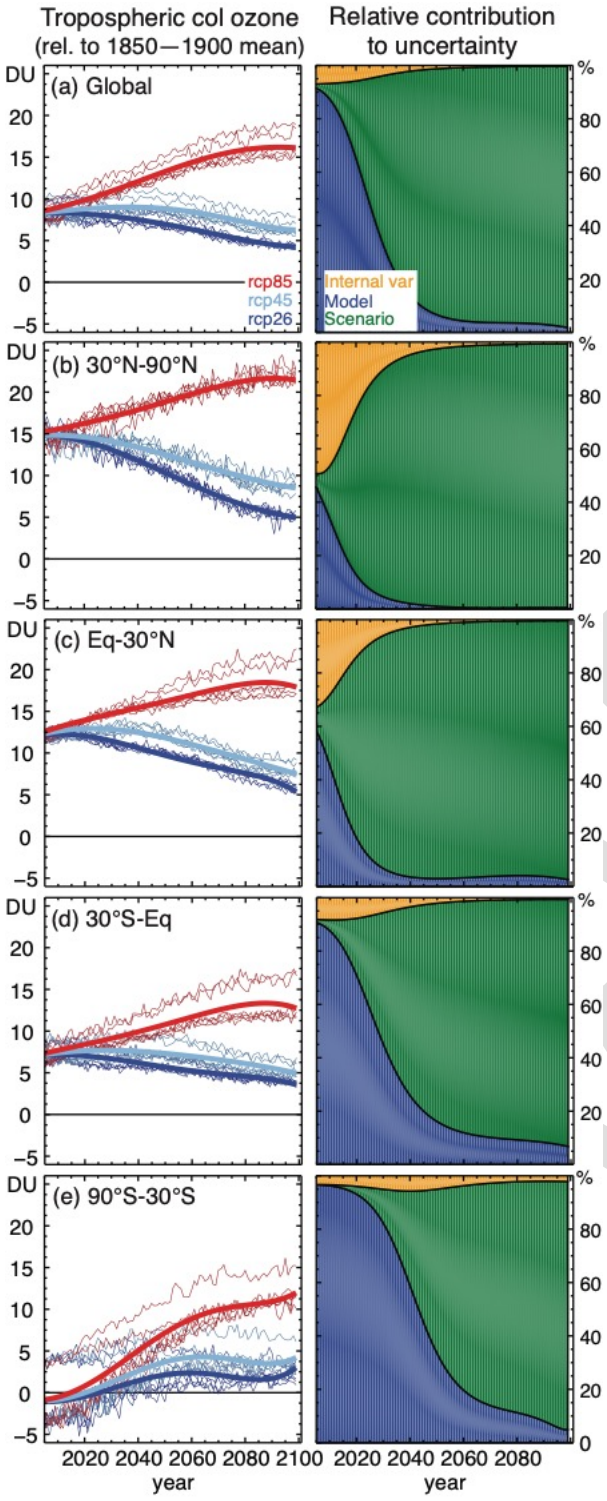

Figure 10: Projected changes in tropospheric column ozone and their uncertainties in CMIP5 models over the 21st century. The left-hand panels show the change in the modelled ozone column, the right-hand panels show the relative contribution to the uncertainty (variance) in the change in ozone (decomposed into three components). Panel (a) shows the global change, panels b-e show regional changes. The six models (CESM1-WACCM, GFDL-CM3, GISS-E2-H-p2, GISS-E2-H-p3, GISS-E2-R-p2, and GISS-E2-R-p3) represent only three independent modelling centers (NCAR, NOAA GFDL and NASA GISS), but these are the only models that provided output for more than two scenarios.

5 Challenges to modelling the budget and burden of ozone: chemical processes

Whilst model simulations are vital for projecting changes in the ozone budget, they remain incomplete, and not without error. Figure 10 highlights that the intrinsic differences between models is a large source of uncertainty in near term future projections of the burden of tropospheric ozone. As described in Section 8.2 of *TOAR-Model Performance,* one of the main sources of uncertainty in global models is their limited representation of tropospheric chemistry (Young et al., 2018). Here, we review recent studies describing a range of processes that are believed to be important for tropospheric ozone and are, to-date, not included in the types of models we have reviewed in Section 4.

5.1 Nitryl chloride photolysis

The importance of nitryl chloride ($ClNO_2$) for the simulation of ozone formation has only recently been recognized. $ClNO_2$ is formed from the reaction of dinitrogen pentoxide (N_2O_5) with chloride-containing aerosol at night. $ClNO_2$ is an important nocturnal reservoir for NO_x and atomic Cl, particularly in polluted coastal environments. Photolysis of $ClNO_2$ in the early morning regenerates NO_2 and atomic Cl, which affects oxidant photochemistry and enhances photochemical ozone production, especially in polluted environments where the concentrations of N_2O_5 precursors (nitrogen oxide radicals and ozone) are high (Osthoff et al., 2008; Sarwar et al., 2012). In environments where $ClNO_2$ yields are appreciable, overnight conversion of NO_x to $HONO_2$ (i.e., permanent NO_x loss) would be considerably reduced, leaving more NO_x available for ozone formation the next day. In addition, the reactive chlorine atoms from $ClNO_2$ photolysis can significantly enhance VOC oxidation rates – particularly in a VOC-rich areas such as Houston – in the early morning when other common oxidants (for example, NO_3, OH) are scarce (Osthoff et al., 2008; Mielke et al., 2011).

(R13) $HCl + N_2O_5 \xrightarrow{(het)} ClNO_2(g) + HONO_2(aq)$

(R14) $ClNO_2 + hv \rightarrow Cl + NO_2$

Recent studies (Riedel et al., 2012; 2014; Sommariva et al., 2014) have found that photolysis of $ClNO_2$ increases boundary layer mixing ratios of ozone by 7-30% (e.g., Riedel et al., 2014).

At a mountain-top (957 m a.s.l) site in southern China, $ClNO_2$ mixing ratios as high as 4.7 nmol/mol were observed in December 2013 (Wang et al., 2016), suggesting strong production of this compound in highly polluted regions. Wang et al. (2016) estimate that such large amounts of $ClNO_2$ were responsible for up to 40% of daytime production of ozone in the upper boundary layer (Figure 11). More effort is required to integrate this process based understanding of this chemistry into regional and global chemistry-climate models.

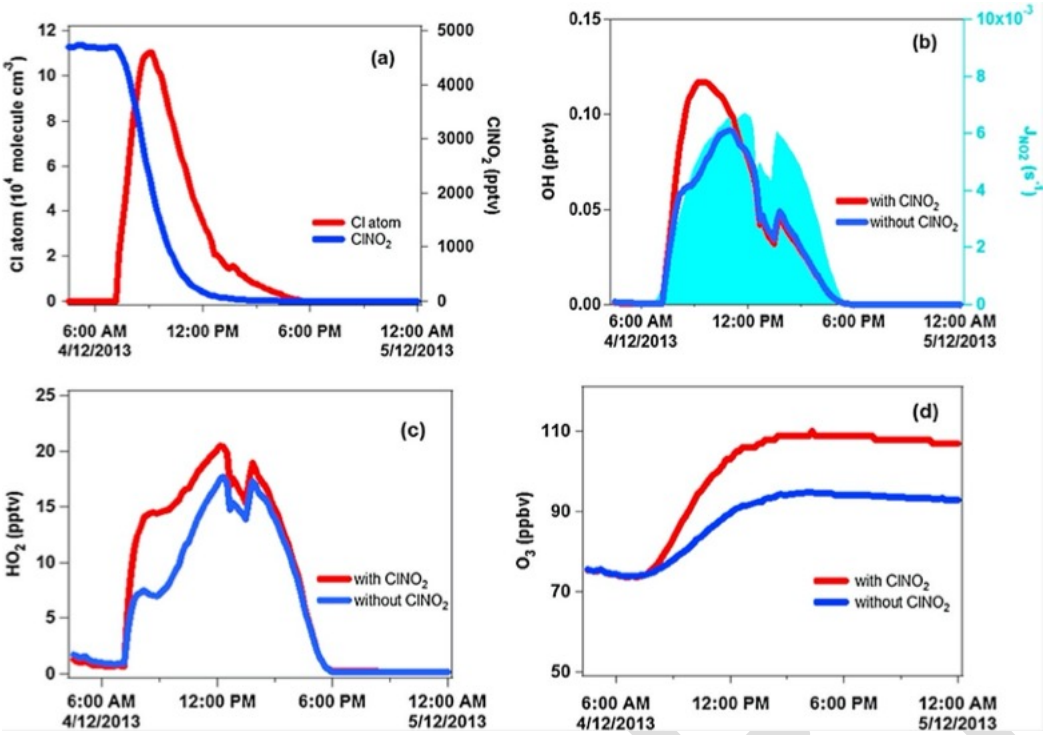

Figure 11**:** Model simulated concentrations/mixing ratios of (a) $ClNO_2$ and Cl, (b) OH, (c) HO_2, and (d) ozone during the day following plume sampling from the Mt. Tai Mao Shan site (957 m a.s.l) in Hong Kong, with and without the inclusion of $ClNO_2$ chemistry. The measured photolysis rate constant of NO_2 is shown by the light blue shading. The model was initiated with the measured concentrations of $ClNO_2$ and other relevant chemical constituents at 06:00. Figure adopted from Wang et al. (2016).

5.2 HONO photolysis

Nitrous acid (HONO) was first recognized as a morning source of OH radical by Perner and Platt (1979). Recent field studies have found much higher daytime HONO concentrations than those calculated based on the gas-phase reaction of NO+OH in both urban and rural areas, implying a missing source or sources of HONO and thus of OH during daytime (Kleffmann et al., 2005; Elshorbany et al., 2009, Li et al., 2014b; Wong et al., 2013). Kleffmann, et al., (2005) showed that HONO measured above a forest canopy close to the Jülich Research Center, Germany, was on average a factor of 10 larger than model predictions.

The search for the source of the “missing” HONO has taken place across the globe, with observations pointing to a pervasive source of HONO that does not appear to be limited to specific geographical regions or times of year. Possible additional sources of daytime HONO include heterogeneous formation on humid surfaces (Kleffmann, 2007), traffic emissions (Kurtenbach et al., 2001), gas-phase photolysis of potential precursors such as nitro-aromatic compounds (Bejan et al., 2006; Kleffmann, 2007), and biological sources in soils (Su et al., 2011; Maljanen et al., 2013; Oswald et al., 2013). The presently known sources and sinks of HONO are summarized in Figure 12. The search for the missing daytime sources is still an active area of research.

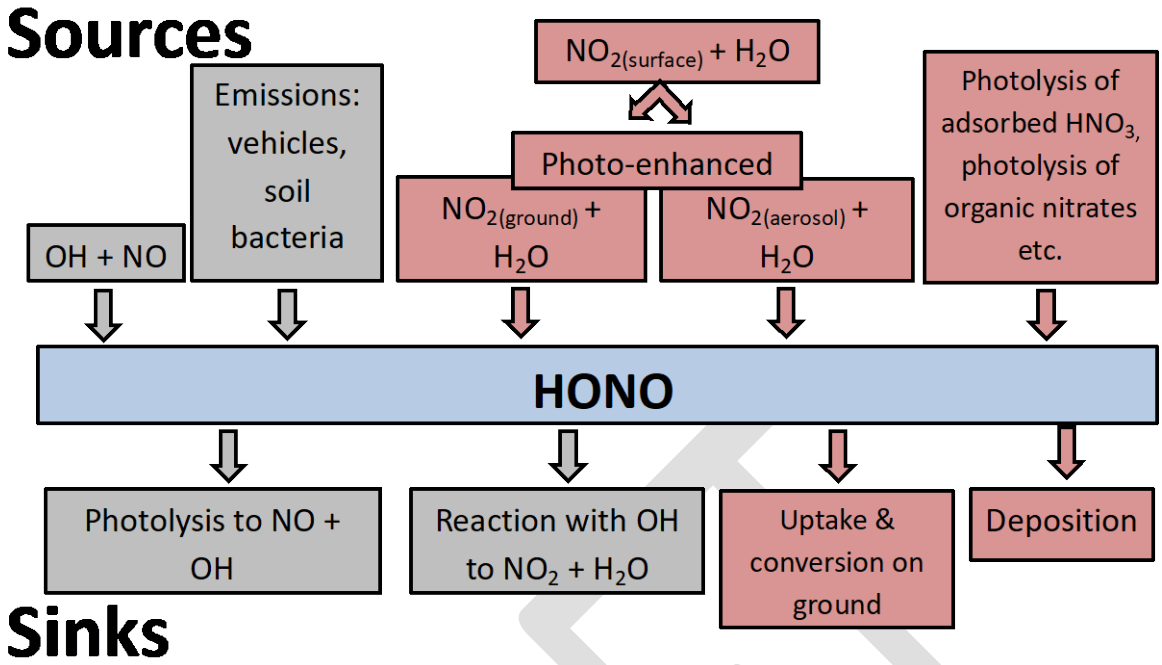

Figure 12: Diagram of major HONO sources and sinks in the troposphere. Boxes in grey represent the traditionally understood sources and sinks, boxes in red show more recently established processes (see text for references).

Models that consider the gas phase homogenous pathways of HONO formation predict low daytime HONO concentrations (Lei et al., 2004; Vogel et al., 2003). To improve simulations of the OH radical and its effect on photochemistry, more recent models have attempted to incorporate additional direct and/or secondary HONO sources (e.g. Figure 13), which improves simulation of HONO, ozone production, and secondary aerosols in polluted urban areas (Sarwar et al., 2008; Li et al. 2010; An et al., 2011; Li et al., 2011; Czader et al., 2012; Zhang et al., 2016). Nonetheless, uncertainties remain in representing these sources in the current state-of-the-art models due to simplifications in their source parameterizations and to adopting different values of key parameters. For instance, model values for the uptake coefficient on aerosol surfaces range from 10^{-6} to 10^{-4}, leading to different conclusions regarding the importance of atmospheric aerosols in HONO formation (An et al., 2013; Aumont et al., 2003; Li et al., 2010; Li et al., 2011; Sarwar et al., 2008). A recent study incorporated up-to-date HONO sources, including gaseous formation, emissions from soil bacteria, and heterogeneous formation of HONO on ocean, aerosol, urban, and vegetation surfaces into a regional chemistry transport model (WRF-Chem) (Figure 13). The improved model led to improvements in simulated HONO at a suburban site in Hong Kong and increased simulated ground-level ozone by 5-10% in a multi-day photochemical episode in southern China (Zhang et al., 2016). This result highlights the importance of accurately representing the additional HONO sources in simulations of ground-level ozone over polluted regions.

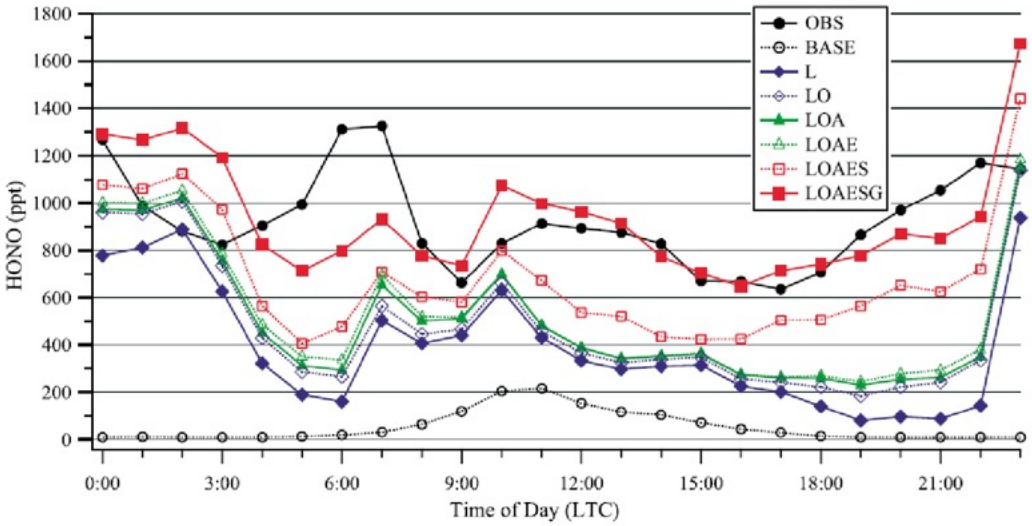

Figure 13: Observed and simulated average diurnal concentration of HONO at Tung Chung, Hong Kong during the polluted period (25–31 August 2011). OBS: observed values; BASE: Only consider HO+NO; L: heterogeneous source from land surfaces; LO: heterogeneous source from land and ocean surfaces; LOA: heterogeneous source from land, ocean, and aerosol surfaces; LOAE: heterogeneous source from land, ocean, and aerosol surfaces plus traffic emission; LOAES: LOAE plus soil emission; LOAESG: LOAES plus additional gas-phase reactions (see Zhang et al., 2016 for detail).

Ye et al. (2016) reported trace gas measurements from aircraft flights over the western subtropical North Atlantic Ocean during summer 2013. From these data, they developed a novel mechanism that links particle-bound nitrate (p-NO_3) to the production of HONO via photolysis (Ye et al., 2016). The data from Ye et al. (2016) suggest that the photolysis of p-NO_3 is orders of magnitude faster than that of gas-phase $HONO_2$. Kasibhatla et al. (2019) show that inclusion of p-NO_3 photolysis in a global model can lead to increases in ozone of 10-30% in the tropical and subtropical marine boundary layer. They find that using a photolysis rate for p-NO_3 that is 25-100 times that of gas-phase $HONO_2$ provides the best agreement with observations of NO_x and HONO at the Cape Verde Atmospheric Observatory. These values for p-NO_3 photolysis are at the lower end of those determined by Ye et al. (2016). Further work is required to quantify and understand the impacts that this process has on the tropospheric ozone budget and its expected evolution in the future.

5.3 Halogen chemistry

Ozone depletion events (ODE) were discovered in the troposphere, more specifically in the spring polar boundary layer, about three decades ago. They were first observed in the Arctic at Barrow (now called Utqiaġvik), Alaska (Oltmans, 1981) and Alert, Canada (Bottenheim et al., 1986) and later also in the Antarctic (Kreher et al., 1996). During ODEs, surface ozone levels decrease from typical values of approximately 30-40 nmol mol^{-1} to levels below the detection limit of ozone sensors, 1-2 nmol mol^{-1}. This phenomenon makes the polar regions one of the environments where chemical loss of tropospheric ozone is most efficient.

In the mid-1980s, it was recognized that the loss of polar boundary layer ozone during ODEs was coupled to halogen chemistry – primarily involving bromine and, to a lesser extent, chlorine. This was confirmed in the following decades by a myriad of observations with different measurement techniques, which identified levels of boundary layer BrO in the range of 30-40 pmol mol^{-1} (Simpson et al.,2007; Saiz-Lopez and von Glasow, 2012). To understand chemical sources and sinks of ozone in this unique environment, detailed modelling exercises were performed focusing on HO_x, NO_x, and halogen chemistry (Bloss et al., 2010) (see discussion below for details of the ozone loss catalytic cycles). The exact mechanisms of bromine activation in the polar regions remain uncertain, but experimental and modelling

studies have shown that gas exchange between the atmosphere and snow/ice surfaces plays a key role (Abbatt et al., 2012). Space-based observations of column BrO enhancements are correlated with modeled sea-salt aerosol (SSA) generated from blowing snow (Choi et al., 2018). Yang et al. (2010) found that the inclusion of blowing snow as a source of bromine in a global model reduces average modeled high latitude lower tropospheric ozone amounts by as much as 8% in polar spring. Forecasting long-term changes in tropospheric polar ozone is a formidable challenge because of the importance of air-ice exchange processes, which are subject to change as ice covered areas are modified in a warming climate.

Reactive halogens (Cl, Br and I) are also present globally in the marine boundary layer (MBL) due to several processes. It is well established that gaseous photolabile compounds (e.g. Br_2, Cl_2, BrCl, $BrNO_2$, $ClNO_2$) are produced from heterogeneous and multi-phase reactions in/on chloride- and bromide-containing particles such as sea salt (e.g. Finlayson-Pitts et al. 1989, Fickert et al. 1999, Roberts et al. 2009). Iodine is directly emitted from the ocean as HOI or I_2 (R15-16) following the ozonolysis of seawater iodide (Garland and Curtis, 1981, Carpenter et al. 2013).

(R15) $H^+ + I^- + O_3 \rightarrow HOI + O_2$

(R16) $H^+ + HOI + I^- \leftrightarrow I_2 + H_2O$

A number of volatile halocarbons (e.g. CH_2I_2, CH_2IBr, CH_2ICl, CH_3I, $CHBr_3$), with lifetimes ranging from minutes to approximately one month, are also present in the MBL (e.g. Jones et al. 2009). Elevated levels of these biogenic compounds are generally observed in coastal regions due to strong emissions from exposed macroalgae (e.g. Carpenter et al. 1999). In marine air, halogen atoms produced from the photolysis of these halocarbon precursors initiate catalytic ozone loss cycles; e.g. R17-19 and R20-23 (where X/Y = Br, Cl or I).

Cycle 1

(R17) $X + O_3 \rightarrow XO + O_2$

(R18) $Y + O_3 \rightarrow YO + O_2$

(R19) $XO + YO \rightarrow X + Y + O_2$

$2\ O_3 \rightarrow 3\ O_2$ Net

Cycle 2

(R20) $X + O_3 \rightarrow XO + O_2$

(R21) $XO + HO_2 \rightarrow HOX + O_2$

(R22) $HOX + hv \rightarrow X + OH$

(R23) $OH + CO\ [+ O_2] \rightarrow HO_2 + CO_2$

$CO + O_3 \rightarrow O_2 + CO_2$ Net

Halogen chemistry may also indirectly reduce ozone production by decreasing the $[HO_2]/[OH]$ ratio (R21/R22) and by accelerating NO_x loss via the production and the subsequent hydrolysis of halogen nitrates ($XONO_2$) in aerosol and cloud (R24, R25). In regions of elevated NO_x, VOC oxidation by Cl atoms can *enhance* ozone production (Section 2.2).

(R24) $XO + NO_2 \rightarrow XONO_2$

(R25) $XONO_2 + H_2O \rightarrow HOX + HONO_2$

Evidence for significant MBL halogen-driven ozone loss is based on a limited, but growing, body of measurements of XO radicals and their precursors, underpinned by numerical modelling on a range of scales. BrO mixing ratios of <1 to 10 pmol mol^{-1} have been reported using Differential Optical Absorption Spectroscopy in the North Atlantic (Leser et al. 2003; Saiz-Lopez et al. 2004; Mahajan et al. 2009). IO has been detected over the Atlantic (e.g. Allan et al. 2000), East Pacific (e.g. Mahajan et al. 2012) and West Pacific oceans (Großmann et al. 2013) and appears to be fairly ubiquitous in the MBL. A compilation of these and other data suggest typical daytime IO mixing ratios in the range of 0.4 – 1 pmol mol^{-1} over the open ocean (Prados-Roman et al. 2015). Measurement-constrained box model studies suggest halogen chemistry can cause substantial reductions in MBL ozone (e.g. Saiz-Lopez and Plane, 2004; Mahajan et al. 2010). At Cape Verde, a site characterized by low NO_x and thereby representative of the typical open ocean, the combined presence of BrO and IO is estimated to enhance photochemical ozone destruction by about 50% (Read et al., 2008).

Few assessments of the impact of halogens on global ozone have been performed. Available global model studies estimate that bromine decreases the tropospheric ozone burden by ~6-9% (e.g. Yang et al. 2010, Parella et al. 2012), and that bromine and iodine combined lower the ozone burden by about 14% (Saiz-Lopez et al., 2014; Sherwen et al., 2016), relative to model simulations without halogens. In the MBL, ozone loss from halogens may be comparable to that from HO_x chemistry alone (Figure 14), with iodine making the largest contribution (Saiz-Lopez et al. 2014). Such models are subject to a large range of process and parametric uncertainty, notably with respect to their treatment of halogen recycling on aerosol. A major challenge lies in capturing the effects of complex multi-phase halogen processes, given that few models explicitly consider aqueous phase chemistry, whilst retaining a reasonable degree of computational efficiency (Tost et al., 2006). Laboratory investigations of the photochemistry and fate of higher iodine oxides (I_xO_y), in particular, are needed to better quantify the role of iodine in ozone chemistry. A more comprehensive measurement database of halogen radicals and their precursors is also needed to assess the fidelity of model simulations. Measurements of BrO in the MBL, for example, are extremely sparse outside of polar regions.

Quantitatively, it is largely unknown how halogen sources have changed on decadal timescales, though levels of MBL iodine may have increased since the pre-industrial era (Prados-Roman et al. 2015), owing to increases in ozone itself (R15, R16) changing the ozone radiative forcing (Sherwen et al., 2019). Further laboratory and field characterisation of air-ocean and air-ice halogen exchange is needed to assess possible future changes to MBL halogen levels (e.g. Hughes et al. 2012) as a consequence of climate change. Overall, understanding of tropospheric halogen processes is a rapidly evolving field. Given the apparent leverage halogens possess over tropospheric ozone concentrations, research focused on addressing the deficiencies of halogen processes in model simulations of current and future ozone would be beneficial. Iglesias-Suarez et al. (2020) suggest that, while at the global scale halogen chemistry may not be enhanced in future warmer climates, increases in regional iodine driven ozone destruction in the future may help offset the ozone climate penalty and help reduce human exposure to high ozone levels in urban areas.

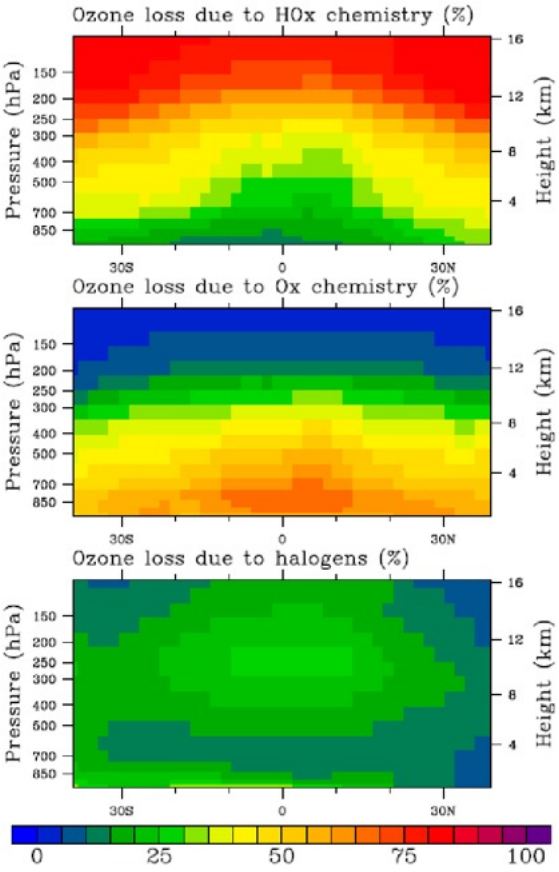

Figure 14: Percentage contribution to chemical ozone loss from HO_x, O_x and halogen photochemistry, between 40° N and 40° S. Approximately 70% of the halogen-mediated ozone loss is calculated to be driven by iodine photochemistry (after Saiz-Lopez et al., 2012).

5.4 Unconventional hydrocarbon extraction

While intense photochemical production of ozone (often resulting in hourly average ozone concentrations exceeding 150 nmol mol^{-1}) near the Earth's surface is considered a summertime, urban phenomenon, rapid diurnal photochemical production of ozone in winter with air temperatures as low as -17 ºC, has been reported (e.g., Schnell et al., 2009; Ahmadov et al., 2015; Oltmans et al., 2016). Schnell et al. (2009) found that in the vicinity of the Jonah–Pinedale Anticline natural gas field in rural Wyoming, high-pressure systems that promote cold temperatures, low wind speeds and limited cloudiness can cause hourly average ozone concentrations to rise from 10–30 nmol mol^{-1} at night to more than 140 nmol mol^{-1} shortly after solar noon (Figure 15). Under these conditions, an intense, shallow temperature inversion develops in the lowest 100m of the atmosphere during the night, which traps high concentrations of ozone precursors (i.e, VOC and NO_x) associated with the production of natural gas. During daytime, photolytic ozone production then leads to the observed high concentrations. They suggested that similar ozone production during wintertime is probably occurring around the world under comparable industrial and meteorological conditions.

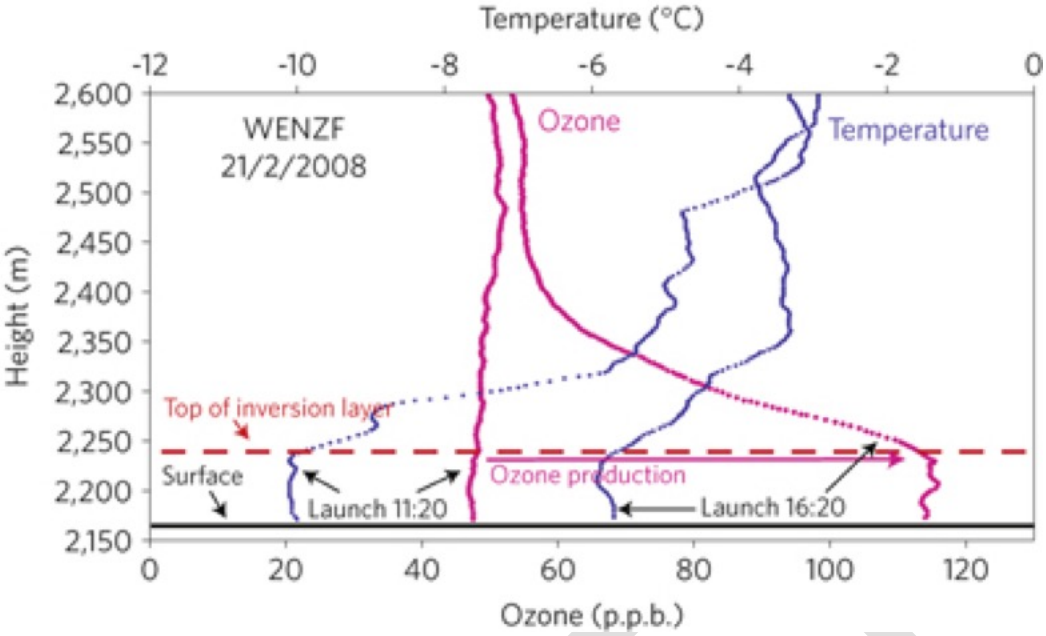

Figure 15: Ozonesonde profile 10 km north of the gas field showing ozone and temperature profiles, surface to 2,600 m, 21 February 2008. Adopted from Schnell et al., 2009.

Ahmadov et al. (2015) observed this same phenomenon over the Uinta Basin in northeastern Utah, which is densely populated by thousands of oil and natural gas wells, during winter 2013. They used a regional-scale air quality model (WRF-Chem) and high-resolution meteorological simulations and were able to qualitatively reproduce the wintertime cold pool conditions as well as the observed multi-day buildup of atmospheric pollutants and the accompanying rapid photochemical ozone formation in the Uinta Basin (Figure 16).

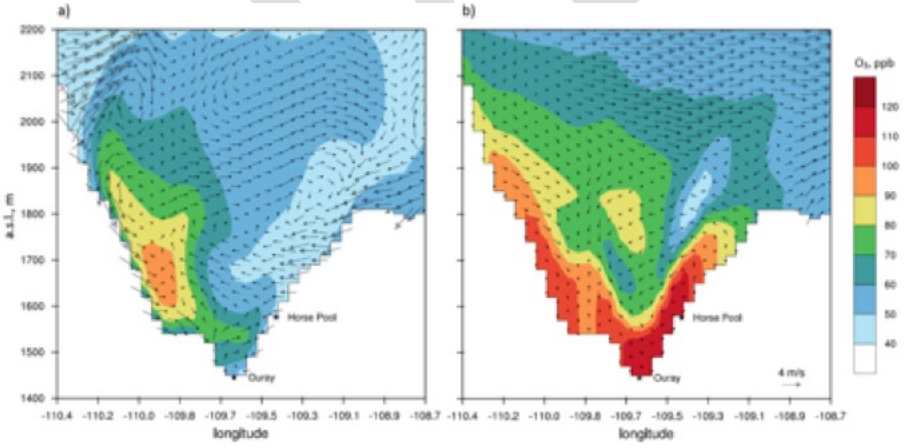

Figure 16**:** Simulated ozone distribution and wind vectors over the Uinta Basin (west-to-east direction in the WRF grid). The Horse Pool and Ouray surface stations along the cross section are shown; (a) early morning (05:00 MST), and (b) afternoon (15:00 MST) on 5 February 2013. The vertical wind components were multiplied by 100 for illustration of the wind vectors. Adopted from Ahmadov et al. (2015)

Edwards et al. (2014) concluded that photolysis of oxidized organic compounds (often containing carbonyl functional groups) from unconventional hydrocarbon extraction was the primary driver for producing radicals that lead to ozone production in the Uinta Basin. However, Archibald et al. (2018) assessed the potential impacts of unconventional

hydrocarbon extraction in the UK and concluded that there is likely to be only a small impact on ozone, even under the assumption of high levels of VOC emissions similar to those observed in locations like Uinta (Edwards et al., 2014). This disparity in the response of ozone to unconventional hydrocarbon extraction emissions seems to be a result of the geography of the emissions region. Indeed, Edwards et al (2014) show that the high levels of ozone they simulated in Uinta occur only in episodes when vertical mixing is limited and when the concentrations of the secondary products (which act as catalysts to the production of ozone) accumulate. Archibald et al. (2018) have shown that such conditions do not occur in the UK in the regions in which unconventional hydrocarbon extraction is likely to take place.

It is worth noting that whilst the impact of emissions from unconventional hydrocarbon extraction is largely a regional issue, the rapid growth in the industry could see it becoming a more widespread problem in the future if the emissions of VOCs and NO_x from hydrocarbon production are not sufficiently controlled.

5.5 Organic peroxy radicals

Peroxy radicals are formed as intermediates during the atmospheric oxidation of all organic compounds and have a rich chemistry. HO_2, CH_3O_2, and $CH_3C(O)O_2$ are the most abundant, but peroxy radicals are present in great diversity in the atmosphere (e.g. Khan et al., 2015). They react with NO, NO_2, HO_2 and other peroxy radicals, undergo unimolecular isomerization, and have lifetimes of the order of 1-100 seconds under typical atmospheric conditions. Atmospheric reactions of peroxy radicals usually proceed via more than one channel, with the different channels having different temperature, and sometimes pressure, dependencies. A large body of work has been performed over the past 30 years to elucidate the complex chemistry of peroxy radicals. While the general features of peroxy radical chemistry are established, many important details remain unclear.

From the perspective of ozone chemistry, the most important reaction of peroxy radicals is that with NO, which produces NO_2 and is responsible for photochemical ozone formation in the troposphere (see Section 3.1). Organic peroxy radicals react with NO via two pathways to give either an alkoxy radical and NO_2 or an alkyl nitrate (Arey et al., 2001).

(R1) $RO_2 + NO \rightarrow RO + NO_2$

(R26) $RO_2 + NO + M \rightarrow RONO_2 + M$

The channel that produces an alkoxy radical and NO_2 leads to radical propagation and promotes photochemical ozone formation. The channel that produces an alkyl nitrate removes radicals and NO_x and hinders local photochemical ozone formation. Alkyl nitrates can be transported and undergo photolysis and reaction with OH, releasing NO_x and promoting ozone formation in downwind locations. The organic nitrate yield increases with decreasing temperature, increasing pressure, and size of the peroxy radical (Atkinson et al., 1983; 1987; Carter and Atkinson, 1989; Harris and Kerr, 1989). Organic nitrate yields for substituted peroxy radicals are lower than those for unsubstituted alkylperoxy radicals of a similar size, particularly when the substituent is located close to the peroxy moiety, although the data are limited and the precise effects are unclear (Arey et al. 2001; Lim and Ziemann, 2005; Matsunaga and Ziemann, 2010). Early studies indicated that nitrate yields were higher for secondary radicals (RCH(OO)R') and lower for primary (RCH_2OO) and tertiary RR'R''COO) radicals (Arey et al., 2001). However, recent studies (Espada et al. 2005; Cassanelli et al. 2007) report approximately equal yields from secondary, primary, and tertiary radicals of the same size. As discussed by Calvert et al. (2015), thermal decomposition of tertiary alkyl nitrates at gas chromatogram (GC) injection temperatures may have led to an underestimation of the yields of tertiary nitrates in the early studies using GC analysis.

Data for the organic nitrate yields of peroxy radicals formed in the oxidation of important biogenic VOCs are limited and often contradictory. Reported organic nitrate yields from the

oxidation of isoprene lie in the range 4-15% (Calvert et al., 2015). Data for the organic nitrate yields for the atmospherically relevant monoterpenes and sesquiterpenes is extremely limited and uncertain. As an example, the organic nitrate yield following the HO-initiated oxidation of α-pinene has been reported as 18±9% by Nozière et al. (1999) and 1% by Aschmann et al. (2002). Clearly, given the importance of well-established branching ratios for organic nitrate formation to atmospheric models of ozone formation, there is an urgent need for further work in this area.

Peroxy radicals have been proposed to form water complexes (e.g. Aloisio and Franscico, 1998; Clark et al., 2008), and it has been estimated that approximately 10-20% of HO_2 radicals in the atmosphere exist as the HO_2•H_2O complex (Archibald et al., 2011) and that approximately 5-15% of organic peroxy radicals in the atmosphere exist as the RO_2•H_2O complex (Khan et al., 2015). Water complexed peroxy radicals may be more reactive and have different product distributions than un-complexed peroxy radicals and may be important in atmospheric ozone chemistry. An increase of approximately 12-14% in ozone production has been estimated for a two-fold increase in reactivity of RO_2•H_2O compared with RO_2 radicals (Khan et al., 2015). Definitive direct experimental studies are required to establish the atmospheric importance of reactions involving water-complexed peroxy radicals.

Finally, we note that much recent attention has focused on isomerization of peroxy radicals, where 1-5 and 1-6 H abstractions can occur rapidly and may switch the peroxy radical from primary to secondary or even tertiary, with concomitant changes in reactivity and possible organic nitrate yields (e.g. Peeters et al., 2009; Praske et al., 2018). As Praske et al. (2018) highlight, given the significant regional reductions in anthropogenic NO_x that have occurred in recent decades, the fate of the RO_2 in VOC source regions may now change from propagating NO-NO_2 conversion to the formation of highly oxygenated compounds. Further work is needed to clarify the role of peroxy radical isomerization in atmospheric chemistry and integrate this in global model studies to understand the potential implications for the tropospheric ozone budget.

5.6 Heterogeneous processes

The largest potential impact of heterogeneous processes on tropospheric ozone is via removal of N_2O_5 (a NO_x and ozone reservoir) and the hydroperoxyl radical HO_2 (Jacob, 2000). Following on from earlier work by Lelieveld and Crutzen (1990), Dentener and Crutzen showed that removal of NO_3 and N_2O_5 by aerosol particles caused decreases in ozone at the Earth's surface of up to 25%, and global decreases in ozone and OH of 9% (Dentener and Crutzen, 1993). Tie et al. (2001) studied the global impact of HO_2, N_2O_5 and CH_2O uptake on aerosols, and found a significant effect of removal of these compounds on ozone. Martin et al. (2003) showed that aerosols have a strong effect not only on chemistry through heterogeneous uptake, but also on photolysis rates, with the two processes having approximately equal impacts on OH.

Our current understanding of the uptake of N_2O_5 from laboratory measurements is based on a large and relatively coherent body of experimental data, which has resulted in a well-validated mechanism. However, there remain significant challenges in parameterizing these results in a reduced form for use in global models, primarily due to the scarcity of data on the temperature dependence of the uptake coefficient and differing determinations of the RH dependence in the literature. Stavrakou et al. (2013) chose three realistic, but different, parameterizations for N_2O_5 loss onto tropospheric aerosol. Figure 17 shows the effect of these parameterizations on rate coefficients of N_2O_5 loss, with Brown et al. (2009) representing a lower limit. A wide range of rate coefficients is simulated by the different parameterizations, corresponding to an uncertainty in the lifetime of N_2O_5 of over 3 orders of magnitude to this process, with implications for simulated ozone. A more robust parameterization is clearly required.

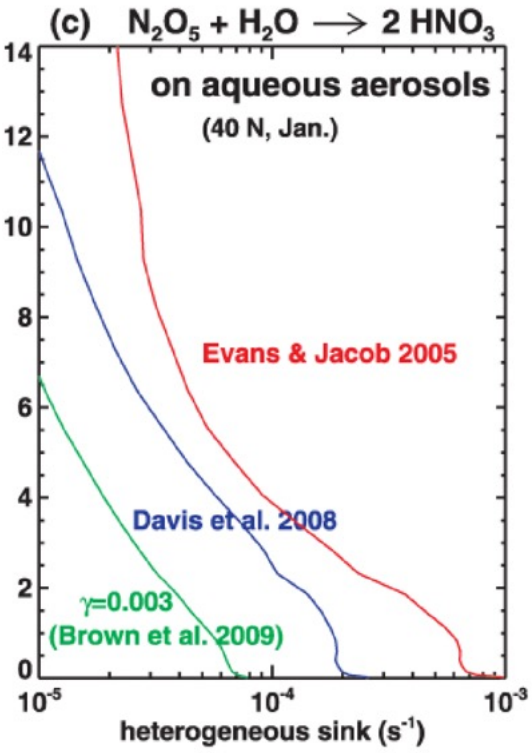

Figure 17: Calculated rate of hydrolysis of N_2O_5 onto tropospheric aerosol (the heterogeneous sink) as a function of altitude, using three different parameterizations widely used in models. The different calculations result in an order of magnitude difference in the rate of heterogeneous sink within the boundary layer.

A more significant challenge for modelling is the inclusion of the effect of nitrate aerosol composition on N_2O_5 removal. It is known that nitrate reduces the reactivity of mixed composition aerosols (Mentel et al., 1999), and the observed strong negative dependence of N_2O_5 on nitrate aerosol concentration means that two important feedbacks are missing from models. With increasing nitrate levels, 1) the contribution of N_2O_5 hydrolysis to the aerosol nitrate burden is reduced, and 2) less NO_x is removed from the gas phase. At present, an online description of the nitrate aerosol mode is not included in a large number of chemistry-climate models. A global study of the aerosol burden by Feng and Penner (2007) highlighted the contribution of N_2O_5 uptake to nitrate levels, but the use of offline (non-interactive) OH and ozone fields means that the feedback of N_2O_5 loss on oxidation rates was missing. Paulot et al. (2016) highlighted the effect of aerosol composition on uptake, noting that decreasing the uptake of N_2O_5 reduced the model bias in nitrate aerosol concentrations at the surface, providing indirect evidence for reduced uptake coefficients onto nitrate aerosol.

The simulation of nitrate aerosol presents a significant challenge, and there are large uncertainties in the expected burden under climate change scenarios. While higher temperatures decrease the nitrate aerosol burden, Pye et al. (2009) projected increases in NO_x emissions lead to a significant increase in nitrate aerosol burden, both in absolute terms and as a fraction of total aerosol amount, due to simultaneous decreases in SO_2 emission. The combined effect of increasing temperature and emissions is not yet resolved, with studies showing no significant change in nitrate aerosol (Pye et al., 2009) or modest increases (Bauer et al., 2007; Bellouin et al., 2011). At this point, the effect of nitrate aerosol on N_2O_5 has not yet been fully quantified, and, in view of the possibility of increasing nitrate aerosol burden in future climate, this should be an area of focus.

The uptake coefficient of HO_2 into aqueous aerosol, and the picture from laboratory data is unclear. Initially, uptake of HO_2 was determined to follow first-order kinetics (Cooper and Abbatt, 1996), but subsequent measurements showed pronounced second-order behavior, consistent with uptake controlled by self-reaction of HO_2 in the absence of transition metals (Thornton, 2005). On this basis, Thornton et al. (2008) proposed a parameterization that gave low values of $\gamma<0.05$ for a surface-weighted uptake coefficient in the lower troposphere. The authors conclude that the effect of temperature on uptake of HO_2 was significant and this should be included in CCM parameterizations.

More recent measurements, using lower mixing ratios of HO_2, indicate that the reaction under ambient conditions is first-order, although the fate of the HO_2 following uptake remains unclear. Taketani et al. (2008, 2009) showed that first-order loss of HO_2 is observed onto aqueous sulfate aerosol, as well as on aerosol regenerated from ambient aerosol filter samples (Taketani et al., 2012). In these experiments, large values of the uptake coefficient, $\gamma>0.1$, were observed. Uptake by solid mineral dust aerosol has been measured and shown to be less efficient but still significant ($\gamma=0.03$) (George et al., 2013). A self-reaction to form H_2O_2 now appears unlikely to be the dominant atmospheric sink, although it may certainly occur in the lab under higher gas phase HO_2 concentrations than are typically observed in the atmosphere.

Mao et al. (2010) showed that including the loss of HO_2 into aerosol improved the agreement between modelled and observed HO_2, but that including subsequent release of H_2O_2 in the model reduced the level of agreement. Although Mao et al. (2013) assessed the role of transition metal in controlling the reactivity of ambient aerosols, the mechanism for other aerosols is unclear. Li et al. (2019) applied the GEOS-Chem CTM with the current knowledge of HO_2 aerosol chemistry and found that the slowing down such sink of HO_2 due to the decrease in ambient aerosol has contributed to recent increasing trend of summer surface ozone in China. However, the lack of mechanistic understanding of the factors controlling uptake of HO_2 limits confident assessment of the impact of this heterogeneous process on ozone.

The role of mineral dust has been highlighted in lab studies as being important. The release of NO and NO_2 from adsorbed nitrate has been observed (Ndour et al., 2009). The release of OH from the photolytic reduction of H_2O adsorbed onto mineral dust seen in the laboratory (Dupart et al., 2012) is indirectly supported by observations of new particle formation following episodes of high mineral dust loading, presumably via enhanced flux of $OH+SO_2$. Observations of Dust from Thar Desert and WRF-Chem study showed that without including dust aerosols through heterogeneous chemistry and perturbation in photolysis rates, ozone loss of 16 nmol/mol and NO_y loss of about 2 nmol/mol remains unexplained (Kumar et al., 2014). It is also shown that dust could lead to ozone loss by 10-15% up to 4 km altitude region.

Several recent studies of ozone uptake indicate a significant perturbation to the oxidation pathways within the aerosol, presumably through the formation of reactive oxygen species (Shiraiwa et al., 2011). The impact of direct loss of ozone onto SOA aerosol surfaces should be examined further, as these latter processes are important to our understanding of the largely unexplored oxidative chemistry within the aerosol and to their impact on human health.

6 Challenges to modelling the budget and burden of tropospheric ozone: emissions and dynamics

As Section 5 highlights, there are numerous chemical processes which have a bearing on our ability to model the tropospheric ozone budget, and potentially its trends. Our understanding of these processes is increasing but they are still poorly represented in models (Young et al., 2018). There are also numerous uncertainties associated with transport of ozone and its precursors and their emissions that provide a challenge for understanding trends in the tropospheric ozone burden, and the details of the tropospheric ozone budget from local to global scales.

6.1 Impacts of dynamical variability on the ozone burden and budget.

While the global tropospheric ozone burden is estimated to have increased from 1960 to 2010 (Parrish et al., 2014; Young et al., 2013; Griffiths et al., 2020), the pattern of changes in ozone is complex, with ozone leveling off after ca. 2000 in some areas but continuing to grow in others (Cooper et al., 2014; Gaudel et al., 2018). Studies have shown that ozone at a given location is strongly influenced by not only emissions changes but also by variability in transport associated with large-scale dynamics. Dynamical variability is generally diagnosed from a constant emission run, while the difference between this "base" simulation and one in which emissions vary realistically with time provides the emissions-driven component. However, these types of experiments tend to be performed ad hoc by modelling groups and there is little coordinated effort to understand the role of dynamical variability in a multi model sense. Lin et al. (2014) highlight the lack of a springtime increase in ozone levels at Mauna Loa Observatory Hawaii during the 2000s – in sharp contrast to trends at other remote Northern midlatitude sites – was driven by a weakening of springtime transport of ozone-rich air from Asia to Hawaii. This occurred as a result of a predominance of La Nina-like conditions associated with the Pacific Decadal Oscillation. Long-range transport from mid-latitudes to the Arctic likewise varies strongly with the phase of the North Atlantic Oscillation (Eckhardt et al., 2003), and the cold temperatures mean that peroxyacetyl nitrate formed in mid-latitudes acts as a significant source of NO_x, accounting for 50-90% of Arctic surface ozone production during spring (Walker et al., 2012).

Even in less remote locations, long-range transport confounds attribution of observed ozone changes to changes in local emissions. Asian emissions have been shown to be a major contributor to springtime ozone increases in the Western US (e.g. Jacob et al., 1999; Zhang et al., 2008). Lin et al. (2017) estimate that transport from Asia has driven as much as 65% of the increase in surface background ozone levels during springtime that has occurred since 1990, despite a 50% reduction in Western US NO_x. Verstraeten et al. (2015) similarly found that from 2005-2010, long-range transport of pollution from China offset ~40% of the reduction in mid-tropospheric ozone that should have occurred over the Western US in response to a 21% decrease in regional NO_x emissions there. Long range transport from both Asia and North America have likewise been found to reduce the efficacy of European emissions controls (e.g. Jonson et al., 2006). In the Southern Hemisphere, large increases (20-30% $decade^{-1}$ since 1990) in mid-tropospheric ozone in the austral winter over two sites in southern Africa have been at least preliminarily attributed to increases in anthropogenic NO_x emissions throughout the hemisphere rather than any significant change in biomass burning (Thompson et al., 2014). On the other hand, a more recent study by Lu et al. (2019) found that the increasing tropospheric ozone over 1990-2015 in the extratropical Southern Hemisphere is not mainly due to increases of anthropogenic emissions. Instead, they attribute the trend to changes in the meridional circulation driven by the poleward expansion of the Southern Hemisphere Hadley circulation, again highlighting the importance of large-scale dynamics to the tropospheric ozone budget.

Variability in STT also plays an important role in tropospheric ozone variability and trends (Hess and Zbinden, 2013), leading to changes in tropospheric ozone levels in the northern mid-latitudes of around 2%, approximately half of the interannual variability (Neu et al., 2014). An increase in STE in 2009-2010 associated with a combination of El Niño and easterly shear in the stratospheric quasi-biennial oscillation was calculated as being responsible for half of the net increase in mid-tropospheric ozone over Eastern China from 2005-2010, with the other half driven by local emissions increases (Verstraeten et al., 2015).

As Figure 10 shows, in the near-term at the regional scale we can expect that dynamical variability will make the greatest relative contribution to the uncertainty of the tropospheric mean ozone column. But key unresolved questions remain regarding the current generation of chemistry-climate models' ability to accurately capture this process, and how changes in climate will affect dynamical variability. We suggest further work be performed to better understand these questions from a multi model perspective.

6.2 Impacts of emission uncertainty on the ozone budget and burden

Whilst projects like ACCMIP, CCMI and AerChemMIP coordinate modelling efforts by providing common sets of emissions data for groups to use, these activities represent an ensemble of opportunity. As a result, modelling groups often make pragmatic decisions that result in teams using different emissions datasets within each model (Young et al., 2013; 2018). Differences in emissions in models may be a key reason for differences in the modelled simulations of the historic changes in the ozone budget and burden (Figure 5-7) and its future evolution (Figure 10). A key issue with emission inventories is the assessment of their uncertainty. Despite the complexity of inventories, systematic uncertainty estimates on these datasets are often not reported. Inventory developers have begun to report uncertainty estimates, and this has become good practice for national greenhouse gas inventories (Penman et al. 2000). Other approaches, including comparisons of different inventories and comparisons of inventory emission ratios with ambient enhancement ratios, have been used for estimating emissions uncertainty (e.g., Hassler et al 2016). Here we consider some examples of these different types of emissions uncertainty estimates, along with a discussion of the possible impacts on ozone simulations. We emphasize that there is no single definitive evaluation method regarding uncertainties on emissions of ozone precursors on a global or national scale. We recommend that the development of such a method be a key component of future MIPS.

Hoesly et al. (2017) summarize a number of existing studies that assess uncertainty on ozone precursors in global and regional inventories that inform the CMIP6 historical (1750-2014) inventory dataset produced by the Community Emissions Database System (CEDS). From their analysis, a few general statements can be made: i) Uncertainties in NOx, CO and VOC emissions are higher than those in CO_2 from fossil fuel combustion; ii) Uncertainties on ozone precursor emissions from specific sectors such as mobile sources can be as high as a factor of two, even in industrialized nations with sophisticated inventory development efforts; iii) Uncertainties vary across sectors, with some sectors having much higher uncertainties due to the manner in which estimates are derived and the lack of independent estimates; iv) Global emissions estimates tend to be less uncertain than those of any particular region and v) More recent estimates (for example, in the past two decades) are generally less uncertain than those from earlier periods.

Emissions inventories are always a few years out of date. Present day emissions are very difficult to estimate, because the main drivers in such estimates, i.e. fuel use, energy production and consumption, etc., are generally available with delays of up to three years at the global scale and of at least two years for country-level data and emission factors which may be derived for a specific country, or city are often used in other regions with missing data. It is therefore very difficult to estimate the most recent trends in emissions and to provide accurate scenarios for future years.

For example, as a result of the rapid industrial growth of China and the development of several densely populated areas, several studies have shown that the emissions of all ozone

precursors significantly increased in China over the past 4-5 decades (Zhang et al., 2007, Kurokawa et al., 2013; Granier et al., 2016) but have recently started to decrease (Krotkov et al., 2016; de Foy et al., 2016). Figure 18 shows the evolution of the emissions of NO_x between 1960-2014 in China from different global and regional emission inventories with all inventories showing the emissions of NO_x constantly, and fairly consistently, increasing up to 2012. However, the more recent observations of decreases in NO_x are not yet available in a multi-inventory sense and highlight the challenge of developing an inventory for a region undergoing rapid change in emissions.

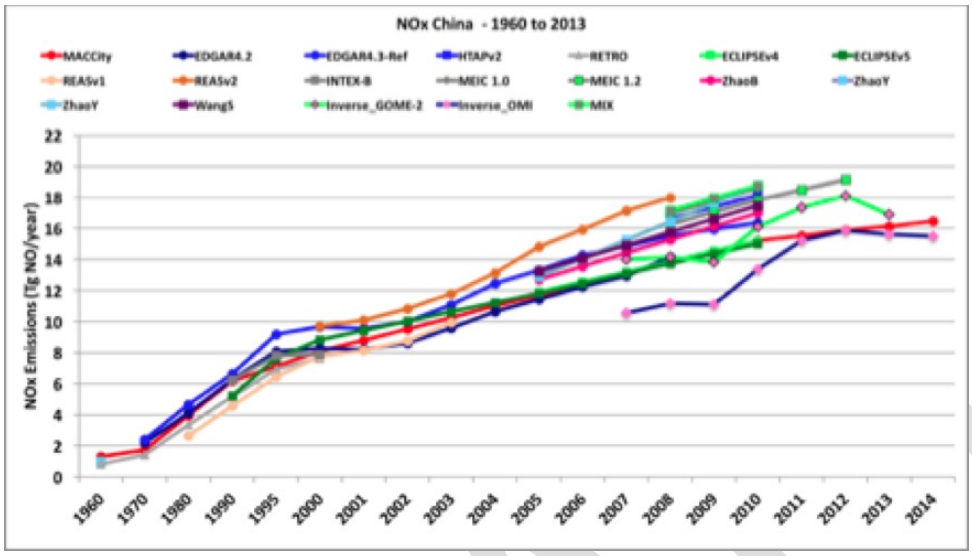

Figure 18: Evolution of the NOx emissions in China from 1960 from different inventories. The emissions optimized through inverse modeling (MPoloG and MPolov5) are also shown (adapted from Granier et al., 2016).

A further uncertainty in the modelling of ozone chemistry is introduced from partitioning of VOC emissions into individual species. This is a complex task which is likely to have particularly large impacts on understanding trends in ozone at the regional scale. von Schneidemesser et al. (2015) highlighted how simulated tropospheric ozone depends on the precise VOC speciation in different inventories, and found that modeled ozone had a greater sensitivity to VOC emissions speciation than to the choice of chemical mechanism used in the simulation. Further research using more realistic chemical-transport models is needed to understand the importance of VOC emissions speciation for determining global and regional budgets of tropospheric ozone.

7 Conclusions and outlook

TOAR has provided an unprecedented review of our understanding of the recent trends in tropospheric ozone and enabled a legacy of new research that will maximize the potential of the TOAR database (Schultz et al., 2017). Furthermore, the insight gained from understanding contemporary (Gaudel et al., 2018) and historic (Tarasick et al., 2019) measurements of tropospheric ozone will enable improved evaluation of model performance (Young et al., 2018).

In addition, TOAR has provided a timely opportunity to reflect on what we've learned since the publication of the 2003 IGAC atmospheric chemistry review (Brasseur et al., 2003), and what we still don't know. In the following sections we review where we have made progress, where uncertainty still remains and some recommendations for future research areas.

7.1 Known uncertainties:

There have been major changes in the locations of anthropogenic ozone precursor emissions; with big reductions in OECD countries counteracted by large increases in non-OECD

countries. This is especially true of Asia, but also in Africa and South and Central America. The impact of this shift in emissions has been shown to be a key driver for increases in the total burden of ozone (Zhang et al., 2016). If emissions of NOx continue to increase in the tropics and subtropics over the next few decades, as technological development and population increases (Jones and O'Neil 2016), we can expect an increase in the tropospheric ozone burden over the next few decades (Kumar et al., 2018). We still don't fully understand the impacts of the uncertainty in emissions, and future work should systematically target this knowledge gap.

Through the reassessment of historical trends (Tarasick et al., 2019) and very recent isotopic constraints (Yeung et al., 2019) we are in a strong position to challenge the validity of some of the early measurements of ozone that would suggest ozone more than doubled between the late 19th century and present-day (i.e. those made at Montsouris, France). Replicating these very low ozone values was a huge challenge to modellers but it now appears that the modelled increase in the burden of tropospheric ozone of around 30% since the pre-industrial (Figure 5) is consistent with observational estimates over shorter time periods. In addition to these historic observations there has been a step change in the ability to understand tropospheric ozone with satellites. Gaudel et al. (2018) reviewed much of this work in TOAR-Climate, but since then recent work has highlighted the power of combining satellite datasets to understand trends in tropospheric ozone (Ziemke et al., 2019). In the next decade, planned satellite measurements of ozone and ozone precursors will be acquired from both low earth orbit (LEO) and geostationary orbit (GEO). LEO observations such as TropOMI on ESA/Sentinel 5P (Beirle et al., 2019) and IASI-NG on Eumetsat/MetOP will continue the global monitoring of the atmosphere obtained by existing LEO satellites, while the GEO perspective will provide temporal coverage that is not possible from LEO over continental-scale observing domains. The new GEO satellite instruments such as NASA/TEMPO (North America), ESA/Sentinel-4 (Europe) and the Korean GEMS (East Asia) should be able to help us quantify diurnal changes in precursor emissions and chemical production of ozone. Both LEO and GEO observations will have finer spatial resolution (< 10 km) than existing assets to aid in distinguishing emissions, chemistry and transport processes. These new measurements will substantially improve air quality prediction along with our understanding of atmospheric composition.

7.2 Outstanding science questions related to understanding the ozone budget:

Whilst this is not a major focus of TOAR, as we highlighted in Section 6.1 and Young et al. (2018) discussed, there is a strong body of evidence which highlights that over the last 15 years we have made great progress in understanding the role of natural climate variability and climate change on tropospheric ozone. CCMs provide a great opportunity for us to explore these interactions and the new AerChemMIP and CMIP6 projects (Collins et al., 2017) will provide the community with larger volumes of data to analyse than ever before.

The discovery of $ClNO_2$ as a ubiquitous reservoir of chlorine and NOx (Mielke et al., 2011) has potential to change our current understanding of the role of N_2O_5 chemistry in the troposphere. Few global modelling studies have been performed to understand the impacts on trends in tropospheric ozone with or without this chemistry, and further studies are necessary. More generally the role of halogens on tropospheric composition is still highly uncertain, but their influence on concentrations and trends may be profound.

The discovery of a significant role for peroxy radical isomerization reactions has also been a breakthrough in the last few decades. It is now widely recognized that the fate of peroxy

radicals in the troposphere is not limited to bimolecular reactions. Indeed, for many peroxy radicals these unimolecular H-shifts may out compete bimolecular reactions in the troposphere. But what role this chemistry plays on the ozone budget and burden is still not completely understood. The most recent isoprene chemistry schemes all include H-shifts (Archibald et al., 2011; Bates and Jacob, 2019b) and suggest that these reactions result in large increases in OH and decreases in ozone in the tropical lower troposphere (Squire et al., 2015; Bates and Jacob 2019b).

The formation of $HONO_2$ as a product from the reaction between HO_2 + NO (Butkovskaya et al., 2005; 2007; 2009) has been shown in modelling studies to have a potentially significant impact on the tropospheric ozone burden (Søvde et al., 2011; Gottschaldt et al., 2013; Archibald et al., 2019). Independent laboratory studies are required to verify this channel in the reaction and to better understand the role of water vapour in this and other peroxy radical reactions.

In spite of the huge role it plays on the ozone budget, relatively little work has focused on the deposition sink of ozone in recent years. As we have reviewed in section 2.1, changes in the deposition of ozone are likely to have significantly impacted historic trends and are likely to continue to do so at the regional scale (Lin et al., 2019) and in particular as land use is altered in the wake of the impacts of climate change and the drive to net zero emissions.

7.3 Recommendations for the future:

In TOAR-Ozone Budget we have reviewed the literature and have highlighted the significant progress in modelling the processes that control the ozone budget. However, progress in constraining these processes has been poorer. We still don't know if a model with an NCP of 500 Tg is more accurate than a model with an NCP of 100 Tg. A huge focus continues to be in the evaluation of simulations around observational campaigns fixed in time. Less work has focused on evaluating the interannual variability and trends in ozone over time – in part owing to limited data on ozone trends in the troposphere. We see two opportunities for work supported by TOAR in this area; firstly by helping to focus efforts on understanding trends and model sensitivities, secondly in encouraging wider use of new constraints when evaluating ozone. For example the work of Yeung et al. (2019) on oxygen isotopes highlights novel approaches to constraining changes in ozone since the pre-industrial, which other modelling teams and observational teams can take forward.

Do we have sufficient data for understanding trends in the ozone burden and budget? As we've shown here and in *TOAR-Model Performance* (Young et al., 2018), there have been a large number of model simulations performed by the community, especially through model intercomparison projects. But much less of the data generated has been made available to the community, particularly in the area of enabling process-oriented model evaluation and quantification of the ozone budget and its changes. In CCMI and AerChemMIP many more models provided output on their simulated tropospheric ozone trends but less data on what drives them. Excellent work has been performed to understand individual models but with such large spread in the few model budgets available, what can we tell from these individual studies? How do we increase the accessibility and interoperability of ozone process data? The new ideas around definitions of the ozone budget (Edwards and Evans, 2017; Bates and Jacob, 2019) provide new opportunities to better understand the role of emissions and the stratosphere, but at a potentially large cost in having to output more data.

So far, we have spent a huge amount of resources on increasing the detail in the representation of processes in models and their resolution. However, the biases against observations of tropospheric ozone have not changed significantly over the last two decades. Formal assessments of model uncertainty are difficult, but when performed even on a small

part of the model (for example on the impact of rate constant uncertainty see Section 4.1) these are often large. Some of these uncertainties could be reduced by further focused laboratory studies, improved emission inventories, etc However, there may also be a need for new measures of success? Such as enabling chemical interactions with strong feedbacks on the Earth system (i.e. through improved coupling of the reactive nitrogen inventory in the atmosphere with the terrestrial biosphere)? Do we need an ozone equivalent of equilibrium climate sensitivity that can be used to summarise performance? One can argue that in general more research is needed to characterise how our understanding of the budget of ozone simulated in models is evolving over time. Are we getting any better at modelling tropospheric ozone? One suggestion is the adoption of a core tropospheric ozone simulation with prescribed emissions of ozone precursors and meteorology that will enable modelling groups to more precisely identify the role of changes in the chemistry of ozone included in models. This methodology builds upon and aspires to emulate the success of the Diagnostic, Evaluation and Characterization of Klima (DECK) experiments, which are used in the CMIP (Eyring et al., 2016). The DECK experiments enable the climate modelling community to understand how changes to climate models impact metrics such as climate sensitivity and include, for example, a 100-year simulation with increasing CO_2 at 1%/yr. A tropospheric ozone "DECK" experiment would require sufficient buy-in from the community but could be used to resolve some of these outstanding questions.

We have made a lot of progress in understanding the burden and budget of ozone in the troposphere, and with the advent of the new generation of GEO and LEO satellites, the availability of more model simulations from CMIP6 than ever before, and an improved understanding of recent and historic trends in ozone observations, enabled by *TOAR*, we are in a great position to close out some of the remaining questions and reduce the uncertainty in predictions of future tropospheric ozone.

Contributions

ATA, JN and YE lead the writing and editing of the paper with significant contributions from ORC, TJW, VN and PJY. All co-authors contributed to reviewing and editing the manuscript and leading specific areas.

Contributed to conception and design: ATA, JN, YE

Contributed to acquisition of data: BJ, PTG, YMS, ATA, PJY, VN.

Contributed to analysis and interpretation of data: ATA, JN, ORC, ASL,

Drafted and/or revised the article: All co-authors contributed to the drafting and revision of the article.

Acknowledgements

ATA and PJY would like to acknowledge the IGAC CCMI project, ACCMIP and CMIP5 for providing simulations which underpinned the analysis in Section 4. VN would like to acknowledge the CEDS emissions inventory developed in support of the CMIP6 shown in Figure 8.

Funding information

ATA and PTG would like to acknowledge support from NCAS. YE would like to acknowledge support from the NSF AGS awards # 1900795 & 1929368. TW acknowledges support from the Hong Kong Research Grants Council (T24-504/17-N) and the National Natural Science Foundation of China (91844301). ASL thanks European Executive Agency under the European Union's Horizon 2020 Research Innovation programme (Project 'ERC-2016-COG 726349 CLIMAHAL'). RH is supported by a NERC Independent Research Fellowship (NE/N014375/1).

Competing interests

None to declare.

References:

Ahmadov, R., McKeen, S., Trainer, M., Banta, R., Brewer, A., Brown, S., Edwards, P. M., de Gouw, J. A., Frost, G. J., Gilman, J., Helmig, D., Johnson, B., Karion, A., Koss, A., Langford, A., Lerner, B., Olson, J., Oltmans, S., Peischl, J., Pétron, G., Pichugina, Y., Roberts, J. M., Ryerson, T., Schnell, R., Senff, C., Sweeney, C., Thompson, C., Veres, P. R., Warneke, C., Wild, R., Williams, E. J., Yuan, B., and Zamora, R.: Understanding high wintertime ozone pollution events in an oil- and natural gas-producing region of the western US, Atmos. Chem. Phys., 15, 411-429, doi:10.5194/acp-15-411-2015, 2015.

Anderson et al.: A pervasive role for biomass burning in tropical high ozone/low water structures, doi: 10.1038/ncomms10267, 2015.

Andersson, C. and Engardt, M., 2010. European ozone in a future climate: Importance of changes in dry deposition and isoprene emissions. Journal of Geophysical Research: Atmospheres, 115(D2).

Archibald, A. T., et al. (2011), Impacts of HOx regeneration and recycling in the oxidation of isoprene: Consequences for the composition of past, present and future atmospheres, Geophys. Res. Lett., 38, L05804, doi:10.1029/2010GL046520.

Archibald, A. T., O'Connor, F. M., Abraham, N. L., Archer-Nicholls, S., Chipperfield, M. P., Dalvi, M., Folberth, G. A., Dennison, F., Dhomse, S. S., Griffiths, P. T., Hardacre, C., Hewitt, A. J., Hill, R., Johnson, C. E., Keeble, J., Köhler, M. O., Morgenstern, O., Mulchay, J. P., Ordóñez, C., Pope, R. J., Rumbold, S., Russo, M. R., Savage, N., Sellar, A., Stringer, M., Turnock, S., Wild, O., and Zeng, G.: Description and evaluation of the UKCA stratosphere-troposphere chemistry scheme (StratTrop vn 1.0) implemented in UKESM1, Geosci. Model Dev. Discuss., https://doi.org/10.5194/gmd-2019-246, in review, 2019.

Atlas, E. and Ridley, B.A. (1996) The Manuna Loa Observatory Photochemistry Experiment: Introduction. Journal of Geophysical Research, 101, 14531–14541.

ATMOFAST: Atmosphärischer Ferntransport und seine Auswirkungen auf die Spurengas-konzentrationen in der freien Troposphäre über Mitteleuropa (Atmospheric Long-range Transport and its Impact on the Trace-gas Composition of the Free Troposphere over Central Europe), Project Final Report, T. Trickl, co-ordinator, M. Kerschgens, A. Stohl, and T. Trickl, subproject co-ordinators, funded by the German Ministry of Education and Research

within the programme “Atmosphärenforschung 2000“, http://www.trickl.de/ATMOFAST.htm, 130 pp., 2005 (in German); revised publication list 2012

Auer, R. (1939) Über den Faglichen Gang des Ozongehalts der bodennahen Luft. Beitraege Zur Geschichte Der Geophysik and Kosmischen Physik, 54, 137−145.

Auvray, M, and I. Bey (2005), Long-range transport to Europe: Seasonal variations and implications for the European ozone budget, J. Geophys. Res, D11303, doi: 10.1029/2004JD005503, 22 pp.

Ayers, G.P., Penkett, S.A., Gillett, R.W., Bandy, B., Galbally, I.E., Meyer, C.P., Elsworth, C.M., Bentley, S.T. and Forgan, B.W. (1992) Evidence for photochemical control of ozone concentrations in unpolluted marine air. Nature, 360, 446–448.

Banerjee, A., Amanda C. Maycock, Alexander T. Archibald, N. Luke Abraham, Paul Telford, Peter Braesicke, and John A. Pyle, Drivers of changes in stratospheric and tropospheric ozone between year 2000 and 2100, Atmos. Chem. 21Phys., 14, 9871-9881, https:// doi:10.5194/acp-16-2727-2016, 2016.

Banerjee, A., Archibald, A. T., Maycock, A. C., Telford, P., Abraham, N. L., Yang, X., 19Braesicke, P., and Pyle, J. A.: Lightning NOx, a key chemistry–climate interaction: impacts of 20future climate change and consequences for tropospheric oxidising capacity, Atmos. Chem. 21Phys., 14, 9871-9881, https://doi.org/10.5194/acp-14-9871-2014, 2014

Barnes, E. A., Fiore, A. M., and Horowitz, L. W. (2016). Detection of trends in surface ozone in the presence of climate variability. J. Geophys. Res. Atmos. 121, 6112–6129. doi:10.1002/2015JD024397.

Barrie, L.A., Botteheim, J.W., Schnell, R.C., Crutzen, P.J. and Rasmussen, R.A. (1988) Ozone destruction and photochemical reactions at polar sunrise in the lower Arctic atmosphere. Nature, 334, 138−141.

Bates, K. H., and Jacob, D. J.. (2019), An expanded definition of the odd oxygen family for tropospheric ozone budgets: Implications for ozone lifetime and stratospheric influence. Geophys. Res. Lett., 46. https://doi.org/10.1029/2019GL084486

Bates, K. H. and Jacob, D. J.: A new model mechanism for atmospheric oxidation of isoprene: global effects on oxidants, nitrogen oxides, organic products, and secondary organic aerosol, Atmos. Chem. Phys., 19, 9613–9640, https://doi.org/10.5194/acp-19-9613-2019, 2019b.

Beekmann, M., G. Ancellet, S. Blonsky, D. De Muer, A. Ebel, H. Elbern, J. Hendricks, J. Kowol, C. Mancier, R. Sladkovic, H. G. J. Smit, P. Speth, T. Trickl, P. Van Haver (1997) Regional and Global Tropopause Fold Occurrence and Related Ozone Flux across the Tropopause, J. Atmos. Chem., 28, 29-44.

Beirle, S., Borger, C., Dörner, S., Li, A., Hu, Z., Liu, F., Wang, Y. and Wagner, T., 2019. Pinpointing nitrogen oxide emissions from space. Science advances, 5(11), p.eaax9800.

Bethan, S, G. Vaughan, C. Gerbig, A. Volz-Thomas, H. Richer and D. A. Tiddeman (1998) Chemical air mass differences near fronts, J. Geophys. Res., 103, 13413-13434.

Bey, I., D. J. Jacob, J. A. Logan and R. M. Yantosca (2001) Asian chemical outflow to the Pacific in spring: Origins, pathways, and budgets, J. Geophys.-Res., 106, 23091-23113.

Bithell, M., Vaughan, G., and Gray, L. J. (2000) Persistence of stratospheric ozone layers in the troposphere, Atmos. Environ., 34, 2563-2570.

Bloomer, B. J., J. W. Stehr, C. A. Piety, R. J. Salawitch, and R. R. Dickerson (2009), Observed relationships of ozone air pollution with temperature and emissions, Geophys. Res. Lett., 36, L09803, doi:10.1029/2009GL037308.

Boersma et al. (2011), An improved retrieval of tropospheric NO2 columns from the Ozone Monitoring Instrument, Atmos. Meas. Tech., 4, 1905-1928.

1833 Bowman, K., and D. K. Henze (2012), Attribution of direct ozone radiative forcing to spatially
1834 resolved emissions, Geophys. Res. Lett., 39, L22704, doi:10.1029/2012GL053274

1835 Brasseur, G.P., Hauglustaine, D.A. and Walters, S. (1996) Chemical compounds in the remote
1836 Pacific troposphere: Comparison between MLOPEX measurements and chemical transport
1837 model calculations. Journal of Geophysical Research, 101, 14795–14813.

1838 Brasseur, G.P., Prinn, R.G., Pszenny A.A.P. (Eds.). (2003). Atmospheric Chemistry in a
1839 Changing World. Springer Verlag, Heidelberg, Germany. IBSN: 978-3-642-62396-7. p 300.

1840 Brewer, A.M. (1949), Evidence for a world circulation provided by the measurements of helium
1841 and water vapor distribution in the stratosphere. Quarterly Journal of the Royal Meteorological
1842 Society, 75, 351–363.

1843 Brown-Steiner, B., Selin, N. E., Prinn, R. G., Monier, E., Tilmes, S., Emmons, L., et al. (2018).
1844 Maximizing ozone signals among chemical, meteorological, and climatological variability.
1845 Atmos. Chem. Phys. 18, 8373–8388. doi:10.5194/acp-18-8373-2018.

1846 Butkovskaya, N.I., Kukui, A., Pouvesle, N., and Le Bras, G.: J. Phys. Chem. A, 109, 6509,
1847 2005.

1848 Butkovskaya, N., Kukui, A., and Le Bras, G.: J. Phys. Chem. A, 111, 9047, 2007.

1849 Butkovskaya, N., Rayez, M.-T., Rayez, J.-C., Kukui, A., and Le Bras, G.: J. Phys. Chem. A,
1850 113, 11327, 2009.

1851 Cammas, J.-P., Jacoby-Koaly, S., Suhre, K., Rosset, R., and Marenco, A. (1998) Atlantic
1852 subtropical potential vorticity barrier of Ozone by Airbus In-Service Aircraft (MOZAIC) flights,
1853 J. Geophys. Res., 103, 25681-25693.

1854 Carpenter, L.J., Monks, P.S., Galbally, I.E., Meyer, C.P., Bandy, B.J. and Penkett, S.A. (1997)
1855 A study of peroxy radicals and ozone photochemistry at coastal sites in the northern and
1856 southern hemispheres. Journal of Geophysical Research, 102, 25417−25427.

1857 Chameides, W.L. and Walker, J.C.G. (1973) A photochemical theory for tropospheric ozone.
1858 Journal of Geophysical Research, 78, 8751−8760.

1859 Chang K-L, I. Petropavlovskikh, O. R. Cooper, M. G. Schultz T. Wang (2017), Regional trend
1860 analysis of surface ozone observations from monitoring networks in eastern North America,
1861 Europe and East Asia, Elem Sci Anth., 5:50, DOI: http://doi.org/10.1525/elementa.243

1862 Chen, X. L., Y. M. Ma, H. Kelder and K. Yang (2011) On the behaviour of the tropopause
1863 folding events over the Tibetan Plateau, Atmos. Chem. Phys., 11, 5113-5122.

1864 Clark, S.K., Ward, D.S. and Mahowald, N.M., 2017. Parameterization-based uncertainty in
1865 future lightning flash density. Geophysical Research Letters, 44(6), pp.2893-2901.

1866 Clifton, O.E., Fiore, A.M., Munger, J.W., Malyshev, S., Horowitz, L.W., Shevliakova, E., Paulot,
1867 F., Murray, L.T. and Griffin, K.L., 2017. Interannual variability in ozone removal by a temperate
1868 deciduous forest. *Geophysical Research Letters*, *44*(1), pp.542-552.

1869 Colange, G. and Lepape, A. (1929) Relation entre les titres en ozone de l'air du sol et de l'air
1870 de la haute atmosphere. Comptes Rendus, 189, 53−54.

1871 Colette, A., Ancellet, G. (2005) Impact of vertical transport processes on the tropospheric
1872 ozone layering above Europe. Part II: climatological analysis of the past 30 years. Atmospheric
1873 Environment 39, 5423e5435.

1874 Collins, W. J., Lamarque, J.-F., Schulz, M., Boucher, O., Eyring, V., Hegglin, M. I., Maycock,
1875 A., Myhre, G., Prather, M., Shindell, D., and Smith, S. J.: AerChemMIP: quantifying the effects
1876 of chemistry and aerosols in CMIP6, Geosci. Model Dev., 10, 585–607,
1877 https://doi.org/10.5194/gmd-10-585-2017, 2017.

1878 Cooper, O. R., C. Forster, D. Parrish, M. Trainer, E. Dunlea, T. Ryerson, G. Hübler, F.
1879 Fehsenfeld, D. Nicks, J. Holloway, J. de Gouw, C. Warneke, J. M. Roberts, F. Flocke and J.
1880 Moody (2004a) A case study of transpacific warm conveyor belt transport: Influence of
1881 merging airstreams on trace gas import to North America, J. Geophys. Res., 109, D23508,
1882 doi: 10.1019/2003JD003624, 17 pp.

1883 Cooper, O., Forster, C., Parrish, D., Dunlea, E., Hübler, G., Fehsenfeld, F., Holloway, J.,
1884 Oltmans, S., Johnson, B., Wimmers, A., and Horowitz, L. (2004b) On the life cycle of a
1885 stratospheric intrusion and its dispersion into polluted warm conveyor belts, J. Geophys. Res.,
1886 109, D23S09, doi: 10.1029/2003JD004006, 18 pp.

1887 Cooper, O. R., A. Stohl, G. Hübler, E. Y. Hsie, D. D. Parrish, A. F. Tuck, G, N, Kiladis, S. J.
1888 Oltmans, B. J. Johnson, M. Shapiro, J. L. Moody and A. S. Lefohn (2005) Direct transport of
1889 midlatitude stratospheric ozone into the lower troposphere and marine boundary layer of the
1890 tropical Pacific Ocean, J. Geophys. Res., 110, D23310, doi: 10.1029JD005783, 15 pp.

1891 Cooper, O.R., A. Stohl, M. Trainer, A. M. Thompson, J. C. Witte, S. J. Oltmans, B. J. Johnson,
1892 J. Merrill, J. L. Moody, G. Morris, D. Tarasick, G. Forbes, P. Nédélec, F. C. Fehsenfeld, J.
1893 Meagher, M. J. Newchurch, F. J. Schmidlin, S. Turquety, J. H. Crawford, K. E. Pickering, S.
1894 L. Baughcum, W. H. Brune, C. C. Brown (2006) Large upper tropospheric ozone
1895 enhancements above mid-latitude North America during summer: in situ evidence from the
1896 IONS and MOZAIC ozone monitoring network. Journal of Geophysical Research
1897 111(D24S05). doi:10.1029/2006JD007306.

1898 Cooper, O., C., D. D. Parrish, A. Stohl, M. Trainer, P. Nédélec, V. Thouret, J. P. Cammas, S.
1899 J. Oltmans, B. J. Johnson, D. Tarasick, T. Leblanc, I. S. McDermid, D. Jaffe, R. Gao, J. Stith,
1900 T. Ryerson, K. Aikin, T. Campos, A. Weinheimer and M. A. Avery (2010) Increasing springtime
1901 ozone mixin g ratios in the free troposphere over western North America, Nature, 463, 344-
1902 348.

1903 Cooper, O. R., Parrish, D. D., Ziemke, J., Balashov, N. V., Cupeiro, M., Galbally, I. E., Gilge,
1904 S., Horowitz, L., Jensen, N. R., Lamarque, J.-F., Naik, V., Oltmans, S. J., Schwab, J., Shindell,
1905 D. T., Thompson, A. M., Thouret, V., Wang, Y., Zbinden, R. M., 2014. Global distribution and
1906 trends of tropospheric ozone: An observation-based review, Elementa: Science of the
1907 Anthropocene, 2, 000029, doi: 10.12952/journal.elementa.000029.

1908 Cooper, P.L. and Abbatt, J.P.D., 1996. Heterogeneous interactions of OH and HO2 radicals
1909 with surfaces characteristic of atmospheric particulate matter. The Journal of Physical
1910 Chemistry, 100(6), pp.2249-2254.

1911 Cox, R.A., et al., (1975). Long-range transport of photochemical ozone in north-western
1912 Europe. Nature, 255(5504), pp.118-121.

1913 Cristofanelli, P., A. Bracci, M. Sprenger, A. Marinoni, U. Bonafè, F. Cazolari, R. Duchi, P. Laj,
1914 J. M. Pichon, F. Roccato, H. Venzac, E. Vuillermoz and P. Bonasoni (2010) Tropospheric
1915 ozone variations at the Nepal Climate Observatory-Pyramid (Himalayas, 5079 a.s.l.) and
1916 influence of deep stratospheric intrusion events, Atmos. Chem. Phys., 10, 6537-6549.

1917 Crutzen, P.J. (1970) The influence of nitrogen oxides on atmosphere ozone content. Quarterly
1918 Journal of the Royal Meteorological Society, 96, 320−325.

1919 Crutzen, P.J. (1973) Photochemical reactions initiated by and influencing ozone in unpolluted
1920 tropospheric air. Tellus, 26, 47−57.

1921 Danielsen, E.F. and Mohnen, V.A. (1977) Project Dustorm Report : Ozone Transport, In situ
1922 measurements, and meteorological analyses of tropopause folding. Journal of Geophysical
1923 Research, 82, 5867−5877.

1924 Danielson E.F. (1968) Stratospheric-tropospheric exchange based on radioactivity, ozone and
1925 potential vorticity. Journal of Atmospheric Science, 25, 502-518.

1926 Davidson, EA and Kingerlee, W. (1997) A global inventory of nitric oxide emissions from soils.
1927 Nutrient Cycling in Agroecosystems, 48:37-50.

1928 Davies, T. D., and E. Schuepbach (1994) Episodes of High Ozone Concentrations at the
1929 Earth´s Surface Resulting from Transport down from the Upper Troposphere/Lower
1930 Stratosphere: A review and Case Studies, Atmos. Environ., 28, 53-68.

1931 DeCaria, A. J., Pickering, K. E., Stenchikov, G. L., and Ott, L. E.: Lightning-generated NOx
1932 and its impact on tropospheric ozone production: A three-dimensional modeling study of a
1933 Stratosphere-Troposphere Experiment: Radiation, Aerosols and Ozone (STERAO-A)
1934 thunderstorm, J. Geophys. Res., 110, 1–13, doi:10.1029/2004JD005556, 2005.

1935 de la Torre, D., 2008. Quantification of mesophyll resistance and apoplastic ascorbic acid as
1936 an antioxidant for tropospheric ozone in durum wheat (Triticum durum Desf. cv.
1937 Camacho). *The Scientific World Journal*, *8*, pp.1197-1209.

1938 Dentener F., T. Keating and H. Akimoto (eds.) (2011), Hemispheric Transport of Air Pollution
1939 2010, Part A: Ozone and Particulate Matter, Air Pollution Studies No. 17, United Nations, New
1940 York and Geneva, ISSN 1014-4625, ISBN 978-92-1-117043-6.

1941 Derwent, R. G., P. G. Simmonds, S. Seuring, and C. Dimmer (1998) Observation and
1942 interpretation of the seasonal cycles in the surface concentrations of ozone and carbon
1943 monoxide at Mace Head, Ireland from 1990 to 1994, Atmos. Environ., 32, 145–157

1944 Dickerson, R. R., G. J. Huffman, W. T. Luke, L. J. Nunnermacker, K. E. Pickering, A. C. D.
1945 Leslie, C. G. Lindsay, W. G. N. Slinn, T. J. Kelly, P. H. Daum, A. C. Delany, J. P. Greenberg,
1946 P. R. Zimmerman, J. F. Boatman, J. D. Ray and D. H. Stedman (1987) Thunderstorms: An
1947 Important Mechanism in the Transport of Air Pollutants, Science, 235, 460-465.

1948 Doherty, R. M., O. Wild, D. T. Shindell, D. Zeng, I. A. MacKenzie, W. J. Collins, A. M. Fiore,
1949 D. S. Stevenson, M. G. Schultz, P. Hess, R. G. Derwent and T. Keating (2013) Impacts of
1950 climate change on surface ozone and intercontinental ozone pollution: A multi-model study, J.
1951 Geophys. Res. 118, 3744-3763, doi: 10.1002/jgrd.50266.

1952 Dolwick, P., Akhtar, F., Baker, K., Possiel, N., Simon, H., Tonnesen, G., 2015. Comparison of
1953 background ozone estimates over the western United States based on two separate model
1954 methodologies. Atmospheric Environment 109: 282-296, doi:
1955 10.1016/j.atmosenv.2015.01.005.

1956 Doniki, S., Hurtmans, D., Clarisse, L., Clerbaux, C., Worden, H. M., Bowman, K. W., and
1957 Coheur, P.-F.: Instantaneous longwave radiative impact of ozone: an application on
1958 IASI/MetOp observations, Atmos. Chem. Phys. Discuss., 15, 21177-21218, doi:10.5194/acpd-
1959 15-21177-2015, 2015.

1960 Duncan, B. N., L. N. Lamsal, A. M. Thompson, Y. Yoshida, Z. Lu, D. G. Streets, M. M. Hurwitz,
1961 and K. E. Pickering (2016), A space-based, high-resolution view of notable changes in urban
1962 NOx pollution around the world (2005–2014), J. Geophys. Res. Atmos., 121, 976–996,
1963 doi:10.1002/2015JD024121.

1964 Edwards, P. M. and Evans, M. J.: A new diagnostic for tropospheric ozone production, Atmos.
1965 Chem. Phys., 17, 13669–13680, https://doi.org/10.5194/acp-17-13669-2017, 2017.

1966 Eisele, H., H. E. Scheel, R. Sladkovic (1999) High-Resolution Lidar Measurements of
1967 Stratosphere-Troposphere Exchange, T. Trickl, J. Atmos. Sci., 56, 319-330.

1968 Elshorbany, Y. F., Kurtenbach, R., Wiesen, P., Lissi, E., Rubio, M., Villena, G., Gramsch, E.,
1969 Rickard, A. R., Pilling, M. J., and Kleffmann, J.: Oxidation capacity of the city air of Santiago,
1970 Chile, Atmos. Chem. Phys., 9, 2257-2273, doi:10.5194/acp-9-2257-2009, 2009.

1971 Emmerson, K. M., Galbally, I. E., Guenther, A. B., Paton-Walsh, C., Guerette, E.-A., Cope, M.
1972 E., Keywood, M. D., Lawson, S. J., Molloy, S. B., Dunne, E., Thatcher, M., Karl, T., and
1973 Maleknia, S. D.: Current estimates of biogenic emissions from eucalypts uncertain for

1974 southeast Australia, Atmos. Chem. Phys., 16, 6997-7011, doi:10.5194/acp-16-6997-2016,
1975 2016.

1976 Emmons, L. K., Hess, P. G., Lamarque, J.-F., and Pfister, G. G.: Tagged ozone mechanism
1977 for MOZART-4, CAM-chem and other chemical transport models, Geosci. Model Dev., 5,
1978 1531-1542, doi:10.5194/gmd-5-1531-2012, 2012.

1979 Eyring, V., Arblaster, J.M., Cionni, I., Sedláček, J., Perlwitz, J., Young, P.J., Bekki, S.,
1980 Bergmann, D., Cameron-Smith, P., Collins, W.J. and Faluvegi, G., 2013. Long-term ozone
1981 changes and associated climate impacts in CMIP5 simulations. Journal of Geophysical
1982 Research: Atmospheres, 118(10), pp.5029-5060.

1983 Eyring, V., Bony, S., Meehl, G.A., Senior, C.A., Stevens, B., Stouffer, R.J. and Taylor, K.E.,
1984 2016. Overview of the Coupled Model Intercomparison Project Phase 6 (CMIP6) experimental
1985 design and organization. Geoscientific Model Development (Online), 9(LLNL-JRNL-736881).

1986 Fabry, C. and H. Buisson, 1913: L'absorption de l'ultra-violet par l'ozone et la limite du spectre
1987 solaire. J. Phys. Theor. Appl., 3, 196-206, https://doi.org/10.1051/jphystap:019130030019601

1988 Fares, S., McKay, M., Holzinger, R., & Goldstein, A. H. (2010). Ozone fluxes in a Pinus
1989 ponderosa ecosystem are dominated by non-stomatal processes: Evidence from long-term
1990 continuous measurements. Agricultural and Forest Meteorology, 150(3), 420 – 431.
1991 https://doi.org/10.1016/j.agrformet.2010.01.007

1992 Fehsenfeld, F. C., P. Daum, W. R. Leatch, M. Trainer, D. D. Parrish and G. Hübler (1996)
1993 Transport and processing of nOe3 and O3 precursors over the North Atlantic: An overview of
1994 the 1993 North Atlantic Regional Experiment (NARE) summer intensive, J. Geophys. Res.,
1995 101, 28877-28891; and references therein.

1996 Fiore, A. M. D. J. Jacob, I. Bey. R. M. Yantosca, B. D. Field A. C. Fusco and J. G. Wilkinson
1997 (2002) Background ozone over the United States, and contribution to pollution episodes, J.
1998 Gedophys. Res, 107, 4275, doi: 10.1029/2001JD000982, 25pp.

1999 Fiore, A. M., F. J. Dentener, O. Wild, C. Cuvelier, M. G. Schultz, P. Hess, C. Textor, M. Schulz,
2000 R. M. Doherty, L. W. Horowitz, I. A.. MacKenzie, M. G. Sanderson, D. T. Shindell, D. S.
2001 Stevenson, S. Szopa, R. Van Dingenen, G. Zeng. C. Atherton, D. Bergmann, I. Bey, G.
2002 Carmichael, W. J. Collins, B. N. Duncan, G. Faluwegi, G. Folberth, M. Gaus., S. Gong, D.
2003 Hauglustaine, T. Holloway, I. S. A., Isaksen, D. J. Jacob, J. E. Jonson, J. W. Kaminski, T. J.
2004 Keating, A. Lupu, E. Marmer, V. Montanaro, R. J. Park, G. Pitari, G. Pitari, K. J. Pringle, J. A.
2005 Pyle, S. Schroeder, M. G. Vivanco, P. Wind, G. Woijcik, S. Wu, and A. Zuber (2009)
2006 Multimodel estimates of intercontinental source-receptor relationships for ozone pollution,
2007 J.Geophys. Res., 114, D04301, doi: 10.1029/2008JD010816, 21 pp.

2008 Fiore, A.M., V. Naik, D. Spracklen, A. Steiner, N. Unger, M. Prather, D. Bergmann, P.J.
2009 Cameron-Smith, B. Collins, S. Dalsøren, G. Folberth, P. Ginoux, L.W. Horowitz, B. Josse, J.-
2010 F. Lamarque, T. Nagashima, F. O'Connor, S. Rumbold, D.T. Shindell, R.B. Skeie, K. Sudo, T.
2011 Takemura, G. Zeng, Global Air Quality and Climate (2012), Chem. Soc. Rev., 41, 6663–6683.

2012 Fischer, E.V., Jaffe, D.A., and Weatherhead, E.C. (2011), Free tropospheric peroxyacetyl
2013 nitrate (PAN) and ozone at Mount Bachelor: Potential causes of variability and timescale for
2014 trend detection, Atmospheric Chemistry and Physics, 11, 5641–5654, doi: 10.5194/acp-11-
2015 5641-2011.

2016 Fishman, J. and Seiler, W. 1983. Correlative nature of ozone and carbon-monoxide in the
2017 troposphere – implications for the tropospheric ozone budget. Journal of Geophysical
2018 Research, 88, 3662–3670.

2019 Fishman, J., Solomon, S. and Crutzen, P.J. (1979) Observational and theoretical evidence in
2020 support of a significant in-situ photochemical source of tropospheric ozone. Tellus, 31,
2021 432−446.

2022 Fowler D. et al. (2009) Atmospheric composition change: Ecosystems–Atmosphere
2023 interactions. Atmospheric Environment 43, 5193–5267.

2024 Fowler, D., Flechard, C., Cape, J.N., Storeton-West, R.L. and Coyle, M. (2001) Measurements
2025 of Ozone Deposition to Vegetation Quantifying the Flux, the Stomatal and Non-Stomatal
2026 Components. Water, Air, & Soil Pollution 130: 63-74. doi:10.1023/A:1012243317471

2027 Franz, M., Simpson, D., Arneth, A., and Zaehle, S.: Development and evaluation of an ozone
2028 deposition scheme for coupling to a terrestrial biosphere model, Biogeosciences, 14, 45-71,
2029 doi:10.5194/bg-14-45-2017, 2017.

2030 Furger, M., J. Dommen, W. K. Graber, L. Pioggio, A. Prévôt, S. Emeis, G. Grell, T. Trickl, B.
2031 Gomiscek, B. Neininger, G. Wotawa (2000) The VOTALP Mesolcina Valley Campaign 1996-
2032 concept, background and some highlights, Atmos. Environ., 34, 1395-1412.

2033 Galbally, I. E., Schultz, M.G., Buchmann, B., Gilge, S., Guenther, F., Koide, H., Oltmans, S.,
2034 Patrick, L., Scheel, H.-E., Smit, H., Steinbacher, M., Steinbrecht, W., Tarasova, O., Viallon, J.,
2035 Volz-Thomas, A., Weber, M., Wielgosz, R. and Zellweger, C., 2013. Guidelines for Continuous
2036 Measurement of Ozone in the Troposphere, GAW Report No 209, Publication WMO-No. 1110,
2037 ISBN 978-92-63-11110-4, WMO, Geneva.

2038 Galbally, I.E. (1968) Some measurements of ozone variation and destruction in the
2039 atmospheric surface layer. Nature, 218 (5140), 456–457.

2040 Galbally, I.E. (1971) Ozone profiles and ozone fluxes in the atmospheric surface layer.
2041 Quarterly Journal of the Royal Meteorological Society, 97 (411), 18–29.

2042 Galbally, I.E. (1974) Gas transfer near the earth's surface. Adv. in Geophys., 18B: 329–339.

2043 Galbally, I.E. and Roy, C.R. (1980) Destruction of ozone at the Earth's surface. Quarterly
2044 Journal of the Royal Meteorological Society, 106 (449), 599–620.

2045 Galbally, I.E. and Roy, C.R. (1978) Loss of fixed nitrogen from soils by nitric oxide exhalation.
2046 Nature, 275: 734–735.

2047 Galbally, I.E., Bentley, S.T. and Meyer, C.P. (2000) Mid–latitude marine boundary-layer ozone
2048 destruction at visible sunrise observed at Cape Grim, Tasmania, 41°S. Geophysical Research
2049 Letters, 27 (23), 3841–3844.

2050 Ganzeveld, L., D. Helmig, C. W. Fairall, J. Hare, and A. Pozzer (2009), Atmosphere-ocean
2051 ozone exchange: A global modeling study of biogeochemical, atmospheric, and waterside
2052 turbulence dependencies, Global Biogeochemical Cycles, 23, GB4021,
2053 doi:10.1029/2008GB003301.

2054 Garland, J.A. and Curtis, H., 1981. Emission of iodine from the sea surface in the presence of
2055 ozone. Journal of Geophysical Research: Oceans, 86(C4), pp.3183-3186.

2056 Garland, J.A., Elzerman, A.W. and Penkett, S.A., 1980. The mechanism for dry deposition of
2057 ozone to seawater surfaces. Journal of Geophysical Research: Oceans, 85(C12), pp.7488-
2058 7492.

2059 Gaudel, A., et al. (2018), Tropospheric Ozone Assessment Report: Present-day distribution
2060 and trends of tropospheric ozone relevant to climate and global atmospheric chemistry model
2061 evaluation, Elem Sci Anth, 6(1):39, DOI: https://doi.org/10.1525/elementa.291

2062 Ghude, S. D., C. Jena, D. M. Chate, G. Beig, G. G. Pfister, R. Kumar, and V. Ramanathan
2063 (2014), Reductions in India's crop yield due to ozone, Geophys. Res. Lett., 41, 5685–5691,
2064 doi:10.1002/2014GL060930.

2065 Gottschaldt, K., Voigt, C., Jöckel, P., Righi, M., Deckert, R. and Dietmüller, S., 2013. Global
2066 sensitivity of aviation NO x effects to the HNO 3-forming channel of the HO 2+ NO reaction.
2067 Atmospheric Chemistry and Physics, 13(6), pp.3003-3025.

2068 Gouget, H., Cammas, J.-P., Marenco, A., Rosset, R., and Jonquières, I. (1996) Ozone peaks
2069 associated with a subtropical tropopause fold and with the trade wind inversion: A case study
2070 from the airborne campaign TROPOZ II over the Caribbean in winter, J. Geophys. Res., 101,
2071 25979-25993.

2072 Granier C., Bertrand Bessagnet, Tami Bond, Ariela D'Angiola, Hugo Denier van der Gon,
2073 Gregory J. Frost, Angelika Heil, Johannes W. Kaiser, Stefan Kinne, Zbigniew Klimont, Silvia
2074 Kloster, Jean-François Lamarque, Catherine Liousse, Toshihiko Masui, Frederik Meleux,
2075 Aude Mieville, Toshimasa Ohara, Jean-Christophe Raut, Keywan Riahi, Martin G. Schultz,
2076 Steven J. Smith, Allison Thompson, John van Aardenne, Guido R. van der Werf, Detlef P. van
2077 Vuuren (2011) Evolution of anthropogenic and biomass burning emissions of air pollutants at
2078 global and regional scales during the 1980–2010 period. Climatic Change 109:163–190. DOI
2079 10.1007/s10584-011-0154-1

2080 Granier, C., Bessagnet, B., Bond, T., D'Angiola, A., van der Gon, H. D., et al., 2011. Evolution
2081 of anthropogenic and biomass burning emissions of air pollutants at global and regional scales
2082 during the 1980–2010 period, Climatic Change, 109, 163–190. doi:10.1007/s10584-011-
2083 0154-1.

2084 Grousset, F. E., P. Ginoux, A. Bory and P. E. Biscaye (2003) Case study of a Chinese dust
2085 plume reaching the French Alps, Geophys. Res. Lett., 30, 1277, doi:10.1029/2002GL016833,
2086 4 pp.

2087 Guenther, A., et al. (2006), Estimates of global terrestrial isoprene emissions using MEGAN
2088 (Model of Emissions of Gases and Aerosols from Nature), Atmospheric Chemistry and
2089 Physics, 6: 3181-3210.

2090 Guerova, G., I. Bey, J.-L. Attié, R. V. Martin, J. Cui and M. Sprenger (2006) Impact of
2091 transatlantic transport episodes on summertime ozone in Europe, Atmos. Chem. Phys., 6,
2092 2057-2072.

2093 Hannan, J. R., H. E. Fuelberg, J. H. Crawford, G. W. Sachse and D. R. Blake (2003) Role of
2094 wave cyclones in transporting boundary layer air to the free troposphere durting the spring
2095 2001 NASA/TRACE-P experiment, J. Geophys. Res., 108, 8785, doi:
2096 10.1029/2002JD003105, 17 pp.

2097 Hartley, W. N., 1881: On the absorption of solar rays by atmospheric ozone. J. Chem. Soc.,
2098 Trans., 39, 111-128

2099 Hassler, B., McDonald, B. C., Frost, G. J., Borbon, A., Carslaw, D. C., Civerolo, K., et al.
2100 (2016). Analysis of long-term observations of NOx and CO in megacities and application to
2101 constraining emissions inventories. *Geophys. Res. Lett.* 43, 9920–9930.
2102 doi:10.1002/2016gl069894.

2103 Hauglustaine, D.A., Madronich, S., Ridley, B.A., Walega, J.G., Cantrell, C.A., Shetter, R.E.
2104 and Hüber, G. (1996) Observed and model-calculated photostationary state at Mauna Loa
2105 Observatory during MLOPEX 2. Journal of Geophysical Research, 101 (D9), 14681–14696.

2106 Hawkins, E. and Sutton, R., 2009. The potential to narrow uncertainty in regional climate
2107 predictions. *Bulletin of the American Meteorological Society*, *90*(8), pp.1095-1108.

2108 Helmig, D., E. K. Lang, L. Bariteau, P. Boylan, C. W. Fairall, L. Ganzeveld, J. E. Hare, J.
2109 Hueber, and M. Pallandt (2012) Atmosphere-ocean ozone fluxes during the TexAQS 2006,
2110 STRATUS 2006, GOMECC 2007, GasEx 2008, and AMMA 2008 cruises, Journal of
2111 Geophysical Research, 117, D04305, doi:10.1029/2011JD015955.

2112 Helmig, D., Ganzeveld, L., Butler, T. and S. J. Oltmans S.J. (2007) The role of ozone
2113 atmosphere-snow gas exchange on polar, boundary-layer tropospheric ozone – a review and
2114 sensitivity analysis. Atmospheric Chemistry and Physics, 7, 15–30.

Hilboll, A., A. Richter, and J. P. Burrows. "Supplementary material to “Long-term changes of tropospheric NO2 over megacities derived from multiple satellite instruments”." Atmos. Chem. Phys 13 (2013): 1-3.

Hoesly, R. M., et al. (2017), Historical (1750 – 2014) anthropogenic emissions of reactive gases and aerosols from the Community Emission Data System (CEDS), Geosci. Model Dev. Discuss., doi:10.5194/gmd-2017-43.

Holton, J. R., Douglass, A. R., Haynes, P. H., McIntyre, M. E., Rood, R. B., and Pfister, L. (1996) Stratosphere-troposphere exchange, Rev. Geophys., 33, 403–439.

HTAP (2010), Hemispheric Transport of Air Pollution, Part A: Ozone and Particulate Matter, F. Dentener, T. Keating and H. Akimoto, Eds., United Nations (New York, Geneva), 278 pp., ISSN 1014-4625, ISBN 978-92-1-117043-6, http://www.htap.org/publications/2010_report/2010_Final_Report/HTAP%202010%20Part%20A%20110407.pdf

Hu, L., D.B. Millet,Baasandorj, T.J. Griffis, P. Turner, D. Helmig, A.J. Curtis, J. Hueber (2015), Isoprene emissions and impacts over an ecological transition region in the US Upper Midwest inferred from tall tower measurements, J. Geophys. Res., 120, 3553-3571, doi:10.1002/2014JD022732

Hu, L., D.J. Jacob, X. Liu, Y. Zhang, L. Zhang, P.S. Kim, M.P. Sulprizio, R.M. Yantosca (2017), Global budget of tropospheric ozone: evaluating recent model advances with satellite (OMI), aircraft (IAGOS), and ozonesonde observations, Atmos. Environ., 167, 323-334, doi: 10.1016/j.atmosenv.2017.08.036

Huntrieser, H., Heland, J., Schlager, H., Forster, C., Stohl, A., Aufmhoff, H., Arnold, F., Scheel, H. E., Campana, M., Gilge, S., Eixmann, R., and Cooper, O. (2005) Intercontinental air pollution transport from North America to Europe: Experimental evidence from aircraft measurements and surface observations, J. Geophys. Res., 110, DO1305, doi: 10.1029/2004JD005045, 22 pp.

IPCC (2013), Climate Change 2013: The Physical Science Basis. Contribution of Working Group I to the Fifth Assessment Report of the Intergovern-mental Panel on Climate Change [Stocker, T.F., D. Qin, G.-K. Plattner, M. Tignor, S.K. Allen, J. Boschung, A. Nauels, Y. Xia, V. Bex and P.M. Midgley (eds.)]. Cambridge University Press, Cambridge, United Kingdom and New York, NY, USA, 1535 pp.

Jacob, D. J., J. A. Logan, and P. P. Murti (1999) Effect of rising Asian emissions on surface ozone in the United States, Geophys. Res.Lett., 26, 2175-2178.

Jacob, D.J., 2000. Heterogeneous chemistry and tropospheric ozone. Atmospheric Environment, 34(12-14), pp.2131-2159.

Jaffe, D., Anderson, T., Covert, D., Kotchenruther, R., Trost, B., Danielson, J., Simpson, W., Berntsen, T., Karlsdottir, S., Blake, D., Harris, J., Carmichael, G., and Uno, I.: Transport of Asian Air Pollution to North America, Geophys. Res. Lett., 26, 711-714, 1999.

Jaffe, D.A., and Wigder, N.L. Ozone production from wildfires: A critical review. Atmospheric Environment 51, 1–10, doi:10.1016/j.atmosenv.2011.11.063, 2012.

Janssens-Maenhout, G., et al. "HTAP_v2. 2: a mosaic of regional and global emission grid maps for 2008 and 2010 to study hemispheric transport of air pollution." Atmospheric Chemistry and Physics 15.19 (2015): 11411-11432.

Jenkin, M.E., Watson, L.A., Utembe, S.R. and Shallcross, D.E., 2008. A Common Representative Intermediates (CRI) mechanism for VOC degradation. Part 1: Gas phase mechanism development. *Atmospheric Environment*, *42*(31), pp.7185-7195.

Jenkin, M.E., Khan, M.A.H., Shallcross, D.E., Bergström, R., Simpson, D., Murphy, K.L.C. and Rickard, A.R., 2019. The CRI v2. 2 reduced degradation scheme for isoprene. *Atmospheric Environment*, *212*, pp.172-182.

2163 Jöckel, P., Tost, H., Pozzer, A., Brühl, C., Buchholz, J., Ganzeveld, L., Hoor, P., Kerkweg, A.,
2164 Lawrence, M. G., Sander, R., Steil, B., Stiller, G., Tanarhte, M., Taraborrelli, D., van Aardenne,
2165 J., and Lelieveld, J.: The atmospheric chemistry general circulation model ECHAM5/MESSy1:
2166 consistent simulation of ozone from the surface to the mesosphere, Atmos. Chem. Phys., 6,
2167 5067–5104, https://doi.org/10.5194/acp-6-5067-2006, 2006.

2168 Jöckel, P., Tost, H., Pozzer, A., Kunze, M., Kirner, O., Brenninkmeijer, C. A. M., Brinkop, S.,
2169 Cai, D. S., Dyroff, C., Eckstein, J., Frank, F., Garny, H., Gottschaldt, K.-D., Graf, P., Grewe,
2170 V., Kerkweg, A., Kern, B., Matthes, S., Mertens, M., Meul, S., Neumaier, M., Nützel, M.,
2171 Oberländer-Hayn, S., Ruhnke, R., Runde, T., Sander, R., Scharffe, D., and Zahn, A.: Earth
2172 System Chemistry integrated Modelling (ESCiMo) with the Modular Earth Submodel System
2173 (MESSy) version 2.51, Geosci. Model Dev., 9, 1153–1200, https://doi.org/10.5194/gmd-9-
2174 1153-2016, 2016.

2175 Jones, B. and O'Neill, B.C., 2016. Spatially explicit global population scenarios consistent with
2176 the Shared Socioeconomic Pathways. Environmental Research Letters, 11(8), p.084003.

2177 Jones, I.T.N. and Wayne, R.P. (1970) The photolysis of ozone by ultraviolet radiation: IV.
2178 Effect of photolysis wavelength on primary step. Proceedings of the Royal Society, A319, 273.

2179 Jonson, J. E., A. Stohl, A. M. Fiore, P. Hess, S. Szopa, O. Wild, G. Weng, F. J. Dentener, A.
2180 Lupu, M. G. Schultz, B. N. Duncan, K. Sudo, P. Wind, M. Schulz, E. Marmer, C. Cuvelier, T.
2181 Keating, A. Zuber, A. Valdebenito, V. Dorokov, H. De Backer, J. Davies, G. H. Chen, B.
2182 Johnson, D. W. Tarasick, R. Stübi, M. J. Newchurch, P. von der Gathen, W. Steinbrecht and
2183 H. Claude (2010) A multi-model analysis of vertical ozone profiles, Atmos. Chem. Phys., 10,
2184 5759-5783.

2185 Junge, C.E. (1962) Global ozone budget and exchange between stratosphere and
2186 troposphere. Tellus, 14, 363−377.

2187 Junge, C.E. (1972) The cycle of atmospheric gases – natural and man made. Quarterly
2188 Journal of the Royal Meteorological Society, 98, 711–729.

2189 Kentarchos, A. S., and G. J. Roelofs (2003) A model study< of stratospheric ozone in the
2190 troposphere and its contribution to tropospheric OH formation, J. Geophys. Res., 8517, doi:
2191 10.1029/2002JD002598, 9 pp.

2192 Keyser, D., and M. A. Shapiro (1986) Monthly Wea. Redv., 114, 452-499.

2193 Krotkov, Nickolay A., et al. "Aura OMI observations of regional SO2 and NO2 pollution
2194 changes from 2005 to 2015." Atmospheric Chemistry and Physics16.7 (2016): 4605-4629.

2195 Khan, M.A.H., Cooke, M.C., Utembe, S.R., Archibald, A.T., Derwent, R.G., Jenkin, M.E.,
2196 Morris, W.C., South, N., Hansen, J.C., Francisco, J.S. and Percival, C.J., 2015. Global
2197 analysis of peroxy radicals and peroxy radical-water complexation using the STOCHEM-CRI
2198 global chemistry and transport model. Atmospheric environment, 106, pp.278-287.

2199 Kumar, R., M. C. Barth, S. Madronich, M. Naja, G. R. Carmichael, G. G. Pfister, C. Knote, G.
2200 P. Brasseur, N. Ojha, T. Sarangi (2014) Effects of dust aerosols on tropospheric chemistry
2201 during a typical pre-monsoon season dust storm in northern India, *Atmos. Chem. Phys,, 14,*
2202 *6813-6834.*

2203 Kumar, R., et al., (2018). How Will Air Quality Change in South Asia by 2050? Journal of
2204 Geophysical Research, 123. https://doi.org/10.1002/2017JD027357.

2205 Kurokawa, J., et al. "Emissions of air pollutants and greenhouse gases over Asian regions
2206 during 2000–2008: Regional Emission inventory in ASia (REAS) version 2." Atmospheric
2207 Chemistry and Physics 13.21 (2013): 11019-11058.

2208 Kurpius, M. R., and A. H. Goldstein, Gasphase chemistry dominates O3 loss to a forest,
2209 implying a source of aerosols and hydroxyl radicals to the atmosphere, Geophysical Research
2210 Letters, 30 (7), 1371, doi:10.1029/2002GL016785, 2003.

2211 Lamarque, J. F., Bond, T. C., Eyring, V., Granier, C., Heil, A., Klimont, Z., et. al. (2010).
2212 Historical (1850–2000) gridded anthropogenic and biomass burning emissions of reactive
2213 gases and aerosols: methodology and application. Atmospheric Chemistry and Physics,
2214 10(15), 7017-7039.

2215 Lamarque, J.-F., A. O. Langford and M. H. Proffitt (1996) Cross-tropopause mixing of ozone
2216 through gravity wave breaking: Observation and modeling, J. Geophys. Res., 101,22969-
2217 22976.

2218 Lamarque, J.-F., T. C. Bond, V. Eyring, C. Granier, A. Heil, Z. Klimont, D. Lee, C. Liousse, A.
2219 Mieville, B. Owen, M. G. Schultz, D. Shindell, S. J. Smith, E. Stehfest, J. Van Aardenne, O. R.
2220 Cooper, M. Kainuma, N. Mahowald, J. R. McConnell, V. Naik, K. Riahi, and D. P. van Vuuren
2221 (2010), Historical (1850–2000) gridded anthropogenic and biomass burning emissions of
2222 reactive gases and aerosols: methodology and application, Atmos. Chem. Phys., 10, 7017-
2223 7039.

2224 Lamarque, J.F., P.G. Hess, and X.X. Tie (1999), Three-dimensional model study of the
2225 influence of stratosphere-troposphere exchange and its distribution on tropospheric chemistry,
2226 Journal of Geophysical Research, 104, 26,363–26,372.

2227 Lamsal, L. N., Martin, R. V., Padmanabhan, A., van Donkelaar, A., Zhang, Q., Sioris, C. E.,
2228 Chance, K., Kurosu, T. P., and Newchurch, M. J. (2011), Application of satellite observations
2229 for timely updates to global anthropogenic NOx emission inventories, Geophys. Res. Lett., 38,
2230 L05810, 10.1029/2010gl046476.

2231 Lamsal, L. N., R. V. Martin, A. van Donkelaar, E. A. Celarier, E. J. Bucsela, K. F. Boersma, R.
2232 Dirksen, C. Luo, and Y. Wang (2010), Indirect validation of tropospheric nitrogen dioxide
2233 retrieved from the OMI satellite instrument: Insight into the seasonal variation of nitrogen
2234 oxides at northern midlatitudes, J. Geophys. Res., 115, D05302, doi:10.1029/2009JD013351.

2235 Langford, A. O. (1999) Stratosphere-troposphere exchange at the subtropical jet, contribution
2236 to the tropospheric ozone budget at midlatitudes, Geophys. Res. Lett, 26, 2449-2452.

2237 Langford, A. O., R. B. Pierce and P. J. Schultz (2015) Stratospheric intrusions, the Santa Ana
2238 winds, and wildland fires in Southern California, Geophys. Res.Lett., 42, 6091-6097, dir:
2239 10.1002/2015GL064964.

2240 Lefohn, A. S., H. Wernli, D. Shadwick, S. J. Oltmans, M. Shapiro (2011) Quantifying the
2241 importance of stratospheric-tropospheric transport on surface ozone concentrations at high-
2242 and low-elevation monitoring sites in the United States, Atmos. Environ., 62, 646-456.

2243 Lefohn, A. S., H. Wernli, D. Shadwick, S. Limbach, S. J. Oltmans, M. Shapiro (2011) The
2244 importance of stratospheric-tropospheric transport in affecting surface ozone concentrations
2245 in the western and northern tier of the United States, Atmos. Environ., 45, 4845-4857.

2246 Lelieveld, J. and Crutzen, P. J. (1994) Role of Deep Cloud Convection in the Ozone Budget
2247 of the Troposphere, Science, 264, 1759-1761.

2248 Lelieveld, J. and Crutzen, P.J. (1990) Influences of cloud photochemical processes on
2249 tropospheric ozone. Nature, 343 (6255), 227−233.

2250 Lelieveld, J., Gromov, S., Pozzer, A. and Taraborrelli, D., 2016. Global tropospheric hydroxyl
2251 distribution, budget and reactivity. Atmos. Chem. Phys, 16, pp.12477-12493.

2252 Levy II, H. (1971) Normal atmosphere: Large radical and formaldehyde concentrations
2253 predicted. Science, 173, 141−143.

2254 Levy II, H. (1972) Photochemistry of the lower troposphere. Planetary and Space Science, 20,
2255 919−935.

2256 Levy II, H. (1973) Photochemistry of minor constituents in the troposphere. Planetary and
2257 Space Science, 21 (4), 575−591.

Li, Q., D. L. Jacob, I. Bey, P. I. Palmer, B. N. Duncan, B. D. Field, R. V. Martin, A. M., Fiore, R. M. Yantosca, D. D. Parrish, P. G. Simmonds, and S. J. Oltmans (2002) Transatlantic transport of pollution and its effects on surface ozone in Europe and North America, J. Geophys. Res., 107, 4166, doi: 10.1029/2001JD001422, 16 pp.

Li, K., D. J. Jacob, H. Liao, L. Shen, Q. Zhang, and K. H. Bates (2019), Anthropogenic drivers of 2013–2017 trends in summer surface ozone in China, *Proceedings of the National Academy of Sciences*, *116*(2), 422, doi:10.1073/pnas.1812168116.

Liang, Q., L. Jaeglé, D. A. Jaffe, P. Weiss-Penzias, A. Heckman and J. A. Snow (2004) Long-range transport of pollution to the northeast Pacific: Seasonal variations and transport pathways of carbon monoxide, J. Geophys. Res., 109, D23S07, doi: 10.1029/2003JD004402, 16 pp.

Liang, Q., L. Jaeglé, R. C. Hudman, S. Turquety, D. J. Jacob, M. A. Avery, E. V. Browell, G. W. Sachse, D. R. Blake, W. Brune, X. Ren, R. C. Cohen, J. E. Dibb, A. Fried, H. Fuelberg, M. Porter, B. G. Heikes, G., Huey, H. B. Singh, and P. O. Wennberg (2007) Summertime influence of Asian pollution in the free troposphere over North America, J. Geophys. Res., 112, D12S11, doi: 10.1029/2006JD007919, 20 pp.

Lin, M., A. M. Fiore, L. W. Horowitz, O. R. Cooper, V. Naik,J. Holloway, B. J. Johnson, A. M. Middlebrook, S. J. Oltmans, I. B. Pollack, T. B. Ryerson, J. X. Warner, C. Widinmyer, J. Wilson and B. Wyman (2012) J. Geophys. Res., 117, D00V07, doi: 10.1029/2011JD016961, 20 pp.

Lin, M., A. M. Fiore, O. R. Cooper, L. W. Horowitz, A. O. Langford, H. Levy II, B. J. Johnson, V. Naik, S. J. Oltmans and C. J. Senff (2012) Springtime high ozone events over the western United States: Quantifying the role of stratospheric intrusions, Geophys. Res., 117, D00V22, doi: 10.1029/2012JD018151, 20 pp.

Lin, M., L.W. Horowitz, S. J. Oltmans, A. M. Fiore and S. Fan (2014), Tropospheric ozone trends at Mauna Loa Observatory tied to decadal climate variability, Nature Geoscience, 7, 136-143 doi:10.1038/ngeo2066.

Lin, M., Fiore, A.M., Horowitz, L.W., Langford, A.O., Oltmans, S.J., Tarasick, D. and Rieder, H.E., 2015. Climate variability modulates western US ozone air quality in spring via deep stratospheric intrusions. Nature Communications, 6(1), pp.1-11.

Lin, M., Z. Zhang, L. Su, J. Hill-Falkenthal, A. Priyadarshi, Q. Zhang, G. Zhang, S. Kang, C.-Y. Chan and M. H. Thiemens (2016) Resolving the impact of stratosphere-to-troposphere transport on the the sulfur cycle over the Tibetan Plateau using a cosmogenic 35S tracer, J. Geophys Res., 121, 439-456, doi: 10.1002/2015JD023801.

Lin, M.Y., W. Horowitz, R. Payton, A.M. Fiore, G. Tonnesen (2017). US surface ozone trends and extremes from 1980 to 2014: Quantifying the roles of rising Asian emissions, domestic controls, wildfires, and climate. Atmos. Chem. Phys.,doi:10.5194/acp-17-2943-2017

Lin, M., Malyshev, S., Shevliakova, E., Paulot, F., Horowitz, L.W., Fares, S., Mikkelsen, T.N. and Zhang, L., 2019. Sensitivity of Ozone Dry Deposition to Ecosystem-Atmosphere Interactions: A Critical Appraisal of Observations and Simulations. Global Biogeochemical Cycles, 33(10), pp.1264-1288.

Liu, H., D. J. Jacob, I. Bey, R. M. Yantosca, B. N. Duncan (2003) Transport pathways for Asian outflow over the Pacific: Interannual and seasonal varikations, J. Geophys. Res., 108, 878t6, doi: 10.1029/2002JD003102, 18 pp.

Liu, S.C., Trainer, M., Carroll, M.A., Hübler, G., Montzka, D.D., Norton, R.B., Ridley, B.A., Walega, J.G., Atlas, E.L., Heikes, B.G., Huebert, B.J. and Warren, W. (1992) A study of the photochemistry and ozone budget during the Mauna Loa Observatory photochemistry experiment. Journal of Geophysical Research, 97 (D10), 10463−10471.

LRTAP Convention, 2015. Draft Chapter III: Mapping Critical levels for Vegetation, of the Manual on Methodologies and Criteria for Modelling and Mapping Critical Loads and Levels and Air Pollution Effects, Risks and Trends. Available at: http://icpmapping.org/Mapping_Manual

Lu, X., L. Zhang, Y. Zhao, D. J. Jacob, Y. Hu, L. Hu, M. Gao, X. Liu, I. Petropavlovskikh, A. McClure-Begley, and R. Querel (2018), Surface and tropospheric ozone trends in the Southern Hemisphere since 1990: possible linkages to poleward expansion of the Hadley Circulation, Science Bulletin, doi:https://doi.org/10.1016/j.scib.2018.12.021.

Luhar, A. K., Galbally, I. E., Woodhouse, M. T., and Thatcher, M.: An improved parameterisation of ozone dry deposition to the ocean and its impact in a global climate-chemistry model, Atmos. Chem. Phys., 17, 3749–3767, doi:10.5194/acp-17-3749-2017, 2017.

Luo, C., Y. Wang, and W. J. Koshak (2017), Development of a self-consistent lightning NOx simulation in large-scale 3-D models, J. Geophys. Res. Atmos., 122, 3141–3154, doi:10.1002/2016JD026225.

Ma, J., W. L. Lin, X. D. Zheng, X. B. Xu, Z. Li, L. L. Yang (2014) Influence of air mass downward transport on the variability of surface ozone at Xianggelila Regional Atmospheric Background Station, southwest China, Atmos. Chem. Phys., 14, 5311-5325.

Ma, Z., et al. (2016), Significant increase of surface ozone at a rural site, north of eastern China, Atmos. Chem. Phys., 16, 3969–3977, doi:10.5194/acp-16-3969-2016.

Marais, E.A., D.J. Jacob, T.P. Kurosu, K. Chance, J.G. Murphy, C. Reeves, G. Mills, S. Casadio, D.B. Millet, M.P. Barkley, F. Paulot, and J. Mao, *Isoprene emissions in Africa inferred from OMI observations of formaldehyde columns*, Atmos. Phys., 12, 6,219-6,235, 2012.

Martin, R.V., Jacob, D.J., Yantosca, R.M., Chin, M. and Ginoux, P., 2003. Global and regional decreases in tropospheric oxidants from photochemical effects of aerosols. Journal of Geophysical Research: Atmospheres, 108(D3).

Mielke, L. H., Amanda Furgeson, Osthoff, H. D.: Observation of ClNO2in a Mid-Continental Urban Environment, Environmental Science & Technology, 45 (20), p.8889, doi:10.1021/es201955u, 2011.

Mijling, B., R. J. van der A, and Q. Zhang. "Regional nitrogen oxides emission trends in East Asia observed from space." Atmospheric Chemistry and Physics 13.23 (2013): 12003-12012.

Miyazaki et al. (2017), Decadal changes in global surface NOx emissions from multi-constituent satellite data assimilation, Atmos. Chem. Phys., 17, 807–837.

Miyazaki, Y., Y. Kondo, M. Koike, H. E. Fuelberg, C. M. Kiley, K. Kita, N. Takegawa, G. W. Sachse, F. Flocke, A. J. Weinheimer, H. B. Singh, F. L. Eisele, M. Zondlo, R. W. Talbot, S. T. Sandholm, M. A. Avery, and D. R. Blake (2003) Synoptic-scale transport of reactive nitrogen over the western Pacific in spring, J. Geophys. Res, 108, 8788, doi:10.1029/2002JD003248, 14 pp.

Monks, P. S., Archibald, A. T., Colette, A., Cooper, O., Coyle, M., Derwent, R., Fowler, D., Granier, C., Law, K. S., Mills, G. E., Stevenson, D. S., Tarasova, O., Thouret, V., von Schneidemesser, E., Sommariva, R., Wild, O., and Williams, M. L., 2015. Tropospheric ozone and its precursors from the urban to the global scale from air quality to short-lived climate forcer, Atmos. Chem. Phys., 15, 8889-8973, doi:10.5194/acp-15-8889-2015.

Monks, P.S., Carpenter, L.J., Penkett, S.A., Ayers, G.P., Gillett, R.W., Galbally, I.E. and Meyer, C.P. (1998) Fundamental ozone photochemistry in the remote marine boundary layer: The SOAPEX experiment, measurement and theory. Atmospheric Environment, 32, 3647−3664.

2352 Müller, J.-F., and G. Brasseur (1995) IMAGES: A three-dimensional chemical transport model
2353 of the global troposphere, Journal of Geophysical Research, 100, 16,445 – 16,490.

2354 Murphy, D.M., and D.W. Fahey (1994) An estimate of the flux of stratospheric reactive nitrogen
2355 and ozone into the troposphere, Journal of Geophysical Research, 99, 5325– 5332.

2356 Myhre, G., D. Shindell, F.-M. Bréon, W. Collins, J. Fuglestvedt, J. Huang, D. Koch, J.-F.
2357 Lamarque, D. Lee, B. Mendoza, T. Nakajima, A. Robock, G. Stephens, T. Takemura and H.
2358 Zhang, 2013: Anthropogenic and Natural Radiative Forcing. In: Climate Change 2013: The
2359 Physical Science Basis. Contribution of Working Group I to the Fifth Assessment Report of
2360 the Intergovernmental Panel on Climate Change [Stocker, T.F., D. Qin, G.-K. Plattner, M.
2361 Tignor, S.K. Allen, J. Boschung, A. Nauels, Y. Xia, V. Bex and P.M. Midgley (eds.)]. Cambridge
2362 University Press, Cambridge, United Kingdom and New York, NY, USA.

2363 Ndour, M., Conchon, P., D'Anna, B., Ka, O. and George, C., 2009. Photochemistry of mineral
2364 dust surface as a potential atmospheric renoxification process. Geophysical research letters,
2365 36(5).

2366 Neu, J. L., T. Flury, G. L. Manney, M. L. Santee, N. J. Livesey, and J. Worden (2014),
2367 Tropospheric ozone variations governed by changes in stratospheric circulation, Nature
2368 Geosci., 7, 340-344, doi:10.1038/ngeo2138.

2369 Nisbet, E. G., E. J. Dlugokencky and P. Bousquet (2014), Methane on the rise – again,
2370 Science, 343, 493-494, 10.1126/science.1249230.

2371 NOAA (2016), Earth Systems Research Laboratory, Global Monitoring Division
2372 http://www.esrl.noaa.gov/gmd/

2373 Ohja, N., M. Naja, T. Sarangi, R. Kumar, P. Bhardwaj, S. Lakl, S. Venkataramani, R. Sagar,
2374 A. Kumar and H. C. Chandola (2014) On the processes influecning the vertical distribution of
2375 ozone over the central Himalayas: Analysis of yearlong ozonesonde observations, Atmos.
2376 Environ., 88, 201-211.

2377 Olsen, M. A., M. R. Schoeberl, and A. R. Douglass (2004), Stratosphere-troposphere
2378 exchange of mass and ozone. Journal of Geophysical Research, 109, D24114,
2379 doi:10.1029/2004JD005186.

2380 Oltmans S.J., Johnson B.J., Helmig D., (2008), Episodes of high surface ozone amounts at
2381 South Pole during summer and their impact on the long-term ozone variation. Atmospheric
2382 Environment, 42, 2804–2816, doi:10.1016/j.atmosenv.2007.01.020.

2383 Ordoñez, C., Brunner, D., Staehelin, J., Hadjinicolaou, P., Pyle, J. A., Jonas, M., Wernli, H.,
2384 and Prévôt, A. S. H. (2007) Strong influence of lowermost stratospheric ozone on lower
2385 tropospheric background ozone changes over Europe, Geophys. Res. Lett., 34, L07805, doi:
2386 10.1029/2006GL029113, 5 pp.

2387 Orlando, J.J., and G.S. Tyndall. "Laboratory studies of organic peroxy radical chemistry: an
2388 overview with emphasis on recent issues of atmospheric significance." Chemical Society
2389 Reviews 41.19 (2012): 6294-6317.

2390 Ott, L. E., B. N. Duncan, A. M., Thompson, G. Diskin, Z. Fasnacht, A. O. Langford, M. Lin, A.
2391 M. Molod, J. E. Nielsen, A. J. Weinheimer and Y. Yoshida (2016) Frequency and impact of
2392 summertime stratospheric intrusions over Maryland during DISCOVER-AQ (2011): New
2393 evidence from NASA´s GEOS-5 simulations, J. Geophys. Res., 121, 3687-37006, doi:
2394 10.1002/2015JD024052.

2395 Parrish, D. D., J. S. Holoway, R. Jakoubek, M. Trainer, T. B. Ryerson, G. Hübler, F. L. Moody
2396 and O. R. Cooper, Mixing of anthropogenic pollution with stratospheric ozone: A case study
2397 from the North Atlantic wintertime troposphere, *J.Res*., *105*, 24,363-24,374, 2000.

2398 Parrish, D. D., et al. (2014), Long-term changes in lower tropospheric baseline ozone
2399 concentrations: Comparing chemistry-climate models and observations at northern mid
2400 latitudes, J. Geophys. Res.Atmos.,119, 5719–5736, doi:10.1002/2013JD021435.

2401 Penkett, S.A., C. E. Reeves, B. J. Bandy, J. M. Kent and H. R. Richer (1998) Comparison of
2402 calculated and measured peroxide data collected in marine air to investigate prominent
2403 features of the annual cycle of ozone in the troposphere, J. Geophys. Res., 101, 13377-13388.

2404 Penkett, S.A., Monks, P.S., Carpenter, L.J., Clemitshaw, K.C., Ayers, G.P., Gillett, R.W.,
2405 Galbally, I.E. and Meyer, C.P. (1997) Relationships between ozone photolysis rates and
2406 peroxy radical concentrations in clean marine air over the Southern Ocean. Journal of
2407 Geophysical Research, 102, 12805−12817.

2408 Penman, J., Kruger, D., Galbally, I.E., Hiraishi, T., Nyenzi, B., Emmanuel, S., Buendia, L.,
2409 Hoppaus, R., Martinsen, T., Meijer, J., Miwa, K., and Tanabe, K., editors. (2000). Good
2410 practice guidance and uncertainty management in national greenhouse gas inventories
2411 [Electronic publication]. Kanagawa, Japan: Intergovernmental Panel on Climate Change. 1 v.
2412 http://www.ipcc-nggip.iges.or.jp/public/gp/english/

2413 Pound, R. J., Sherwen, T., Helmig, D., Carpenter, L. J., and Evans, M. J.: Influences of oceanic
2414 ozone deposition on tropospheric photochemistry, Atmos. Chem. Phys. Discuss.,
2415 https://doi.org/10.5194/acp-2019-1043, in review, 2019.

2416 Prados-Roman, C., Cuevas, C. A., Fernandez, R. P., Kinnison, D. E., Lamarque, J.-F., and
2417 Saiz-Lopez, A.: A negative feedback between anthropogenic ozone pollution and enhanced
2418 ocean emissions of iodine, Atmos. Chem. Phys., 15, 2215–2224, https://doi.org/10.5194/acp-
2419 15-2215-2015, 2015.

2420 Prather, M.J., et al. "An atmospheric chemist in search of the tropopause." Journal of
2421 Geophysical Research: Atmospheres (1984–2012)116.D4 (2011).

2422 Price, C., Penner, J., and Prather, M.: NOx from lightning: 1. Global distribution based on
2423 lightning physics, J. Geophys. Res., 102, 5929–5941, doi:10.1029/96JD03504, 1997.

2424 Price, J. D., and G. Vaughan (1993) The potential for stratosphere-troposphere exchange in
2425 cut-off-low systems, Q. J. R. Meteorol. Soc., 119, 343-365.

2426 Rannik, Ü., Altimir, N., Mammarella, I., Bäck, J., Rinne, J., Ruuskanen, T. M., Hari, P., Vesala,
2427 T., and Kulmala, M.: Ozone deposition into a boreal forest over a decade of observations:
2428 evaluating deposition partitioning and driving variables, Atmos. Chem. Phys., 12, 12165-
2429 12182, doi:10.5194/acp-12-12165-2012, 2012.

2430 Read, K. A., Mahajan, A. S., Carpenter, L. J., Evans, M. J., Faria, B. V. E., Heard, D. E.,
2431 Hopkins, J. R., Lee, J. D., Moller, S. J., Lewis, A. C., Mendes, L., McQuaid, J. B., Oetjen, H.,
2432 Saiz-Lopez, A., Pilling, M. J., and Plane, J. M. C.: Extensive halogen-mediated ozone
2433 destruction over the tropical Atlantic Ocean, Nature, 453, 1232–1235,
2434 doi:10.1038/nature07035, 2008

2435 Regener, V.H. (1938) Neue messungen der vertikalen verteilung des ozons in der
2436 atmosphere. Zeitschrift für Physik, 109, 642−670.

2437 Regener, V.H. (1957) The vertical flux of atmospheric ozone. Journal of Geophysical
2438 Research, 62, 221−228.

2439 Reiter, R. (1990) The ozone trend in the layer of 2 to 3 km a.s.l. since 1978 and the typical
2440 time variations of the ozone profile between ground and 3 km a.s.l. Meteor. Atmos. Phys., 42,
2441 91-104.

2442 REVIHAAP, 2013. Review of evidence on health aspects of air pollution – REVIHAAP Project
2443 technical report. World Health Organization (WHO) Regional Office for Europe. Bonn.
2444 Available at: http://www.euro.who.int/data/assets/pdf_file/0004/193108/REVIHAAP-Final-
2445 technical-report-final-version.pdf.

2446 Richter, Andreas, et al. "Increase in tropospheric nitrogen dioxide over China observed from
2447 space." Nature 437.7055 (2005): 129-132.

2448 Ridley, B. A., J. G.Walega, J. E. Dye, and F. E. Grahek (1994), Distributions of NO, NOx, NOy
2449 and O3 to 12 km altitude during the summer monsoon season over New Mexico, J. Geophys.
2450 Res., 99, 25,519 – 25,534, doi:10.1029/94JD02210.

2451 Ridley, B., Madronich, S., Chatfield, R., Walega, J., Shetter, R., Carroll, M. and Montzka, D.
2452 (1992) Measurements and model simulations of the photostationary state during the Mauna
2453 Loa Observatory photochemistry experiment: Implications for radical concentrations and
2454 ozone production and loss rates. Journal of Geophysical Research, 97 (D10), 10375−10388.

2455 Roelofs G.-J. and J. Lelieveld (1997) Model study of the influence of cross-tropopause O3
2456 transports on tropospheric O3 levels, Tellus B, 49, 38-55.

2457 Roth, P.M., Roberts, P.J.W., Liu, M., Reynolds, S.D. and Seinfeld, J.H. (1974) Mathematical
2458 modeling of photochemical air pollution – II. A model and inventory of pollutant emissions.
2459 Atmospheric Environment, 8, 97–130.

2460 Saiz-Lopez, A., Fernandez, R. P., Ordóñez, C., Kinnison, D. E., Gómez Martín, J. C.,
2461 Lamarque, J.-F., and Tilmes, S.: Iodine chemistry in the troposphere and its effect on ozone,
2462 Atmos. Chem. Phys., 14, 13119–13143, https://doi.org/10.5194/acp-14-13119-2014, 2014.

2463 Scheel, H. E. (2003) Ozone Climatology Studies for the Zugspitze and Neighbouring Sites in
2464 the German Alps, pp. 134-139 in: Tropospheric Ozone Research 2, EUROTRAC-2 Subproject
2465 Final Report, A. Lindskog, Co-ordinator, EUROTRAC International Scientific Secretariat
2466 (München, Germany); www.trickl.de/scheel.pdf

2467 Schönbein, C.F., 1840: On the odour accompanying electricity and on the probability of its
2468 dependency on the presence of a new substance. Philos. Mag., 17, 293-294

2469 Schuepbach, E., T. D. Davies, A. C. Massacand and H. Wernli (1999) Mesoscale modelling
2470 of vertical atmospheric transport in the Alps associated with the advection of a tropopause fold
2471 – a winter ozone episode, Atmos. Environ., 33, 3613-3626.

2472 Schultz, M., R. Schmitt, K. Thomas and A. Volz-Thomas (1998) Photochemical box modelling
2473 of long-range transport from North America to Tenerife during the North Atlantic Regional
2474 Experiment (NARE) 1993, J. Geophys. Res. 103, 13477-13488.

2475 Schultz, M.G., Schröder, S., Lyapina, O., Cooper, O.R., Galbally, I., Petropavlovskikh, I., Von
2476 Schneidemesser, E., Tanimoto, H., Elshorbany, Y., Naja, M. and Seguel, R.J., 2017.
2477 Tropospheric Ozone Assessment Report: Database and metrics data of global surface ozone
2478 observations. Elementa: Science of the Anthropocene, 5.

2479 Schumann, U., and H. Huntrieser (2007), The global lightening - induced nitrogen oxides
2480 source, Atmospheric Chemistry and Physics, 7: 3823-3907.

2481 Seinfeld, J.H. and S.N. Pandis (1998) Atmospheric Chemistry and Physics, John Wiley and
2482 Sons, New York, USA, 1326 pp.

2483 Shapiro, M. A. (1976) The Role of Turbulent Heat Flux in the Generation of Potential Vorticity
2484 of Upper-Level Jet Stream Systems, Mon. Wea. Rev., 104, 892-906.

2485 Shapiro, M. A. (1978) Further Evidence of the Mesoscale and Turbulent Structure of Upper
2486 Level Jet Stream-Frontal Zone Systems, Mon. Wea. Rev., 106, 1100-1111.

2487 Shapiro, M. A. (1980) Turbulent Mixing within Tropopause Folds as a Mechanism for the
2488 Exchange of Chemical Constituents between the Stratosphere and Troposphere, J. Atmos.
2489 Sci., 37, 994-1004, 1980.

2490 Shiraiwa, M., Ammann, M., Koop, T. and Pöschl, U., 2011. Gas uptake and chemical aging of
2491 semisolid organic aerosol particles. Proceedings of the National Academy of Sciences,
2492 108(27), pp.11003-11008.

2493 Shaw, M.D. and L.J. Carpenter (2013) Modification of Ozone Deposition and I2 Emissions at
2494 the Air−Aqueous Interface by Dissolved Organic Carbon of Marine Origin. Environmental
2495 Science and Technology 47, 10947−10954, dx.doi.org/10.1021/es4011459

2496 Sherwen, T., Evans, M.J., Carpenter, L.J., Andrews, S.J., Lidster, R.T., Dix, B., Koenig, T.K.,
2497 Sinreich, R., Ortega, I., Volkamer, R. and Saiz-Lopez, A., 2016. Iodine's impact on
2498 tropospheric oxidants: a global model study in GEOS-Chem. Atmospheric Chemistry and
2499 Physics, 16(2), pp.1161-1186.

2500 Sherwen, T., Evans, M.J., Carpenter, L.J., Schmidt, J.A. and Mickley, L.J., 2017. Halogen
2501 chemistry reduces tropospheric O_3 radiative forcing. Atmospheric Chemistry and Physics,
2502 17(2), pp.1557-1569.

2503 Sitch, S., et al. "Indirect radiative forcing of climate change through ozone effects on the land-
2504 carbon sink." Nature 448.7155 (2007): 791-794.

2505 Škerlak, B., M. Sprenger, H. Wernli (2014) a global climatology of stratosphere-troposphere
2506 exchange using the ERA-Interim data set from 1979 to 2011, Atmos. Chem. Phys., 14, 913-
2507 937.

2508 Škerlak, B., Pfhal, S., Sprenger, M., Wernli, H., 2019. A numerical process study on the rapid
2509 transport of stratospheric air down to the surface over western North America and the Tibetan
2510 Plateau. Atmospheric Chemistry and Physics, 19, 6535–6549, https://doi.org/10.5194/acp-19-
2511 6535-2019.

2512 Sklaveniti, S., Locoge, N., Stevens, P. S., Wood, E., Kundu, S., and Dusanter, S.:
2513 Development of an instrument for direct ozone production rate measurements: measurement
2514 reliability and current limitations, Atmos. Meas. Tech., 11, 741–761,
2515 https://doi.org/10.5194/amt-11-741-2018, 2018.

2516 Söderlund, R. and Svensson, B.H. (1976) The Global Nitrogen Cycle, In: Svensson, B.H. &
2517 Söderlund, R. (eds), Nitrogen, Phosphorus and Sulphur - Global Cycles. SCOPE Report 7.
2518 Ecological Bulletins (Stockholm) 22, 23−73.

2519 Søvde, O.A., Hoyle, C.R., Myhre, G. and Isaksen, I.S.A., 2011. The HNO3 forming branch of
2520 the HO2+ NO reaction: pre-industrial-to-present trends in atmospheric species and radiative
2521 forcings. Atmospheric Chemistry and Physics, 11(17), pp.8929-8943.

2522 Sprenger, M., Croci Maspoli, M., and Wernli, H.: Tropopause folds and cross-tropopause
2523 exchange: A global investigation based upon ECMWF analyses for the time period March
2524 2000 to February 2001, J. Geophys. Res., 108, 8518, doi: 10.1029/2002JD002587, STA 3, 11
2525 pp., 2003.

2526 Squire, O. J., Archibald, A. T., Griffiths, P. T., Jenkin, M. E., Smith, D., and Pyle, J. A.: Influence
2527 of isoprene chemical mechanism on modelled changes in tropospheric ozone due to climate
2528 and land use over the 21st century, Atmos. Chem. Phys., 15, 5123–5143,
2529 https://doi.org/10.5194/acp-15-5123-2015, 2015.

2530 Staehelin, J., F. Tummon, L. E. Revell, A. Stenke and T. Peter (2017). "Tropospheric ozone
2531 at northern mid-latitudes: modeled and measured long-term changes." Atmosphere 8(9): 163.

2532 Stavrakou, Trissevgeni, et al. "How consistent are top-down hydrocarbon emissions based on
2533 formaldehyde observations from GOME-2 and OMI?." Atmospheric Chemistry and Physics
2534 15.20 (2015): 11861-11884.

2535 Stevenson, D.S., Dentener, F.J., Schultz, M.G., Ellingsen, K., van Noije, T.P.C., Wild, O.,
2536 Zeng, G., Amann, M., Atherton, C.S., Bell, N., Bergmann, D.J., Bey, I., Butler, T., Cofala, J.,
2537 Collins, W.J., Derwent, R.G., Doherty, R.M., Drevet, J., Eskes, H.J., Fiore, A.M., Gauss, M.,
2538 Hauglustaine, D.A., Horowitz, L.W., Isaksen, I.S.A., Krol, M.C., Lamarque, J.-F., Lawrence,
2539 M.G., Montanaro, V., Müller, J.-F., Pitari, G., Prather, M.J., Pyle, J.A., Rast, S., Rodriguez,
2540 J.M., Sanderson, M.G., Savage, N.H., Shindell, D.T., Strahan, S.E., Sudo, K. and Szopa, S.

(2006) Multimodel ensemble simulations of present-day and near-future tropospheric ozone. Journal of Geophysical Research, 111, D08301, doi:10.1029/2005JD006338

Stauffer, R. M., A. M. Thompson, J. C. Witte (2018) Characterizing global ozonesonde profile variability from surface to the UT/LS with a clustering technique and MERRA-2 reanalysis, J. Geophys. Res., 123, doi: 10.1002/2017JD028465

Stohl, A. (2001) A 1-year Lagrangian "climatology" of airstreams in the Northern Hemisphere and lowermost stratosphere, J. Geophys. Res., 106, 7263-7279.

Stohl, A., Bonasoni, P., Cristofanelli, P., Collins, W., Feichter, J., Frank, A., Forster, C., Gerasopoulos, E., Gäggeler, H., James, P., Kentarchos, T., Kromp-Kolb, H., Krüger, B., Land, C., Meloen, J., Papayannis, A., Priller, A., Seibert, P., Sprenger, M., Roelofs, G. J., Scheel, H. E., Schnabel, C., Siegmund, P., Tobler, L., Trickl, T., Wernli, H., Wirth, V., Zanis, P., and Zerefos, C. (2003) Stratosphere-troposphere exchange - a review, and what we have learned from STACCATO, J. Geophys. Res., 108, 8516, doi:10.1029/2002JD002490, STA 1, 15 pp.

Stohl, A., Forster, C., Eckhardt, S., Spichtinger, N., Huntrieser, H., Heland, J., Schlager, H., Wilhelm, S., Arnold, F. and Cooper, O., 2003. A backward modeling study of intercontinental pollution transport using aircraft measurements. Journal of Geophysical Research: Atmospheres, 108(D12).

Stohl, A., C. Forster, H. Huntrieser, H. Mannstein, W.W. McMillan, A. Petzold, H. Schlager and B. Weinzierl (2007) Aircraft measurements over Europe of an air pollution plume from Southeast Asia – aerosol and chemical characterization, Atmos. Chem. Phys., 7, 913-937.

Stohl, A., S. Eckhardt, C. Forster, P. James and N. Spichtinger (2002) On the pathways and timescales of intercontinental transport, J. Geophys. Res., 107, 4684, doi: 10.1029/2001JD001396, 17 pp.

Strode, S. A., J. M. Rodriguez, J. A. Logan, O. R. Cooper, J. C. Witte, L. N. Lamsal, M. Damon, B. Van Aartsen, S. D. Steenrod, and S. E. Strahan (2015), Trends and variability in surface ozone over the United States, J. Geophys. Res. Atmos., 120, 9020–9042, doi:10.1002/2014JD022784.

Sun, L., L. Xue, T. Wang, J. Gao, A. Ding, O. R. Cooper, M. Lin, P. Xu, Z. Wang, X. Wang, L. Wen, Y. Zhu, T. Chen, L. Yang, Y. Wang, J. Chen, and W. Wang (2016), Significant increase of summertime ozone at Mount Tai in Central Eastern China, Atmos. Chem. Phys., 16, 10637-10650, doi:10.5194/acp-16-10637-2016, 2016

Tarasick, D., Galbally, I.E., Cooper, O.R., Schultz, M.G., Ancellet, G., Leblanc, T., Wallington, T.J., Ziemke, J., Liu, X., Steinbacher, M., Staehelin, J., Vigouroux, C., Hannigan, J.W., García, O., Foret, G., Zanis, P., Weatherhead, E., Petropavlovskikh, I., Worden, H., Osman, M., Liu, J., Chang, K.-L., Gaudel, A., Lin, M., Granados-Muñoz, M., Thompson, A.M., Oltmans, S.J., Cuesta, J., Dufour, G., Thouret, V., Hassler, B., Trickl, T. and Neu, J.L., 2019. Tropospheric Ozone Assessment Report: Tropospheric ozone from 1877 to 2016, observed levels, trends and uncertainties. *Elem Sci Anth*, 7(1), p.39. DOI: http://doi.org/10.1525/elementa.376

Thompson, A.M., Balashov, N.V., Witte, J.C., Coetzee, J.G.R., Thouret, V. and Posny, F., 2014. Tropospheric ozone increases over the southern Africa region: bellwether for rapid growth in Southern Hemisphere pollution?. *Atmospheric Chemistry and Physics*, p.9855.

Thompson, A. M., J. B. Stone, J. C. Witte, S. K. Miller, S. J. Oltmans, K. L. Ross, T. L. Kucsera, J. T. Merrill, G. Forbes, D. W. Tarasick, E. Joseph, F. J. Schmidlin, W. W. McMillan, J. Warner, E. J. Hintsa, J. E. Johnson, Intercontinental Transport Experiment Ozonesonde Network Study (IONS, 2004): 2. Tropospheric Ozone Budgets and Variability over Northeastern North America, Journal of Geophysical Research, 112, D12S13, doi: 10.1029/2006JD007670.

Tost, H., Jöckel, P., Kerkweg, A., Sander, R., and Lelieveld, J.: Technical note: A new comprehensive SCAVenging submodel for global atmospheric chemistry modelling, Atmos. Chem. Phys., 6, 565–574, https://doi.org/10.5194/acp-6-565-2006, 2006.

Trickl, T., H. Feldmann, H.-J. Kanter, H. E. Scheel, M. Sprenger, A. Stohl, H. Wernli (2010) Deep stratospheric intrusions over Central Europe: case studies and climatological aspects, Atmos. Chem. Phys., 10, 499-524.

Trickl, T., Eisele, H., Bärtsch-Ritter, N. Furger, M., Mücke, R., Sprenger, M., and Stohl, A.: High-ozone layers in the middle and upper troposphere above Central Europe: potential import from the stratosphere along the subtropical jet stream, Atmos. Chem. Phys., 11, 9343-9366, 2011.

Trickl, T., H. Vogelmann, H. Giehl, H. E. Scheel, M. Sprenger, A. Stohl (2014) How stratospheric are deep stratospheric intrusions? Atmos. Chem. Phys., 14, 9941-9961.

Trickl, T., H. Vogelmann, H. Flentje, L. Ries (2015) Stratospheric ozone in boreal fire plumes - the 2013 smoke season over Central Europe, Atmos. Chem. Phys., 15, 9631-9649.

Trickl, T., H. Vogelmann, A. Fix, A. Schäfler, M. Wirth, B. Calpini, G. Levrat, G. Romanens, A. Apituley, K. M. Wilson, R. Begbie, J. Reichardt, H. Vömel, M. Sprenger (2016) How Stratospheric Are Deep Stratospheric Intrusions into the Troposphere? LUAMI 2008, Atmos. Chem. Phys., 16, 8791-8815.

Trickl, T., Vogelmann, H., Ries, L., and Sprenger, M. (2020) Very high stratospheric influence observed in the free troposphere over the northern Alps – just a local phenomenon? Atmos. Chem. Phys., 20.

Tuovinen, J.-P., M.R Ashmore, L.D Emberson, D Simpson (2004) Testing and improving the EMEP ozone deposition module. Atmospheric Environment, 38 (15) 2373-2385. ISSN 1352-2310, https://doi.org/10.1016/j.atmosenv.2004.01.026.

U.S. Environmental Protection Agency, 2013. Integrated Science Assessment for Ozone and Related Photochemical Oxidants. EPA/600/R-10/076F. Office of Research and Development, Research Triangle Park, NC (February).

van Vuuren, D. P., Edmonds, J., Kainuma, M., Riahi, K., Thomson, A., Hibbard, K., Hurtt, G. C., Kram, T., Krey, V., Lamarque, J.-F., Masui, T., Meinshausen, M., Nakicenovic, N., Smith, S. J., and Rose, S. K. (2011), The representative concentration pathways: an overview, Clim. Change, 109, 5–31, doi:10.1007/s10584-011-0148-z.

Vogt, R., Sander, R., von Glasow, R. and Crutzen, P.J. (1999) Iodine chemistry and its role in halogen activation and ozone loss in the marine boundary layer: A model study. Journal of Atmospheric Chemistry, 32 (3), 375−395.

Von Schneidemesser, E., et al. "Chemistry and the linkages between air quality and climate change." Chemical Reviews 115.10 (2015): 3856-3897.

Wallington, T.J., Seinfeld, J.H. and Barker, J.R., 2019. 100 Years of progress in gas-phase atmospheric chemistry research. *Meteorological Monographs*, *59*, pp.10-1.

Weiss-Penzias, P., D. A. Jaffe, L. Jaeglé and Q. Liang (2004) Influence of long-range-transported pollution on the annual and diurnal cycles of carbon monoxide and ozone at Cheaka Peak Observatory, J. Geolphys. Res., 109, D23814, doi: 10.1029/2004JD004505, 15 pp.

Xia, L., Nowack, P. J., Tilmes, S., and Robock, A.: Impacts of stratospheric sulfate geoengineering on tropospheric ozone, Atmos. Chem. Phys., 17, 11913–11928, https://doi.org/10.5194/acp-17-11913-2017, 2017.

Ye C, Zhou X, Pu D, Stutz J, Festa J, Spolaor M, Tsai C, Cantrell C, Mauldin RL, Campos T, Weinheimer A, Hornbrook RS, Apel EC, Guenther A, Kaser L, et al. Rapid cycling of reactive nitrogen in the marine boundary layer. Nature. PMID 27064904 DOI: 10.1038/nature17195, 2016

Yeung, L.Y., Murray, L.T., Martinerie, P., Witrant, E., Hu, H., Banerjee, A., Orsi, A. and Chappellaz, J., 2019. Isotopic constraint on the twentieth-century increase in tropospheric ozone. Nature, 570(7760), p.224.

Young, P. J., et al. (2013a), Pre-industrial to end 21st century projections of tropospheric ozone from the Atmospheric Chemistry and Climate Model Intercomparison Project (ACCMIP), Atmos. Chem. Phys 13, 2063–2090. doi:10.5194/acp-13-2063-2013.

Young, P. J., et al. (2013b), Corrigendum to “Pre-industrial to end 21st century projections of tropospheric ozone from the Atmospheric Chemistry and Climate Model Intercomparison Project (ACCMIP)” published in Atmos. Chem. Phys., 13, 2063–2090, 2013, Atmos. Chem. Phys., 13, 5401–5402, doi:10.5194/acp-13-5401-2013.

Young, P.J., Naik, V., Fiore, A.M., Gaudel, A., Guo, J., Lin, M.Y., Neu, J., Parrish, D., Reider, H.E., Schnell, J.L. and Tilmes, S., 2018. Tropospheric Ozone Assessment Report: Assessment of global-scale model performance for global and regional ozone distributions, variability, and trends. Elementa: Science of the Anthropocene, 6(1).

Zachariasse, M., van Velthoven, P. F. J., Smit, H. G. J., Lelieveld, J., Mandal, T. K., and Kelder, H. (2000) Influence of stratosphere-troposphere exchange over the tropical Indian Ocean during the winter monsoon, J. Geophys. Res., 105, 15403-15416.

Zahn, A., Brenninkmeijer, C. A. M., Asman, W. A. H., Crutzen, P. J., Heinrich, G., Fischer, H., Cuijpers, J. W. M., and van Velthoven, P. F. J. (2002) Budgets of O3 and CO in the upper troposphere: CARIBIC passenger aircraft results 1997-2001, J. Geophys. Res., 107, 4337, doi: 10.1029/2001JD001529, 19 pp.

Zhang, M., W. Tian, L. Chen, and D. Lü (2010) Cross-Tropopause Mass Exchange Associated with a Tropoause Fold Event over the Northeastern Tibetean Plateau, Adv. Atmos. Scik., 27, 1344-1360

Zhang, Q., et al. "NOx emission trends for China, 1995–2004: The view from the ground and the view from space." Journal of Geophysical Research: Atmospheres 112.D22 (2007).

Zhang, R., Tie, X. and Bond, D.W., 2003. Impacts of anthropogenic and natural NOx sources over the US on tropospheric chemistry. Proceedings of the National Academy of Sciences, 100(4), pp.1505-1509.

Zhang, Y., O. R. Cooper, A. Gaudel, A. M. Thompson, P. Nédélec, S.-Y. Ogino and J. J. West (2016), Tropospheric ozone change from 1980 to 2010 dominated by equatorward redistribution of emissions, Nature Geoscience, doi: 10.1038/NGEO2827.

Ziemke, J. R., S. Chandra, G.J. Labow, P.K. Bhartia, L. Froidevaux, and J.C. Witte (2011), A global climatology of tropospheric and stratospheric ozone derived from Aura OMI and MLS measurements, Atmos. Chem., Phys., 11, 9237-9251

Ziemke, J. R., Oman, L. D., Strode, S. A., Douglass, A. R., Olsen, M. A., McPeters, R. D., Bhartia, P. K., Froidevaux, L., Labow, G. J., Witte, J. C., Thompson, A. M., Haffner, D. P., Kramarova, N. A., Frith, S. M., Huang, L.-K., Jaross, G. R., Seftor, C. J., Deland, M. T., and Taylor, S. L.: Trends in global tropospheric ozone inferred from a composite record of TOMS/OMI/MLS/OMPS satellite measurements and the MERRA-2 GMI simulation , Atmos. Chem. Phys., 19, 3257–3269, https://doi.org/10.5194/acp-19-3257-2019, 2019.